Master's thesis

NTNU
Norwegian University of Science and Technology
Faculty of Engineering
Department of Civil and Environmental Engineering

Nora Rydland Fjøsne

Demonstrating the retrofitting potential of non-powered dams for hydropower production

Master's thesis in Civil and Environmental Engineering
Supervisor: Tor Haakon Bakken
June 2020

NTNU
Norwegian University of Science and Technology

Nora Rydland Fjøsne

Demonstrating the retrofitting potential of non-powered dams for hydropower production

Master's thesis in Civil and Environmental Engineering
Supervisor: Tor Haakon Bakken
June 2020

Norwegian University of Science and Technology
Faculty of Engineering
Department of Civil and Environmental Engineering

NTNU
Norwegian University of
Science and Technology

Abstract

A large number of the world's dams and reservoirs are built for other purposes than hydropower production. With an increased focus on renewable energy and environmentally friendly solutions, hydropower is both praised for producing large and flexible quantities of renewable energy, and yet criticized for causing negative impacts on the natural environments. Retrofitting of non-powered dams to dams with a hydropower generating unit require only small interventions compared to the construction of an entirely new dam and power plant. However, reservoirs made for irrigation, domestic water supply, or other purposes often have different regulation patterns than those made solely for hydropower production. The compatibility of the different demand patterns should therefore be assessed and evaluated by investigating the water balance in the relevant basin over several years.

This study aims at demonstrating the hydropower potential of non-powered dams following the current water regulation. In order to quantify the hydropower potential of retrofitting non-powered dams, this study is based on a case study of the Guadalquivir basin in Southern Spain including 13 non-powered dams. The entire basin is simulated over the time period from 2009 to 2018 using the software WEAP with a monthly timestep. Parameters are calibrated using streamflow data for unregulated sub-catchments within the Guadalquivir basin, and transposed to the entire basin. Climate data is averaged within the different sub-catchments of the basin. The software QGIS is used for the processing of georeferenced data concerning the authorized withdrawals and potential evaporation from the reservoirs.

An economic analysis of the retrofitting potential is made in order to compare retrofitting of existing dams, with new hydropower projects and other renewable energy developments. The included costs in the analysis are the cost of construction, the cost of necessary equipment, and the operation and maintenance cost. The revenues are calculated assuming a fixed interest rate, and a fixed electricity price for the lifetime not covered by the simulation period. Levelized cost of electricity is calculated for the retrofitting of all the non-powered dams and compared to other renewable energy sources, whereas the net present values are calculated to quantify the economic viability of the retrofitting considering the future electricity rate.

The results show a retrofitting potential of 64.61 GWh with a corresponding capacity of 45.33 MW for the 13 non-powered dams in Guadalquivir. When considering turbine capacities designed to fit the observed outflow of the non-powered dams, five of the 13 included non-powered dams are found to be economically viable. These five represent a net present value of 13.67 million 2018 EUR and a hydropower potential of 46.79 GWh. The results have a percent bias of 6% when the total simulated streamflow is compared with the measured values at the most downstream gauge in the basin. A linear regression between the results and selected parameters in the ICOLD database is performed, and a global retrofitting potential is estimated to 277.33 TWh from the resulting regression. Summarized, the case study presents important results that indicate the hydropower potential and demonstrates the economic viability of retrofitting existing non-powered dams.

Sammendrag

En stor andel av verdens dammer og reservoarer er bygget for andre grunner enn vannkraft. Med et økt fokus på fornybar energi og miljøvennlige løsninger blir vannkraft både lovprist for å produsere store og fleksible mengder fornybar energi, men også kritisert for å ha en negativ påvirkning på miljøet. Ettermontering av eksisterende dammer uten vannkraftproduksjon til dammer med vannkraftproduksjon krever kun små ingrep sammenlignet med byggingen av en helt ny dam og kraftverk. Derimot kan reservoar bygget for jordvanning, vannforsyning eller andre forbruk ofte ha andre tidsmessige reguleringsmønster enn de som er bygget spesielt for vannkraft. Kompatibiliteten til de forskjellige behovsmønstrene bør derfor undersøkes og evalueres ved å se på vannbalansen i det aktuelle nedbørsfeltet over flere år.

Denne studien tar sikte på å demonstrere vannkraftpotensialet som følger den nåværende vannreguleringen ved eksisterende dammer uten vannkraftproduksjon. For å kvantifisere dette potensialet er denne studien basert på en casestudie av nedbørsfeltet Guadalquivir sør i Spania med 13 slike dammer. Hele nedbørsfeltet er simulert over perioden 2009 til 2018 ved bruk av programvaren WEAP med en månedlig tidsoppløsning. Parametere er kalibrert ved å benytte vannføringsdata for uregulerte nedbørsfelt innenfor Guadalquivir nedbørsfeltet, før de er overført til hele nedbørsfeltet. Klimadata er fordelt i nedbørsfeltet som gjennomsnittsverdier innad de mindre nedbørsfeltene. Programvaren QGIS er brukt for prosesseringen av de geografisk spesifiserte punktene for autoriserte vannuttak og evaporasjonspotensialet fra reservoarene.

En økonomisk analyse av ettermonterings-potensialet er utført for å sammenligne den økonomiske levedyktigheten av å ettermontere turbiner til eksisterende dammer med nye vannkraftprosjekt og andre fornybare energikilder. Analysen inkluderer kostnadene av bygging, installasjoner, drift og vedlikehold. Inntektene er beregnet ved å anta en fast rente og en fast strømpris for perioden av levetiden som ikke er dekket av simuleringene. Faktiske elektrisitetskostnader over levetiden (LCOE) er beregnet for ettermontering av alle dammene uten vannkraftproduksjon og sammenlignet med andre fornybare energikilder, mens netto nåverdiene er beregnet for kvantifisering av den økonomiske levedyktigheten til ettermonteringen med tanke på den antatte fremtidige strømprisen.

Resultatene viser et ettermonteringspotensiale på 64,61 GWh og 45,33 MW for de 13 dammene uten vannkraftproduksjon i Guadalquivir. Når turbiner dimensjonert for observerte uttak fra dammene er tatt med i bestraktningen er fem av de 13 inkluderte dammene uten vannkraftproduksjon funnet å være økonomisk levedyktige. Disse fem representerer en netto nåverdi på 13,67 millioner 2018 EUR og et vannkraftpotensial på 46,79 GWh. Resultatene har et prosentvis avvik på 6% for den totale simulerte vannføringen sammenlignet med målte verdier fra den målestasjonen som er plassert lengst nedstrøms i nedbørsfeltet. En lineær regressjon mellom resultatene og utvalgte parametre i ICOLDs damregister er utført, og det resulterende uttrykket gir et estimat for det globale potensiale for ettermontering på 277,33 TWh. Oppsummert presenterer casestudien viktige resultater som indikerer vannkraftpotensialet og demonstrerer levedyktigheten av ettermontering av dammer uten vannkraftproduksjon.

Preface

This thesis is submitted in partial fulfillment of the requirements for a Master of Science in Civil and Environmental Engineering at the Norwegian University of Science and Technology. The study covered in this thesis has been performed between January 2020 and June 2020, in addition to some parts being based on the project work done during the autumn semester of 2019. Professor Tor Haakon Bakken has supervised the work.

The process of doing this master thesis has been highly rewarding, especially due to the completeness of the task. Covering many of the stages in the initial planning process of general hydropower projects, it has been necessary to include knowledge about hydrology, hydrological modelling, modelling of water resource management, geoinformatics, statistics, hydraulics, technical hydropower solutions as well as economics. Gaining more experience with QGIS and WEAP has been among the most important attributes to this project and is likely to be among the most useful for my future career, directly or indirectly.

This study was intended to be a desktop study from the beginning of the semester and has therefore not been directly affected by the COVID-19 virus and the lockdown it caused in Norway from the 12th of March. The fact that the offices have been closed since the lockdown and the resulting limited communication with other students in the same writing process has however felt like an additional challenge to the study.

There are many people who have contributed to this work. I want to thank my supervisor Professor Tor Haakon Bakken for invaluable support throughout the entire master process. Your quick and positive advice have been highly appreciated, and I am grateful for having gotten the opportunity to study a topic I personally find very interesting from both an engineering, environmental and societal point of view. I also want to thank Ana Juarez for her enthusiastic and encouraging help with finding and understanding Spanish references, and Professor Leif Lia and Professor Oddbjørn Bruland for their professional and technical advice. Finally, I want to thank my friends and family for their support and patience, jogging discussions, and calls in this special period. A special thanks to my proofreader, home office colleague, and partner Alex.

Trondheim, 11.06.2020

Nora Rydland Fjøsne

Table of Contents

List of Figures

List of Tables

List of Abbreviations

DC	Deep Conductivity
CHG	Confederación Hidrográfica del Guadalquivir, O.A.
CLC	CORINE Land Cover
CPI	Consumer Price Index
CRU	Climate Research Unit
DWC	Deep Water Capacity
ET	Evapotranspiration
FAO	Food and Agriculture Organization of the United Nations
GIS	Geographic Information System
GRanD	Global Reservoir and Dam database
GW	Giga Watt
GWh	Giga Watt hours
HICP	Harmonized Index of Consumer Prices
HRWL	Highest Regulated Water Level
ICOLD	International Commission on Large Dams
IRENA	International Renewable Energy Agency
IPCC	Intergovernmental Panel on Climate Change
LCOE	Levelized Cost of Electricity
LEAP	Long-range Energy Alternatives Planning system
NetCDF	Network Common Data Form
NPD	Non-powered dam
NPV	Net Present Value
NTNU	The Norwegian University of Science and Technology
NVE	The Norwegian Water Resources and Energy Directorate
PBIAS	Percent Bias
PET	Potential Evapotranspiration
PFD	Preferred Flow Direction
RES	Renewable Energy Sources
RRF	Runoff Resistance Factor
RZC	Root Zone Conductivity
SAIH	Sistema Automático de Información Hidrológica de la Cuenca del Guadalquivir
SSB	Statistics Norway
SWC	Soil Water Capacity
WACC	Weighted Average Cost of Capital
WEAP	Water Evaluation And Planning system

1 Introduction

1.1 Background

People have since ancient times been managing water for irrigation, navigation and flood control. Water is one of our essential resources, being essential for our bodies as well as a part of nature and the hydrological cycle. Both too much and too little water can cause fatal challenges in our society, as it can result in droughts or floods causing direct and indirect impacts.

Renewable energy sources role in relation to climate change has been highlighted during the last decades. The direct use of the force of falling water to turn water wheels has been used since 202 BC, whereas the first electricity generated by hydropower took place in 1878 (IHA, 2019). Today, hydropower is the most common source of renewable energy for electricity production in the world, with a global production of 4 197 TWh in 2017 (IEA, 2019).

The construction and management of reservoirs enables the storage of water for dryer periods and the retention of water during floods. Integrated water resources management is used in order to optimize the regulation of the reservoirs while taking all the water uses in the river basin into consideration. This may include the use of computer models and real-time monitoring of the status of the basin's reservoirs as well as continuous decision-making regarding how big water volumes that should be withdrawn from which reservoir to what time.

In addition to an increased focus on climate change, the environmental aspect of hydropower has also been increasingly discussed. Even though water storage in reservoirs may become increasingly important in areas where climate change cause more frequent and long-lasting droughts, it is uncertain whether the positive effects outweigh the negative impacts. Construction of dams and alteration of river flows are proven to negatively affect the surrounding ecosystems, and larger alterations normally cause larger negative effects. Instead of building new dams, retrofitting of hydropower to non-powered dams can give increased hydropower generation with only limited adaptation to the dam site and without further flow-alteration.

29 163 dams are registered as non-powered dams (NPDs) in the ICOLD World Register of Dams (ICOLD, 2019), representing about 50% of the dams in the register. Although these dams provide both available water and a height difference to exploit for hydropower production, economic and technical factors still have to be evaluated as well as the compatibility of hydropower production with the existing water use. For a dam to be suited for retrofitting, it needs feasible technical solutions at acceptable costs that can exploit sufficient water volumes without negatively impacting the initial water uses.

There are currently few studies assessing the hydropower potential of retrofitting existing dams that limits the availability of water to the current availability, thus excluding further alteration of the streamflow. The development of water balance models covering whole river basins allows for the simulation of water availability and the effects of different water management strategies. Conserving the current outflow pattern from the dams eliminates possible conflicts between hydropower, environmental requirements and existing water users, and is therefore an interesting and valuable research topic for the assessment of hydropower retrofitting. The case study performed in this thesis is meant to address this potential, and thus hopefully provide useful results that can facilitate the initiation and planning of future retrofitting projects.

1.2 Objectives

The main objectives of this study are the following:

- Develop a method to calculate the retrofitting potential in a basin with non-powered dams
- Demonstrate the hydropower potential of a chosen drainage basin using the Water Evaluation And Planning software (WEAP)
- Provide a rough estimate of the costs of retrofitting and the revenues of the possible hydropower production for the chosen retrofitting projects
- Compare economic results to other sources of renewable energy production
- Assess the assumptions, limitations and uncertainties in the methodology and calculations
- Outline an approach to calculate the regional/global retrofitting potential and address data and research needs in order to further refine the calculations of the hidden hydropower potential

1.3 Structure of the report

This thesis starts with a theory section covering the principles of hydropower used in this study, the concept of retrofitting, and a description of the chosen river basin for the case study. A presentation and explanation of all the materials and methods are included under Method. The findings of the study are presented in the Results section, followed by a discussion. The Discussion covers the limitations, uncertainties, results, and future research topics. Last is the conclusion, the references, and the appendices.

2 Theory

This section starts by explaining the basic principles of hydropower generation and the concept of retrofitting. These two sub-sections are based on the project thesis *Assessment of the retrofitting potential of dams and reservoirs without hydropower* submitted as project thesis (Fjoesne, 2019). The project thesis was written in December 2019 by the same author as this report for the course *TVM4520 Hydropower and Hydraulic Engineering, Specialization Project* at the Norwegian University of Science and Technology. Following is a description of the chosen case study and its characteristics. The WEAP section describes the WEAP software with its most relevant integrated functions and calculation methods for this study, followed by a section presenting the basis for the economic assessment of retrofitting projects. The literature review included in the project thesis also revealed potential barriers to retrofitting that are mentioned under Discussion.

2.1 Hydropower

An available water volume and a height difference are considered the two main conditions for hydropower generation. By using the falling water to move mechanical components, the force can be directly used as a mechanical force or for the generation of electricity. Due to head losses, the available effective head is always smaller than the gross head. The main sources for head losses are contractions, expansions, bends, and friction losses in the waterways. The following equation expresses generated hydropower, *P [W]*:

$$P = \eta \cdot \rho \cdot g \cdot H \cdot Q, \tag{1}$$

where η is the efficiency factor, ρ the density of water [kg/m^3], g the gravitational force [m/s^2], H the effective head [m], and Q the water discharge [m^3/s]. Energy, E, is defined as power integrated over time, and can be calculated as:

$$E = P \cdot t, \tag{2}$$

where the energy, E, is expressed in [Wh], P is the average power [W], and t is the time [h].

The capacity factor describes the ratio of actual produced energy to the maximum hypothetical potential (Hadjerioua et al., 2012) and is considered a key value for describing hydropower projects. The maximum hypothetical potential considers a constant production of the installed capacity during the entire year. Variable turbine flow due to limited water availability, changing head due to changing reservoir levels and head losses, and different generation efficiencies all contribute to the gap between the hypothetical potential and the actual production. The capacity factor can be expressed by the following equation:

$$Capacity\ factor = \frac{Annual\ produced\ energy\ \left[\frac{MWh}{year}\right]}{Installed\ capacity\ [MW] \cdot 8760 \frac{h}{year}}. \tag{3}$$

For an estimation of hydraulic conditions in existing pipelines and intakes, a comparison between the calculated theoretical capacity and the official capacity can be performed. A big theoretical capacity compared to the official capacity can indicate that the waterway is dimensioned in such a way that it causes big head losses or that it comprises a pressure reduction valve. For a conservative estimation of the theoretical capacity of intakes, an estimation assuming intake-controlled capacity and sharp edges can be performed. This is done

by using the continuity equation for steady flow with the velocity term based on the physical principle of potential energy:

$$Q = A \cdot v = \frac{D^2}{4} \cdot \pi \cdot C \cdot \sqrt{2 \cdot g \cdot H_1}, \quad (4)$$

where A is the area of the flow cross section [m²], v the flow velocity [m/s], D the pipe diameter [m], C the contraction coefficient, and H_1 the height difference between the water level an the center of the intake [m] (Jenssen et al., 2006). The resulting capacity is considered to be conservative when assuming the contraction coefficient to be 0.6.

New waterways that supply the turbine with water should be designed according to the installed discharge capacity of the turbine. Bigger dimensions of the waterways reduce the friction losses, but increase the construction costs. Optimizing the dimensions of the waterway is therefore about finding the balance point between increased construction costs and lost revenue from head losses. From the contiuity equation for steady flow, the following equation for the necessary pipe diameter, D [m], is deduced:

$$D = \sqrt{\frac{4 \cdot Q}{C_{max} \cdot \pi}}, \quad (5)$$

where C_{max} is the maximum velocity of the water that flows in the pipe [m]. C_{max} is often found to be between 2 m/s and 4 m/s after optimization (SWECO Norge et al., 2010).

2.2 Retrofitting

2.2.1 Technical solutions

Retrofitting of hydropower to non-powered dams (NPDs) consists of adding a hydropower generating unit to an existing dam and is in this study simply referred to as *retrofitting*. The main advantage of retrofitting is that the costs, efforts and negative environmental impacts of constructing a dam is avoided, as the initial dam structure already provides an exploitable head and a regulated reservoir. Retrofitting can be done with or without structural modifications on the initial structure, since the turbines can be built into the dam construction or installed separately. If installed separately from the dam, the turbine can be supplied by water from existing or new waterways away from the dam. A replacement of existing pressure valves by turbines in existing outlet structures can reduce the need for any constructional work for retrofitting to a minimum and hence reduce the construction time and costs. The friction losses in existing structures may in many cases not be optimized for hydropower generation, and the construction of new intakes should in such cases be considered.

Special technical solutions have been developed for retrofitting, and some are still under development. These include intake solutions and turbines that focus on an easier installation process at NPDs, maximizing the overall efficiency of low head installations, or limiting further impacts on the aquatic life. The updraft free-exit-flow turbine is one of the technical solution especially suited for simple retrofitting, as it can be connected to the existing outlet of the dam (Kao et al., 2009). The updraft flow causes an aeration of the flow and can therefore both improve the oxygen levels in the water downstream and avoid the need for a draft tube. This turbine is suited for hydraulic heads up to 80 meters but is considered to still be under development.

Another technical solution to retrofitting is the siphon turbine. The turbine is in this case placed in a siphon reaching from the reservoir over the top of the dam structure to downstream the dam (Zhou et al., 2019). On one side, the solution eliminates the need to modify the original structure and is found to be the easiest low head turbine to retrofit (Loots et al., 2015). On the

other side, the siphon turbine pose a higher risk of fish injuries (Martinez et al., 2019) and is only suited for low heads as the generation efficiency decreases with increasing head.

A matrix of pre-assembled turbines is an alternative solution for retrofitting of dams with low head. Several turbine manufacturers deliver Kaplan turbines put together in a matrix that faces the water flow (Hydropower Equipment Association, 2015). This solution is easy and quick to install, and require minimal maintenance (Corà, 2020). The multiple turbines allow for the optimization of generation efficiency, as one or several turbines can be switched of when the total outflow of the dam is too small to serve all the turbines. Manufacturers, such as Andritz, have installed this type of solution proving it to be cost competitive.

2.2.2 Practical considerations

The presence of water in an area is not alone sufficient to generate hydropower. The water must be available when there is an energy demand and in volumes that exceeds the minimum flow required for the turbine to run. In drier regions, the available water is limited and not always enough to meet all the water demands. It is therefore important that the generation of hydropower does not further stress the water scarcity. A safe way to avoid negative impacts of retrofitting is then to only produce hydropower of the water releases serving the existing demands. That way, the hydropower generation will not impact the reservoir volume and surface area of the reservoir and does therefore not increase the evaporated volume from the reservoir. As no water then is lost due to the hydropower generation, the water consumption of the retrofitted hydropower can be considered negligible (Bakken et al., 2016).

Dam safety can be considered one of the most important concerns for retrofitting hydropower to existing dam structures. The risks posed by structural modifications of the original dam body has been addressed in a life cycle assessment, highlighting the importance of safety and risk considerations in retrofitting projects (Yugunda et al., 2020). Whereas modifications on the dam structure can increase the risk of dam collapse, retrofitting can also increase the safety level by causing a higher focus on maintenance (Al-Shnynat, 2018).

Environmental impacts due to retrofitting are assumed to be negligible if the water regulation is kept unchanged compared to the initial dam regulation. The construction phase represent the biggest environmental risk during the lifetime of retrofitting projects, but the fauna and flora are considered to be little affected when excluding the construction period (Yugunda et al., 2020). The impacts during the construction period depend on the technical solution chosen for the retrofit and must be considered during the design phase.

The timing of the hydropower generation must also be assessed with regard to the existing electricity grid. On one hand, retrofitting projects have been found to possibly increase the grid flexibility in remote areas (Patsialis et al., 2016). This is because hydropower enables the supply of base load and peak load with a quicker response time than most alternative energy sources (IRENA, 2012). When the electricity demand pattern and water demand pattern follow the same trend, as for water treatment plants, the temporal delay is minimal, and the grid can function well (Kucukali, 2010). On the other hand, differences in temporal demand pattern may cause sudden load rejections and a significant variation in generation efficiency (Loots et al., 2014)

2.3 Description of the case study of Guadalquivir

2.3.1 Geography and history

Guadalquivir is one of the largest river basins in Spain, situated in the most south west part of the country. With a catchment area of 57 527 km^2, it spans across the Andalucía region and

covers parts of 12 of Spain's provinces. The four provinces contributing the most to the catchment are Seville, Córdoba, Jaén and Granada. Mulhacén is the highest point in the catchment with its peak reaching 3479 m.a.s.l. The Guadalquivir river is the main river in the basin, and the fifth longest river in Spain with a length of 657 km. In 2015, the basin had 4 107 598 inhabitants (Berbel et al., 2015).

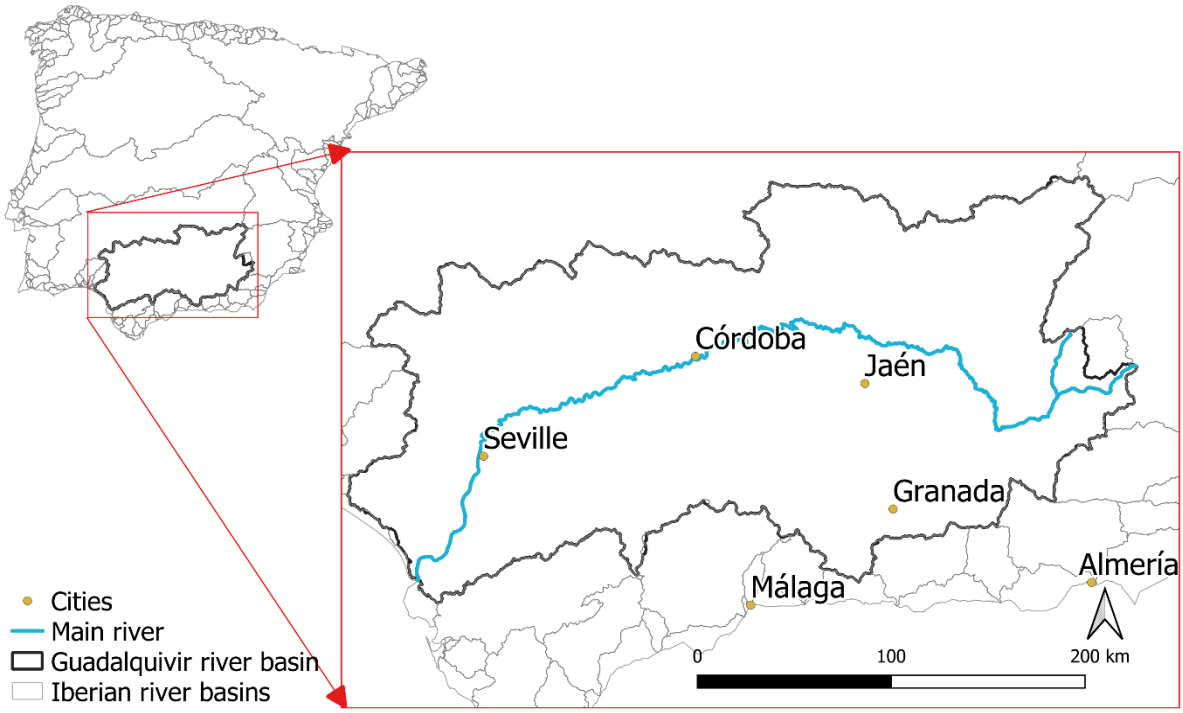

Figure 1: Guadalquivir river basin.

The history of official water management in Guadalquivir started in 1927, when the Hydrographic Confederation of Guadalquivir (CHG) was constituted. Guaranteeing sufficient quantity and quality of water to the region was, and still is, the main objective of the Confederation. This is done by the drafting, monitoring and reviewing of river basin management plans, administration of the public hydraulic structures, and own projects. The Confederation holds a register of all authorized water withdrawals, and sites for water withdrawals over 10 m^3/day or serving more than 50 people are given the status of protected catchments for water supply (CHG, 2011).

2.3.2 Climate and water demands

The climate in Guadalquivir is diverse, much due to its diverse topography. In 2018, the range of monthly average temperature across the river basin spanned from 3.69°c to 10.85°c in February and from 24.85°c to 28.59°c in August (Harris and Jones, 2020). Monthly precipitation varied from 0 mm to 1.88 mm in July and from 127.79 mm to 218.06 mm in March the same year. Torrential rain, and periods of high temperature and drought are weather phenomena common to the region.

The hydrological years can be classified by the means of their deviation from the long-term average yearly precipitation. Normal years in basins of this size can be defined as the hydrological years with precipitation within a 15% difference from the reference precipitation, i.e. being from 85% to 115% of the reference value. The official average yearly precipitation in the period 1980-2011 was of 546 mm (Ministerio para la Transición Ecológica, 2018), and the corresponding classification of the hydrological years used in the simulation are presented in

Table 1. The overall average precipitation in the simulation period is 602 mm, and thus classified as a normal period with regard to this criterion.

Table 1: Average precipitation per hydrological year (CHG, 2019b), and corresponding classification of the hydrological years.

Hydrological year	Precipitation [mm]	Percent of average [%]	Classification
2009/2010	948	174	Wet
2010/2011	781	143	Wet
2011/2012	316	58	Dry
2012/2013	852	156	Wet
2013/2014	470	86	Normal
2014/2015	411	75	Dry
2015/2016	514	94	Normal
2016/2017	480	88	Normal
2017/2018	648	119	Wet

Internal water demands in the Guadalquivir basin consists mainly of irrigation, domestic use, industry and services. In 2007, an estimated 7 000 km^2 of the land was irrigated, consuming roughly 80% of the available water in the basin (CHG, 2011).

In addition to internal water demands, the basin also imports and exports water from and to other neighbor basins. The biggest export is the Negratín-Almanzora transfer, with a capacity of 50 hm^3/year and an average of 37.70 million m^3/year exported from the Negratín reservoir in Guadalquivir to Almanzora in the basin of Almería. The reservoirs Fresneda, Sierra Boyera, Montoro and Aracena are exporting an estimated 24.8 hm^3/year from the Guadalquivir basin in total (Ministerio para la Transición Ecológica, 2018). The main importations of 4.99 hm^3/year are done to the county of Huelva and Doñana, resulting in a net water export out of the Guadalquivir basin of approximately 57.51 hm^3/year. An overview over the water imports and exports are presented in Table 2.

Table 2: Overview of annually transferred water included in the model. Negative numbers represent exports and positive numbers represent imports to the Guadalquivir basin (Ministerio para la Transición Ecológica, 2018).

Reservoir/area	Transfer [hm³/year]
Negratín	-37.70
Fresneda	-3.68
Montoro	-7.04
Sierra Boyera	-7.09
Aracena	-6.99
County of Huelva and Doñana	+4.99

2.3.3 Dams and reservoirs

There are 65 official dams in the Guadalquivir basin with a total reservoir capacity estimated to 8 500 million m³ (CHG). 13 out of the 65 official dams are confirmed to be non-powered dams, excluding additional support dams for reservoirs with several dams. The 13 considered NPDs all have gross heads over 29 meters and reservoir capacities over 13 hm³. An overview over the characteristics of the individual NPDs as included in WEAP are presented in Figure 2.Two of these dams are situated downstream of other dams, and their drainage areas are therefore divided into regulated drainage areas and unregulated drainage areas.

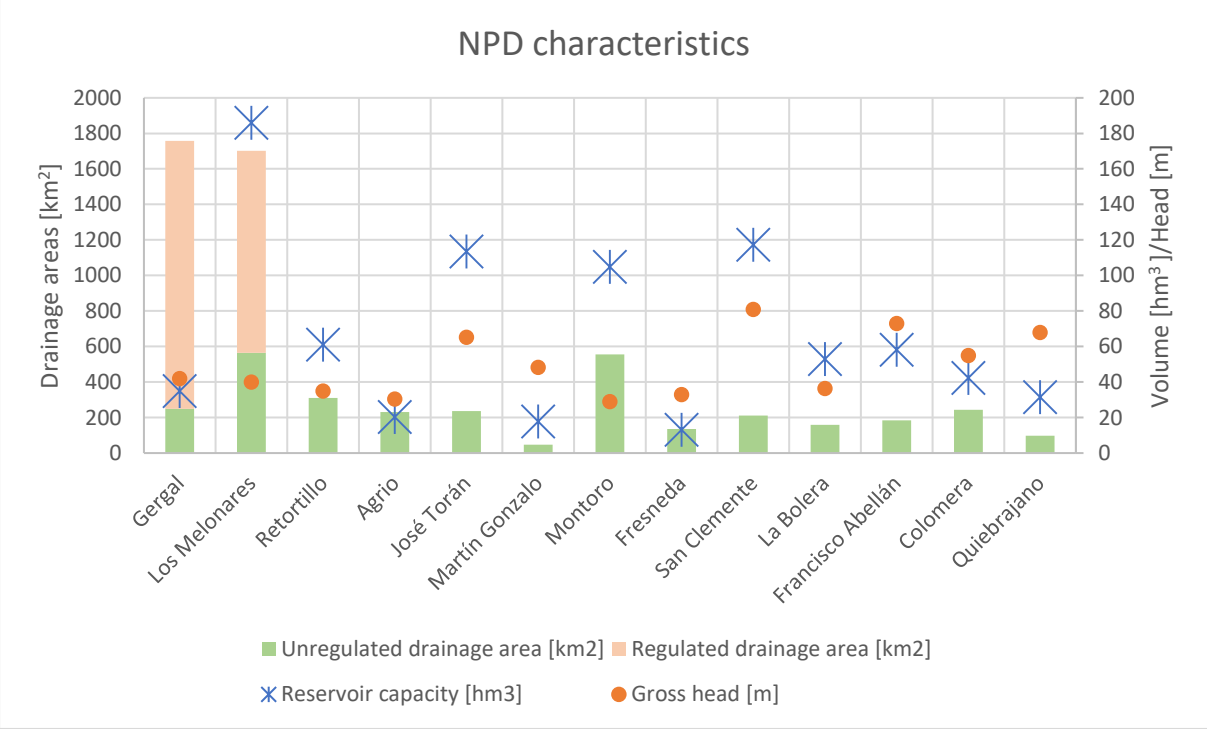

Figure 2: Gross head, reservoir capacity, unregulated drainage area, and regulated drainage area for the included NPDs.

2.4 WEAP

WEAP is a water resources modelling software which was developed in 1988 by Jack Sieber of the Stockholm Environmental Institute (SEI) and has since then been used in several studies worldwide (Stockholm Environment Institute, 2020). In this study, the version 2019.0 published in 2019 is used. The models created by WEAP can consist of one or more river basins, and can include reservoirs, hydropower plants, water demand sites, and transmission links. In order to analyze the effects of possible modifications in the basin, different scenarios can be set up.

2.4.1 Water balance

WEAP allows for simulation of the water balance in the catchment by five different methods of which the Soil Moisture Method is chosen for this study. The method includes algorithms used for the runoff, evaporation and evapotranspiration calculations. The choice of using the Soil Moisture Method is because it allows for more detailed infiltration calculations, in addition to accounting for initial soil moisture content when calculating the runoff from timestep to timestep. The hydrological model in the software is used as a semi-distributed model, meaning that input data are distributed between the different catchments but averaged within the individual catchments. The climate data strictly required by WEAP in order to perform the Soil Moisture Method is time series of temperature and precipitation. In addition, values for cloudiness, wind speed, albedo, freezing point, melting point and initial snow volume can be specified, but are otherwise given default values.

Evapotranspiration (ET) is the term for the processes of water evaporating from the ground and from the plant surface in addition to the transpiration from the plant itself. The processes transform water from liquid form to vapor and thus transfer the water from the soil to the atmosphere. Factors influencing the ET are the solar radiation, shadow conditions, air temperature, wind conditions, moisture availability in the soil, and air humidity (Allen et al., 1998). Soil salinity, soil type, soil management and other factors may also influence the evapotranspiration. The potential ET, PET, expresses the theoretical ET capacity of a standardized crop. In order to adjust this value to fit different vegetation types in the model, a crop coefficient, Kc, is used to calculate the actual ET by the following equation:

$$ET_{actual} = PET \cdot Kc. \tag{6}$$

In WEAP, ET calculations are based on climate data covering temperature, precipitation, wind speed and humidity, and the chosen crop coefficients. The PET is calculated using a modified version of the Penman-Monteith equation for a standard crop (Sieber and Purkey, 2015). The first modification implies that the albedo varies from 0.15 to 0.25 depending on the snow cover, whereas the second modification is the exclusion of the soil heat flux term. Crop coefficients different from the default value of 1 can be implemented manually in the WEAP model. One way of selecting crop coefficients is by analyzing the land cover of the catchments and assign suitable values. Values for crop coefficients are commonly based on the FAO report 56 (Allen et al., 1998). The detection of land cover groups in the basin can be done by using the integrated automatic catchment delineation mode creating land cover bands or by conducting separate GIS analyses. Suitable crop coefficients can then be assigned to the different detected bands or groups.

Irrigation water needs can be implemented manually in the model. Instead of the integrated methods, the water demand for artificial irrigation is then included as water withdrawals from the catchment. The withdrawals' annual activity level must be specified, and a monthly variation can be attributed. Nodes for transmission and return of unconsumed water must be placed along the river, and a corresponding consumption rate for the calculation of return flow must be defined.

The Soil Moisture Method separates the soil into two layers and is therefore called a two-bucket model, as illustrated in Figure 3. The upper bucket represents the soil layer that contributes directly to surface runoff, percolation, and interflow. Evapotranspiration is also calculated based on the water content in the upper bucket. The parameters influencing the runoff, interflow and evapotranspiration are the soil water capacity (*SW),* the runoff-resistance factor (*RRF),* the root zone conductivity (*RZC),* and the preferred flow direction (*PFD)*, whereas the soil moisture in the upper bucket (*z1)* and the input from precipitation and snowmelt are the influencing variables.

The lower bucket represents the soil layer that transports the base flow and receives the percolated water from the upper bucket. The parameters influencing the base flow are the deep-water conductivity (*DWC)* and the deep-water capacity (*DW)*, whereas the soil moisture in the lower bucket (*z2)* and the percolation are the influencing variables. Nodes for where the baseflow recharges the groundwater can be manually added to different reaches but are not included in this study. This is because the interaction between surface water and groundwater is simplified to be included in the soil moisture processes.

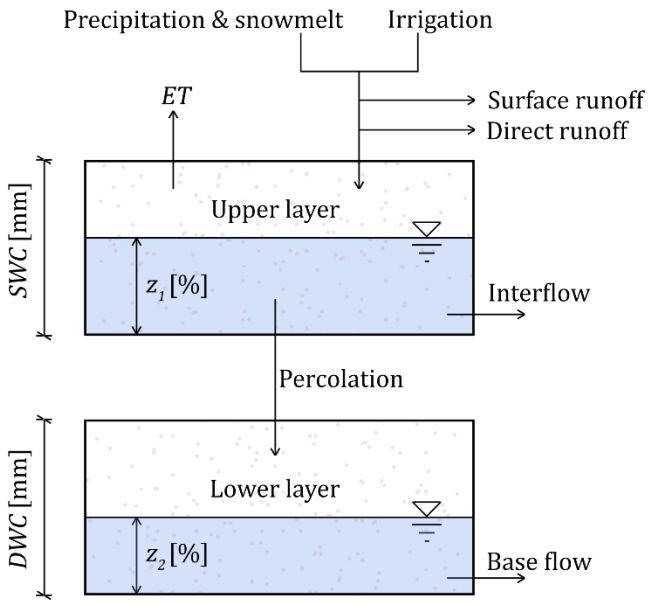

Figure 3: Illustration of the variables and parameters in the Soil Moisture Method. Adapted from (Sieber and Purkey, 2015).

Net evaporation from the reservoirs, also called open water evaporation, is by default neglected in WEAP, whereas specified values can be inserted as input. The net evaporation equals the difference between the evaporation and the precipitation. A positive net evaporation represents a decrease in the reservoir filling and negative net evaporation represent an increase in reservoir filling. As the open water evaporation potential can be difficult to estimate accurately, it can be approximated with the evapotranspiration potential (ET0).

2.4.2 Catchments and reservoirs

WEAP models consist of one or more basins often divided into sub-basins referred to as catchments. An automatic catchment delineation function can be used to generate the basins and can further be used to create catchments within the basins. The function is based on digital elevation models from HydroSHEDS and outlines the catchment area of a chosen point on the world map. The main river in the catchment is included in the generating process and is defined as the river which conveys the largest water volume in the catchment. More rivers flowing into the main river can be added manually. In addition to drawing the main river, the automatic catchment delineation also allows for setting up climate data, elevation and land cover zones using integrated historical data from Princeton, HydroSHEDS and ESA-CCI-LC respectively.

Modelling of the reservoirs in the WEAP models require data on their physical characteristics. The main input is the reservoir capacity and the initial storage volume. To model the reservoirs' response to inflow and releases, it is important to include a volume-elevation curve and

maximum hydraulic flow out of the reservoir. In addition, data for the division of the reservoir into zones with different regulation strategies can be added for more detailed simulations of reservoir regulations.

The water availability in the reservoir is based on a zone system for different purposes and strategies, illustrated in Figure 4. This implies that the volumes of water releases from the reservoir, independent of demand type and priority, depend on the water level at the given timestep. The volume below the outlet level is the *Inactive Zone,* from which no extraction is possible except from evaporation. For the *Buffer Zone,* only a fraction of the volume is accounted as available in order to slow down the emptying of the reservoir and avoid water shortages. Withdrawals from the *Conservation Zone* are fully dependent on the demand downstream and the whole volume can be used to meet the demand without any restrictions. When the water level rises above the *Conservation Zone,* water will be released independent of demand in order to clear the *Flood Control Zone* for possible floods. If the volumes of the different zones are not specified, the whole reservoir volume will be considered as one big *Conservation Zone*.

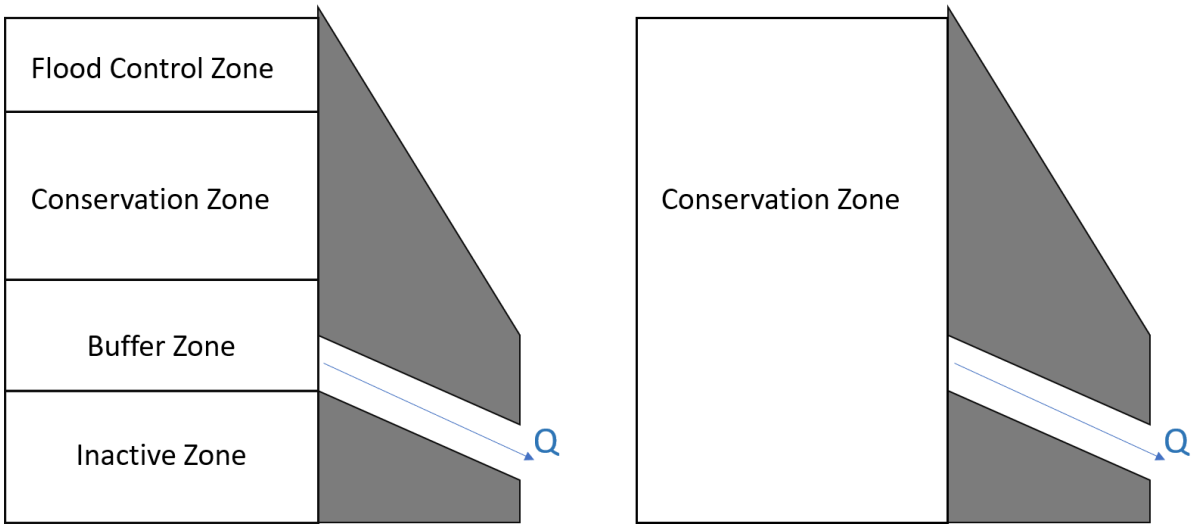

Figure 4: Illustration of the reservoir zone definitions in WEAP. Possible reservoir zones (left) and reservoir zones if unspecified (right). The Q *represents the outflow of the dam. Adapted from (Sieber and Purkey, 2015).*

2.4.3 Hydropower generation

The calculations of the hydropower generation in WEAP are based on the availability of water in the reservoir or in a river in the case of a run of river plant. The different water demands from the reservoir, such as individual water withdrawals, hydropower demand, refilling of the reservoir and environmental flow requirements are assigned specific priorities. In case insufficient water volumes to supply all the demands, the demands with the lowest priorities will be sacrificed and experience unmet demands.

With the calculated water available for hydropower generation, WEAP calculates an energy output. The output is based on the volume that passes through the turbine during the timestep and the *HydroGenerationFactor, HGF.* This factor comprises the density of water, the available head, the plant factor, the plant efficiency and the gravitational force. The available head is estimated as the initial water level at the beginning of the timestep minus the water level of the tailwater. Head losses and other energy losses are accounted for in the *Generating Efficiency* factor, η [%]. Seasonal regulation of the hydropower production is feasible in the WEAP model by adjusting the plant factor. Put together, this results in the following equations:

$$HGF\left[\frac{GJ}{m^3}\right] = \frac{\rho \cdot H \cdot PF \cdot \eta \cdot g}{1\,000\,000\,000} \tag{7}$$

$$\downarrow$$

$$Energy\ generated\ [GJ] = HGF \cdot V \tag{8}$$

where ρ is the density of water [1000 kg/m^3], H the available head [m], PF the plant factor and g the gravitational force [9.806 m^2/s], and V the water volume through the turbine during the timestep [m^3/timestep].

2.5 Economic analysis

2.5.1 Cost of retrofitting and hydropower revenues

In hydropower projects, the costs can be divided into two main groups: investments costs and maintenance and operation (O&M) costs. In retrofitting projects, the costs of constructing the dam as well as possible access roads are already constructed and can therefore be excluded from the investment costs. If the existing water intakes are to be used as the intakes for the turbine, the construction costs of these can also be excluded. Left, are the costs of the mechanic and electric equipment, the costs of transmission and the costs of engineering and project management. The O&M costs are commonly estimated to a specific percentage of the total investment costs (IRENA, 2012).

Revenues from electricity sales are the main economic benefit in the projects and depend on the varying electricity prices. In an economic analysis, the price of electricity considered has to correspond to the costs that are included. If transmission lines are included in the cost calculations, the transmission price must also be included in the electricity price for the calculation of revenues.

2.5.2 NPV and LCOE

The net present value (NPV) of a project is a common measure for the evaluation of the economic viability accounting for the value of time. The NPV represents the value of the project related to a specified year, considering the costs and benefits over its whole lifetime. The costs and benefits included in the NPV are discounted to the specified year using a discount rate. The Weighted Average Cost of Capital (WACC) is used as the discounting rate in cases where the financing of the project is based on both loans and own capital investment. The formula for NPV can be written as:

$$NPV = \sum_{t=0}^{n} \frac{(Cost - revenue)_t}{(1+r)^t}, \tag{9}$$

where r is the discounting rate, t is the year number, and n is the total number of years accounted for in the lifetime.

For a project to be considered economical viable, the NPV must be positive. The positive values of NPV represent how big the estimated profit of the project will be, or alternatively by how much the costs can increase before the project will be non-profitable. When evaluating different alternative projects, the highest NPV is the preferable one. In cases where the NPVs are equal, it is preferable to choose the project with the lowest total costs as this includes the less risks.

Levelized cost of electricity (LCOE) is a measure that can be used for the comparisons of different development projects as it represents the net present cost of commissioning per energy output delivered. In other words, it represents the necessary price of electricity for the

project to be profitable when also accounting for the return on investments of a rate equal to the chosen discount rate. This means that projects with higher LCOE than the projected future electricity price are foreseen to be unprofitable.

The costs of commissioning are calculated by discounting the total costs over the lifetime of the project and dividing by the discounted delivered amount of electricity. Since no revenues are included in the calculations, different alternatives can be compared without assuming future electricity prices. The LCOE can be calculated using the following equation:

$$LCOE\left[\frac{Euros}{kWh}\right] = \frac{\sum_{t=1}^{n} \frac{I_t + M_t + F_t}{(1+r)^t}}{\sum_{t=1}^{n} \frac{E_t}{(1+r)^t}}, \quad (10)$$

where r is the discount rate, n the number of years considered the lifetime, I the investment costs, M the operation and maintenance costs, F the fuel costs, and E [kWh] the electricity generation, all at timestep t (IRENA, 2012). The costs are expressed in Euros.

3 Materials and Methods

This section serves to present the methods used in this study, starting with the main assumptions made for the estimation of the retrofitting potential. Furthermore, the setup of the WEAP model is explained, including what input data is used and how the calibration is performed. The assumptions and sources for the economic analysis are then presented, followed by a description of the upscaling method and what variables it includes.

3.1 Method for estimation of retrofitting potential

3.1.1 Main assumptions

The retrofitting potential is in this study limited to the potential which can be generated with a minimum of negative impacts on the existing water uses and the surrounding environment. First of all, this implies that the water used for hydropower generation cannot reduce the reliability of water supply for the existing water uses. Second of all, the environmental flow requirements, including minimal and maximal limits, are considered equally important as the supply of the existing water uses. Third of all, no construction of pipelines or tunnels in order to increase the available head are considered, as this may cause harmful interventions to the environment.

In order to assess the potential respecting the main assumptions, it is considered necessary to do a simulation of the water balance of an entire river basin. This also allows for the evaluation of different scenarios, including the implementation of different turbine capacities and modifications on the water demands. Different turbine capacities are used to estimate maximum potentials versus more realistic potentials, whereas the scenarios with modified water demands are meant to investigate the possible effects that such alterations may have on the retrofitting potential.

3.1.2 Choice of case study

The choice of drainage basin for use in the case study is based on three criteria. First, the basin must contain several NPDs. Second, there must be easily available data considering streamflow and technical description of the reservoirs. Third, the water availability in the basin must be limited to the extent that there is a risk of unmet demands. This third criterion is set in order to address the conservative cases where retrofitted turbines only can use the existing water flow to not impact the existing water uses.

In Spain, there are 705 NPDs listed in the ICOLD World Register of Dams (ICOLD, 2019), and 127 in the GRanD database version 1_3 (Lehner et al., 2011). 23 of the NPDs in the GRanD database are situated within the Guadalquivir basin, and the basin is thus the river basin in Spain containing the most NPDs according to the GRanD database. Guadalquivir and Spain in general are currently experiencing both droughts and floods, and irrigation water has to be restricted in some periods due to total water demand exceeding the total water availability (Berbel et al., 2015). The local water authorities, Confederación Hidrográfica del Guadalquivir (CHG), provides streamflow data at several points in the basin and downstream the dams, in addition to technical data about reservoirs and weather observations. The Guadalquivir river basin in Southern Spain is therefore considered a suited drainage basin for the case study. The number of NPDs is however reduced to 13 when cross checked with the local water management authorities CHG and data from the Ministry of the Ecological Transition and the Demographic Change (MITECO) provided by the reference medium iAgua (MITECO, 2020).

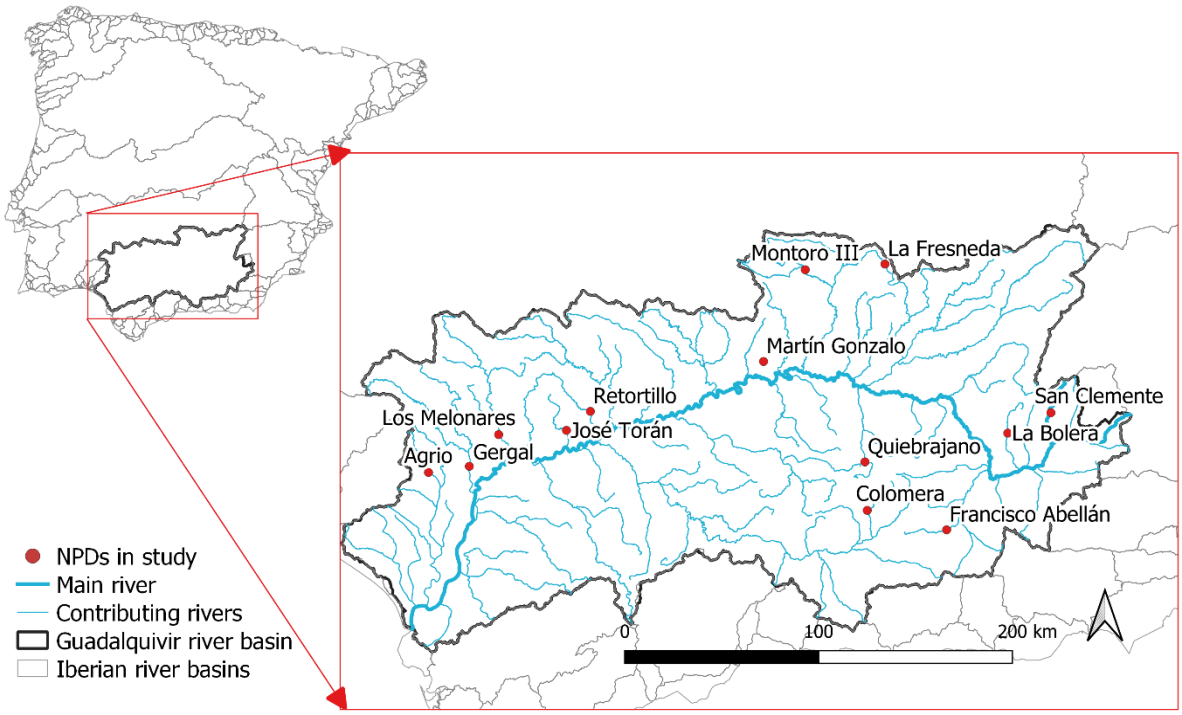

Figure 5: Overview over the Guadalquivir river basin and the studied NPDs.

3.1.3 Tools

The software WEAP (Water Evaluation And Planning system) is found suitable for this study. First of all, it provides a platform for the modelling of basins including reservoirs and hydropower generating units. Second of all, different methods for the implementation of water withdrawals and irrigation water are integrated in the software or made possible to enter manually. Last, the integrated scenario builder and various way of presenting results are considered useful tools for analysis of different factors and for the communication of the results.

QGIS (QGIS Development Team, 2020) is used for the analysis, processing and presentation of georeferenced data. The datasets used in this study are:

- Corine Land Cover (European Environment Agency, 2019)
- Rivers and catchments generated in WEAP (Sieber, 2019)
- Global Reference Evapo-Transpiration dataset (Global-ET0) (Trabucco and Zomer, 2019)
- Authorized withdrawal points (CHG, 2019a)
- Coordinates for the dams and the measuring stations (precipitation, temperature, discharge) (SAIH, 2020b)

3.2 WEAP setup

The hydrological years in the model setup are defined from October to September. The year 2008/2009 starts therefore in October 2008 and ends in September 2009. This follows the definition of hydrological years commonly used on the northern hemisphere, including Spain. At the beginning of the hydrological year, the reservoirs are usually on their lowest levels during the year and the refilling is to start (AleaSoft Energy Forecasting, 2019). The simulation period is chosen to start the 1st of October 2009. The climate data from CRU used in this study ends in 2018 and marks therefore the end of the simulation period. Appendix I provides screen dumps of the WEAP interface with simple explanations of how the model is set up.

3.2.1 Climate data

For wind speed and relative humidity, data from the AQUASTAT Climate Information Tool is used (FAO, 2016). These data are georeferenced monthly averages from the time period 1961-1990 with a spatial resolution of 10 minutes. In order to obtain a representative average for the whole basin, the values for 20 random points inside the basin generated by QGIS are averaged and used for the whole basin. The random points are presented in Figure 6 and the resulting monthly data for wind speed and relative humidity are presented in Table 3.

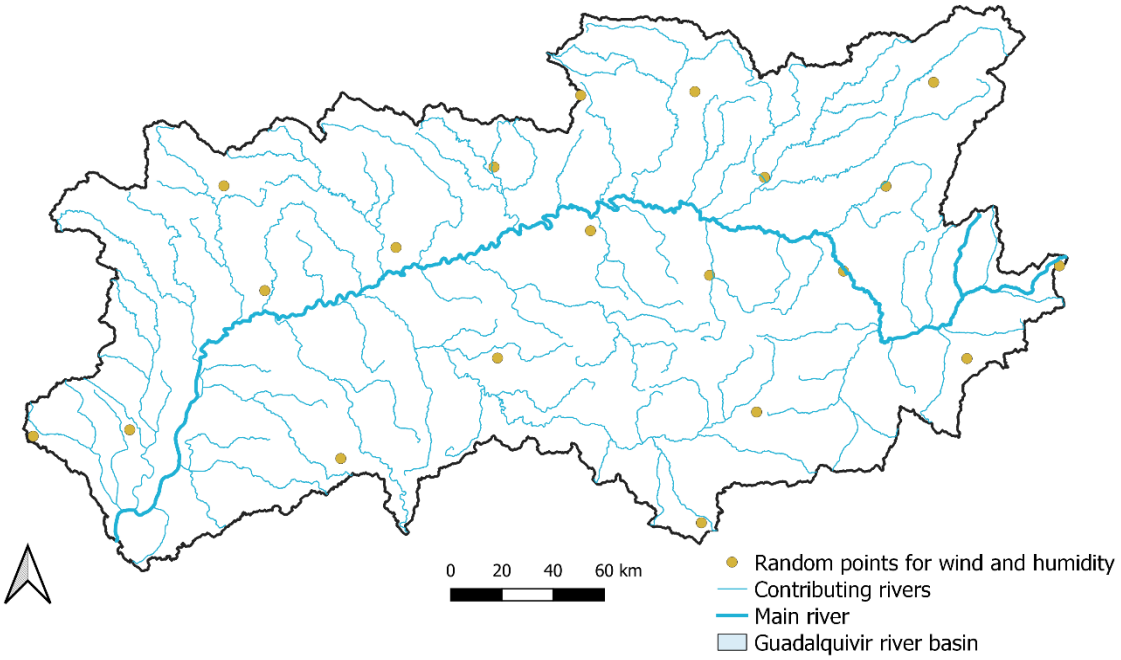

Figure 6: Placement of the 20 random points for extraction of historical wind speed and humidity. The points are generated in QGIS for averaging the wind speed and humidity data from the AQUASTAT Climate Information Tool.

Table 3: Monthly average values for wind speed (2m) and relative humidity.

Month	Wind speed [m/s]	Relative humidity [%]
January	2.9	77.3
February	3.1	73.2
March	3.2	66.6
April	3.0	64.8
May	3.0	59.4
June	2.9	54.5
July	2.9	47.4
August	2.8	49.3
September	2.6	56.7
October	2.7	67.2
November	2.8	75.2
December	3.0	78.0

For the main model, climate data over a longer period is given higher priority than high temporal resolution. Monthly data is considered suitable, as it takes seasonal variation into account without being too data demanding and cause a too accurate presentation compared to the other input data given at an annual resolution. The Climate Research Unit (CRU) provides the database TS4.03 including climate data from 1901 to 2018 with a spatial resolution of 0.5 x 0.5 degrees (56 km x 56 km) (Harris and Jones, 2020). Of the available parameters included in the dataset, temperature, precipitation and cloud cover are used in this study.

The data from CRU is available as NetCDF files containing only one parameter in each file, whereas the WEAP catchment delineation mode only allows for the use of one file for the distribution of climate data over the basin. The catchment delineation mode generates csv files of the NetCDF file corresponding to each of the individual catchments. To read both temperature, precipitation and cloud cover data into WEAP, csv files containing the three parameters are therefore manually merged. A copy of the csv files generated for one parameter is made and stored outside the WEAP model, before this is repeated for the different parameters. The csv files are then merged manually, giving one csv file for each of the catchments containing all three parameters which are uploaded as manual input data.

Gridded precipitation has been found to underestimate high values of precipitation and overestimate low values for precipitation (Yeggina et al., 2020). Observed precipitation at the NPDs are therefore compared to the gridded precipitation of their corresponding catchments. The average difference in precipitation is taken into account by adjusting the gridded precipitation by a global factor. In this case, the comparison shows that the gridded data from CRU gives 18% less water volume during the simulation period considering the whole Guadalquivir basin. The precipitation is therefore increased by 18% compared to the raw data by implementing a correction factor in the input code in WEAP.

Net evaporation is found for each of the reservoirs and included in the model. Historical, georeferenced data for the evapotranspiration potential for the reference crop, ET_0, is in this study chosen as the input for evaporation potential from open water bodies. The Global Reference Evapo-Transpiration dataset (Global-ET0) is used to find the historical average values for each of the reservoirs in the Guadalquivir basin. This is done by extracting the ET_0 values in the dataset for each of the reservoir coordinates in QGIS. The values for ET_0 in the dataset are based on the Penman-Monteith method from the FAO report number 56, using data from WorldClim2 Global Climate Data. In order to estimate the net evaporation, the precipitation data

from CRU for the corresponding catchment is subtracted from the obtained ET_0 values for the individual reservoirs.

3.2.2 Catchments and reservoirs in current state

The WEAP function for automatic catchment delineation is used to create the framework of the Guadalquivir basin and its sub catchments. The basin is first divided into four large catchments named *One* to *Four*, starting at the most downstream part. For each of the 13 NPDs, a sub-catchment is generated from the point where the water course from the NPD meets the main river in the Guadalquivir basin. All the main rivers in the basin are created by the automatic catchment delineation mode and named after the NPD(s) in the catchment rather than the historical names of the rivers. The area between the dam and the main river is included in the catchments in order to analyze the reservoirs' impact on the existing water demands downstream of the dams. The areas not included in the catchments of the NPDs remain in the larger four catchments. Since two of the NPDs are situated in the same smaller catchment, this results in a total of 16 catchments. An overview of how the model is set up is presented in Figure 7.

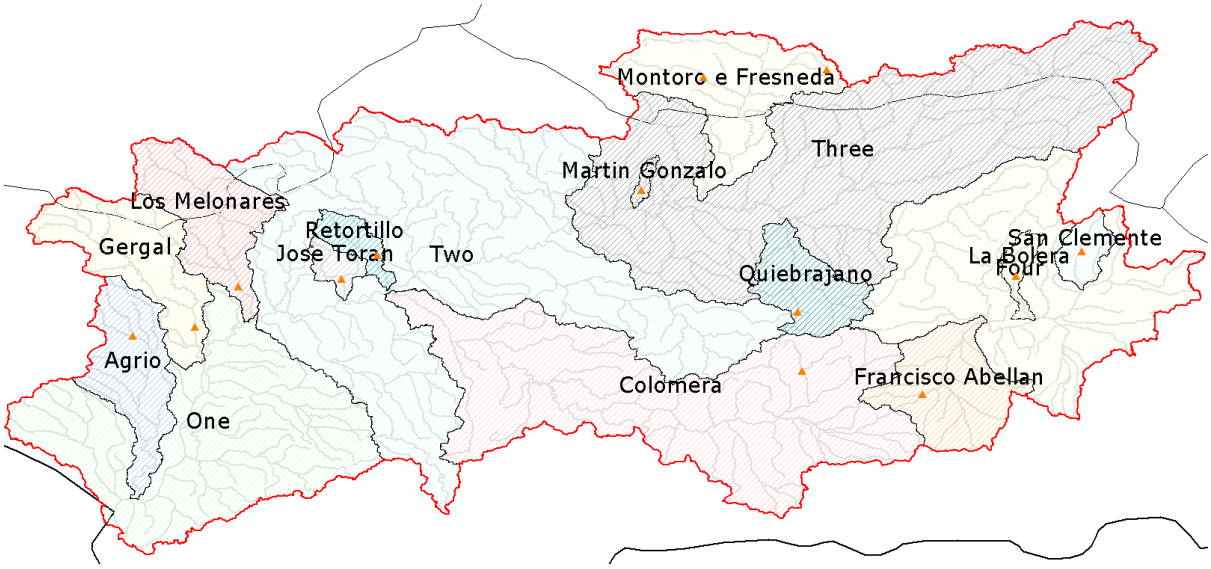

Figure 7: Overview of the division of the Guadalquivir basin into 16 catchments. The orange triangles represent the NPDs included in the model. San Clemente and La Bolera correspond to the two smaller catchments, whereas Four is the bigger, surrounding catchment. The screen dump is taken from WEAP.

WEAP does not calculate runoff distribution within a catchment, but only introduces runoff input to the model where there are placed runoff/infiltration nodes. These nodes are automatically placed at the downstream end of the catchment, resulting in inflow to the downstream catchment. Inflow to the reservoirs within catchments is therefore accounted for in this study by inserting additional runoff/infiltration nodes from the catchment to each of the reservoirs. The share of runoff that drains into the reservoir versus the downstream part of the catchment is calculated using the catchment delineation mode and specified for each of the nodes. As the drainage area found using the catchment delineation mode is sensitive to which point one select on the map, the areas are checked against official data. The drainage areas calculated by WEAP that have a difference larger than 5% are modified to equal the official drainage area.

56 of the 65 official dams in the basin are dams registered in the list of control points from the automatic hydrological information system, SAIH. 54 out of these are chosen to be included in the model of the entire Guadalquivir basin, including the 13 NPDs presented in Figure 2. An

overview of all the included dams and their corresponding reservoirs' storage capacities is included in Appendix B. Power generation for the 8 dams that are currently powered and have official values for intake capacity for the hydropower generation are included in the model for comparison of simulated capacity and official capacity. Data series of observed reservoir fillings for all the reservoirs and observed streamflow at the measuring stations Alcála del Río and Peñaflor (SAIH, 2020a) are implemented in the model in order to evaluate the model simulations.

The physical characteristics of the dams and reservoirs in the Guadalquivir basin are taken from PDFs with official data for each of the dams from CHG (CHG) and completed with data from MITECO (MITECO, 2020). Only one of the four possible reservoir zones for regulation simulation in WEAP is used. This means that the whole reservoir volume is considered as a conservation zone as illustrated in Figure 4, resulting in the whole volume being available for releases. The official values for normal maximal regulated water levels are set to correspond to the maximum storage capacities, and the official elevations of the bottom outlets are set as the lowest level of the reservoir. Two additional sets of volume-elevation values are extracted from historical timeseries of storage volume and water elevation, being the minimum and maximum observed values for the time period 2015-2019. This results in a volume-elevation curve with linear relations between the four inserted sets of values. The volume elevations curves for the included NPDs are included in Appendix H.

Seasonal dependent environmental flow requirements are found in official documents from the Spanish Department of Ecological Transition for 51 of the 54 dams in the model (Agencia Estatal Boletin Oficial del Estado, 2016). These requirements represent the minimal required flow downstream the dams and span from 0.008 m^3/s downstream Fresneda to 0.83 m^3/s downstream Iznajar. The requirements are included in the WEAP model as flow requirement nodes placed directly downstream of the dams. All the environmental flow requirements are presented in Appendix C.

For 14 of the dams, maximum outflows dependent on season also apply. Maximum required flows are like the minimal requirements based on environmental considerations and may limit the hydropower production for plants with higher outlet capacities. These are included in the model as a limit to the maximum hydraulic outflow capacity of the dam if the water level is below the spillway level. This also applies to the turbine capacity when applicable. Additional spawning restrictions are set to the 1st of April in the model, causing a linear decrease from the flow allowance in March and a linear increase to the flow allowance in May downstream the concerned dams. The maximum flow allowances are presented in Figure 8.

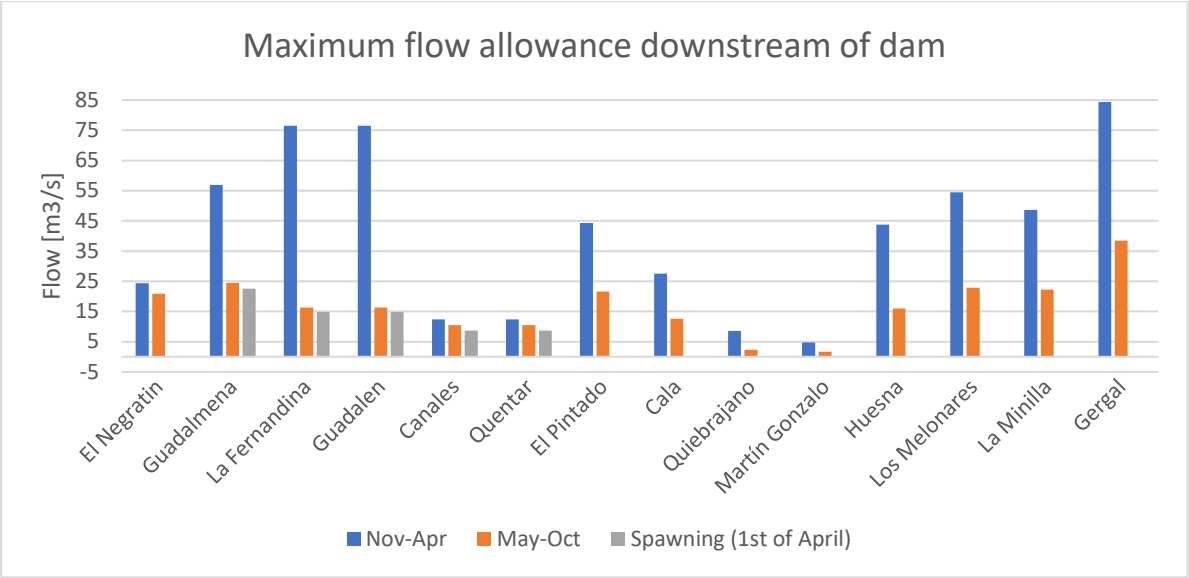

Figure 8: Time dependent maximum flow allowances downstream of dam. Values represent the maximum allowed releases from the dams due to environmental considerations.

For the NPDs, the values for the outlet capacities for water levels below the spillway level are based on maximum daily observed streamflow below the dam. In order to find the capacity excluding the spillway, data of observed daily maximum water levels are used to find the hydraulic capacity for the periods when the water level is below the spillway level. In the cases where the capacity is found to be very high with no similar values the day before and after, the value is excluded and a new capacity set. The NPDs Gergal, Los Melonares and Quiebrajano are found to have higher observed outflows than the maximum allowance for streamflow, and the capacity is therefore set to match the maximum allowance. For the remaining dams, the method is simplified, and the official capacity of the bottom outlets and the other intakes are summarized to define the total hydraulic capacity.

The spillway capacity is simplified to be constantly equal to the maximum hydraulic capacity when the water level reaches above the spillway level, thus not increasing with increasing water level. This is assumed to overestimate the spillway capacity as the maximum capacity is not likely to be reached until the water level reaches the design maximum level. The activation of the spillway capacity is dependent of the water level in the last timestep of the simulation, and is implemented as an if-statement. The values for the spillway capacity are found in the official PDFs with technical data regarding the dams. These values are found to be higher than the maximum observed outflows for several of the dams during the simulation period. Therefore, the official values for maximum spillway capacity are assumed to include the other outlets for the implementation in this model. For Agrio, the spillway capacity is chosen equal to the capacity of an outlet tunnel with higher capacity than the spillway, as the observed capacity is higher than them both. The hydraulic capacities for the NPDs as implemented in WEAP are presented in Figure 9, where minimum and maximum capacities correspond to the seasonal environmental requirements.

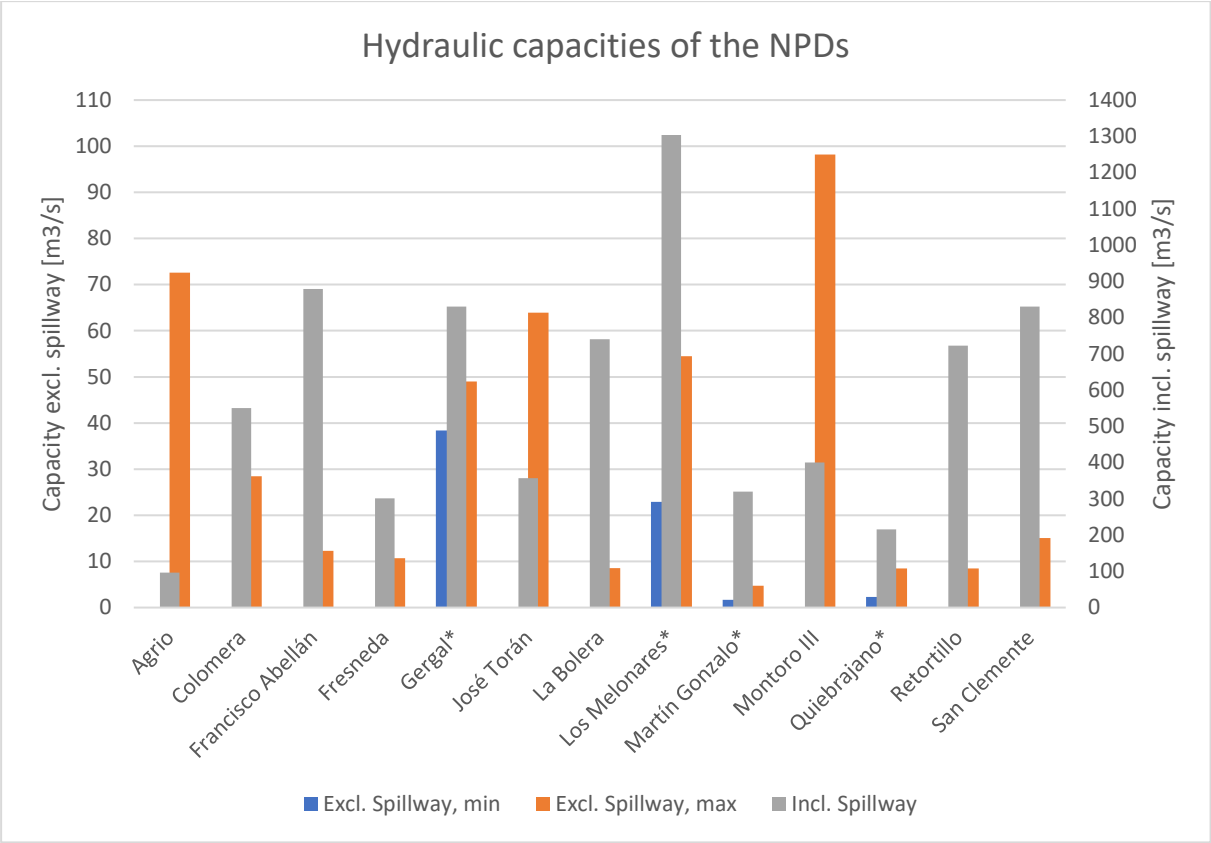

*Figure 9: Hydraulic capacities for the NPDs. The dams marked with * have season dependent maximum flow allowances. The two different allowed capacities are presented as max and min capacity. The capacity including the spillway applies for water levels above the spillway level.*

3.2.3 Water demands

Data from CHG are used to estimate the water withdrawals from the catchments for the main purpose of domestic use and irrigation. The dataset "Captaciones autorizadas" includes the authorized annual withdrawal volumes as well as their status, and to a limited extent their uses (CHG, 2019a). All data described with the words "paralizada" (*paralyzed)*, "denegatoria" (*denial)* or in the category "Con archivo" (*with file)* are considered as inactive withdrawals and are thus excluded from the model. This results in a total withdrawal volume of 6282.5 hm^3 per year. The withdrawal points, shown in Figure 10, are joined to the shapefiles representing the catchments in QGIS and the sum of withdrawals per catchment is calculated. Each of the withdrawal sums for the catchments are added as "Demand Sites" in WEAP with a connected "Transmission Link" and "Return Flow". The transmission links specify the placement of the extractions and the return flows specify the amount and placement of the returning unconsumed withdrawals.

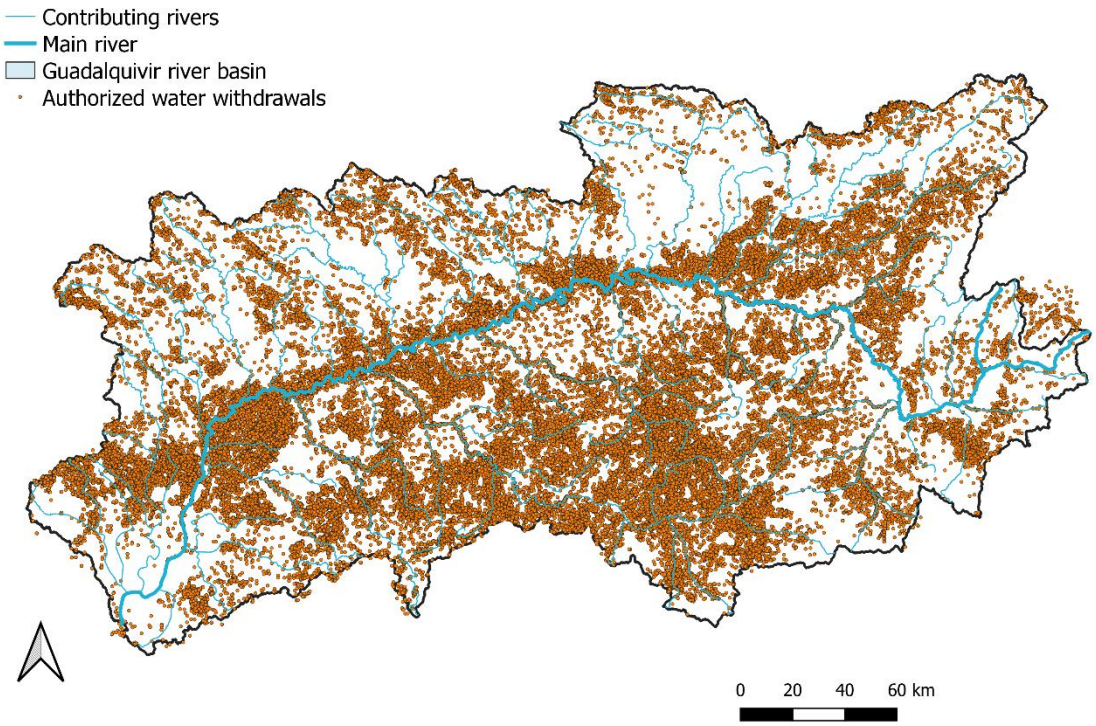

Figure 10: Overview of the georeferenced authorized water withdrawals. Data source: (CHG, 2019a).

For the four large catchments, the aggregated water withdrawals are placed approximately in the middle of the catchments. For the catchments of the NPDs, the withdrawals are aggregated into two groups; upstream and downstream of the dam. The withdrawals upstream the dam and their corresponding return flows are connected directly to the dam, whereas the withdrawals downstream of the dam and their return flows are placed between the dam and where the water course meets the main river. The aggregated values are included in Appendix G. The consumption rate of the withdrawals, i.e. the share of the water withdrawals not returned to the river, is assumed to be 70%. The monthly variations in withdrawal activity is assumed to follow the monthly variation in crop coefficients.

For the selection of crop coefficients, a spatial analysis of the land cover of Guadalquivir using the Corine Land Cover dataset with QGIS is performed. The Corine Land Cover (CLC) data includes data on the biophysical characteristics of the land surface with a spatial resolution up to 100 x 100 m from 2018 (European Environment Agency, 2019). The land uses are divided in to five major groups as the first level, being artificial surfaces, agricultural surfaces, forests and semi-natural areas, wetlands, and waterbodies. The major land cover types detected within Guadalquivir considering these five groups are presented in Figure 11.

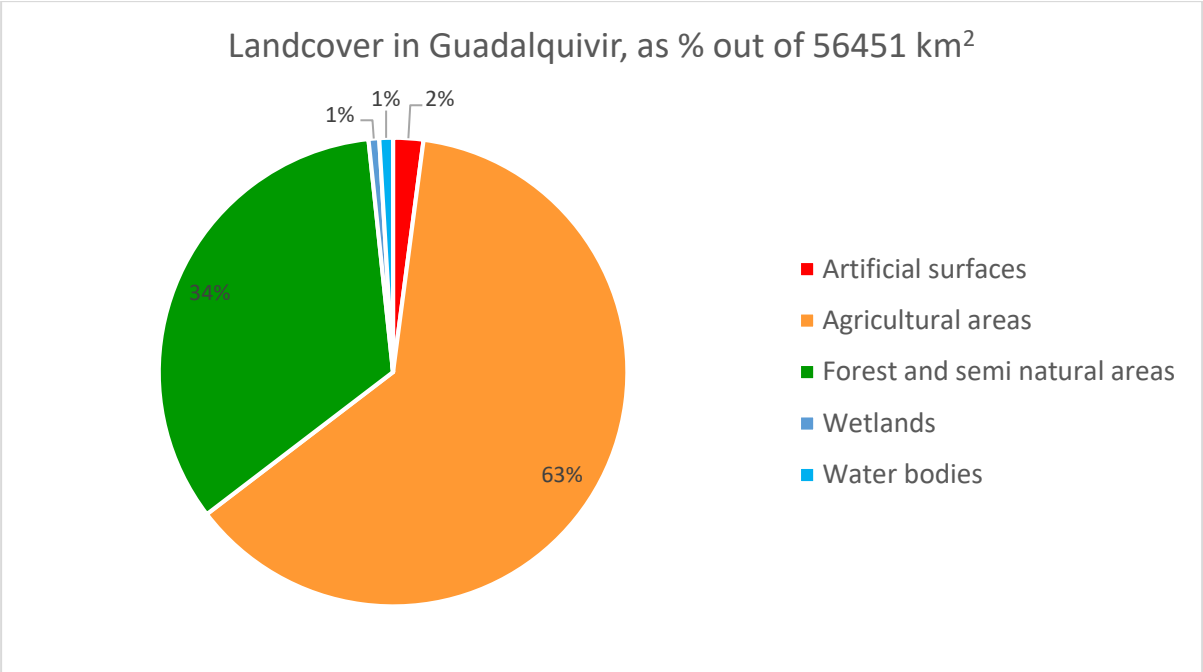

Figure 11: Land cover distribution in Guadalquivir. The values are based on the GIS analysis of the Corine Land Cover dataset (European Environment Agency, 2019).

The five major land cover groups can be further divided into several more detailed groups for a second and a third level. The third and most detailed level contains 50 different groups, making it possible to identify crop types and thus the corresponding crop coefficients with seasonal variations. The area weighted average of the most common crop types in the basin and their corresponding crop coefficients can be used to calculate one generalized crop factor for implementation in the water balance calculations.

In this case, approximately 63% of the land is covered by agricultural areas, whereas the rest is mostly covered by forests and semi natural areas. 25% of the land cover is detected as olive groves, being a significant part of the irrigated area. Since olive is the dominant irrigated crop in the basin, the crop coefficient is chosen to vary according to the seasonal variation of the olive crop factor from the FAO report 56. The value of the crop coefficient generalized for the entire basin is estimated by weighting the olive grove crop coefficient and a constant crop coefficient of 0.8 each by 50%, resulting in the season-dependent crop coefficient for the basin presented in Figure 12.

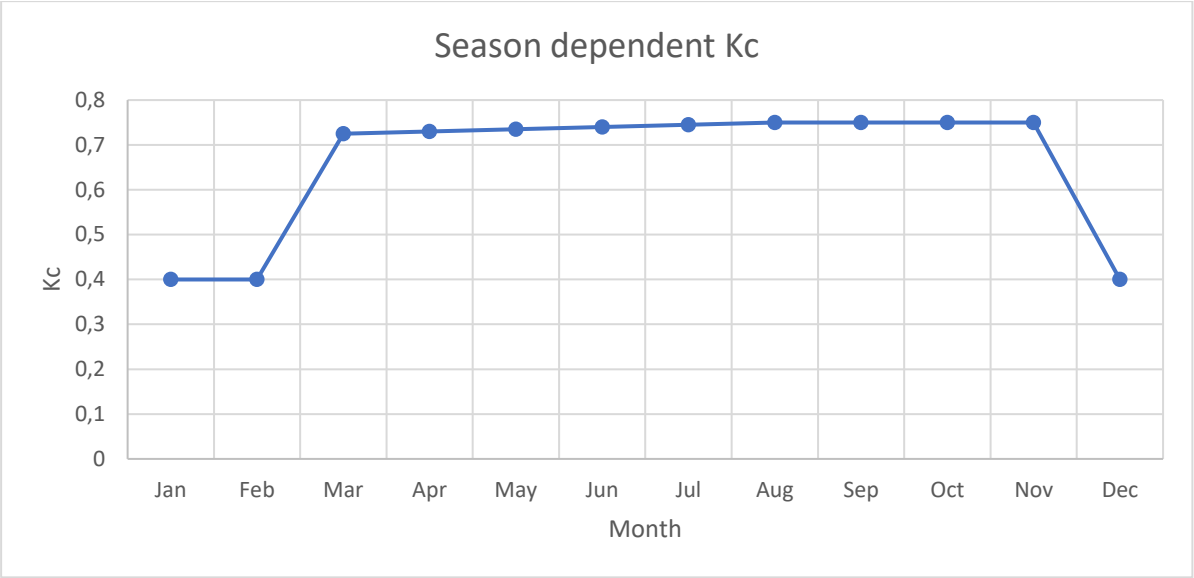

Figure 12: Monthly crop coefficients, Kc.

Six external transfers are included in addition to the authorized, internal withdrawals. The five exports are added individually to each of the corresponding reservoirs Negratín, Fresneda, Montoro, Sierra Boyera and Aracena as demand nodes with no return flow. The import to the Huelva and Doñana county is implemented as "Other supply", as it is not linked to any water source within the catchment. The corresponding values are presented in Table 2, and their monthly variation is chosen to follow the same pattern as for the other withdrawals.

Internal transfers between the reservoirs are not included due to a lack of information. It is however assumed that the available water can be transported within the catchments in order to supply the internal demands, independently on their distance from the rivers.

Groundwater is not considered separately in this study but is assumed to be included in the surface water balance. Official numbers states that almost 25% of the water consumptions are currently supplied by groundwater (CHG, 2016). The surface runoff water is simulated to account for this due to three assumptions implemented in the model. First, the official withdrawals taken from wells and other possible sources of groundwater are considered as consumers of runoff water, and thus included in the withdrawals. Second, no runoff water is considered to infiltrate into the ground and contribute to groundwater recharge. Third, the ground water cycle is assumed to lay within the geographical boundaries of the Guadalquivir, meaning that there is no external transfer of groundwater between the neighbor river basins.

3.2.4 Calibration

Three unregulated sub catchments within Guadalquivir are chosen as calibration catchments in order to avoid uncertainties introduced by regulation strategies. Minimizing the difference between observed and simulated streamflow is considered the most important objective of the calibration. A daily timestep is chosen for the calibration model in order to get a better understanding of how the model is responding to different precipitation values. There are few unregulated river basins left in the Guadalquivir region of considerable size, resulting in the selection of three catchments of a total of 963.21 km^2, thus representing 1.57% of the total basin. The three chosen basins are named Anzur (307.22 km^2), Yeguas (213.36 km^2), and Cabra (442.63 km^2) after their main rivers and are situated south in the middle part of the Guadalquivir basin. CHG provides river discharge data dating back to 1999. The three catchments are defined by the area upstream the stations A10, A16 and A30 from which the

observed streamflow data is collected. The catchments and the measurement stations are shown in Figure 13.

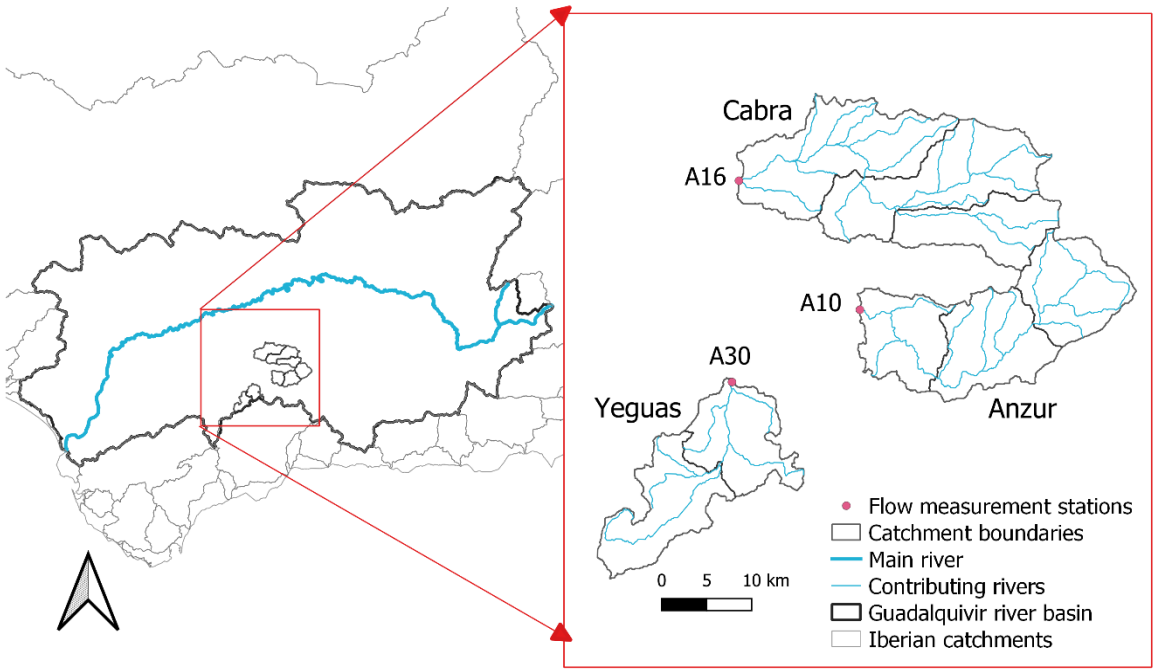

Figure 13: Overview of the three calibration catchments. The inner borders are used for withdrawal aggregation only.

A GIS analysis of the topography and the land cover in the three catchments is performed to compare their characteristics with the characteristics of the whole river basin. The analysis shows that the minimum elevation in the calibration is situated in the Cabra catchment and is 200 m.a.s.l., where the highest elevation is of 1450 m.a.s.l. in the Anzur catchment. The average elevations for the three catchments range from 351-730 m.a.s.l. For the Guadalquivir basin, the elevations range from sea level at the coastal line to 3460 m.a.s.l in the catchment of Colomera. From visual comparison, it can be seen that the calibration catchments have a much less diverse land cover, and that the share of olive groves is much larger in the calibration catchments than in the Guadalquivir basin. An overview of the landcover in Guadalquivir is presented in Figure 14, with the calibration catchments outlined.

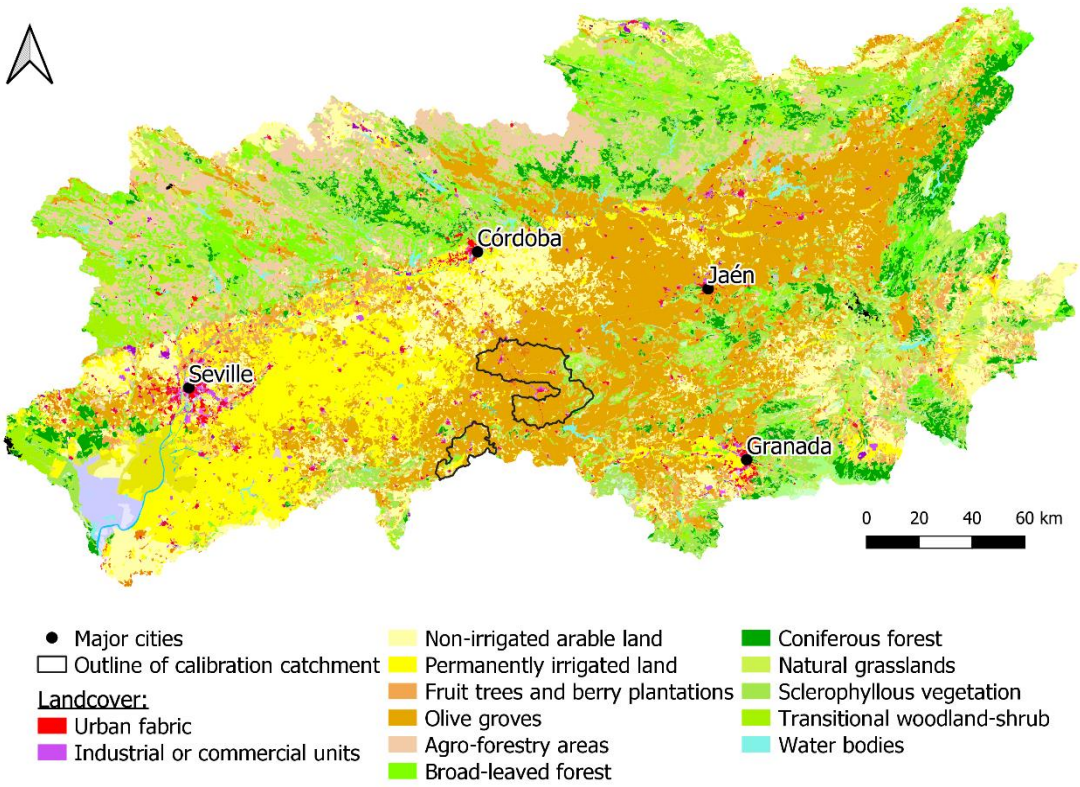

Figure 14: Corine landcover classes in the Guadalquivir basin. Only the descriptions of the most frequent landcovers are included in the legend. Data source: (European Environment Agency, 2019)

Since the calibration areas are smaller than the grid size of the CRU TS4.03 dataset (56 x 56 km), historical timeseries for precipitation and temperature data are taken from local measuring stations close to the calibration catchments. The CHG has measuring points for temperature and precipitation at several locations within the catchment. These data are available at variable resolutions, including daily timesteps. In order to obtain the best calibration, long timeseries of data are preferred as these will have a bigger probability of including extreme events both regarding long drying periods and extreme flood events. The limiting input data in this case is the temperature measurements. Temperature measurements started in 2016 in Guadalquivir at some stations and later at the remaining stations. For the chosen basins for initial calibration, data of temperature is available from 2017, whereas data of precipitation is available from 2015 for all the relevant stations. For the calibration, the time period is therefore set from January 2017 to December 2019.

In order to appoint which measuring stations to be used for which catchment, the theory of Thiessen polygons, also called Voronoi polygons, is used. The theory assumes that the measured observations apply to the area that is closer to the considered gauge than to any of the other neighboring gauges (Schumann, 1998). Voronoi polygons for the measurement stations are created individually for the precipitation measurements and the temperature measurements using the integrated Voronoi polygon function in QGIS. The two resulting maps are shown in Figure 15 and Figure 16.

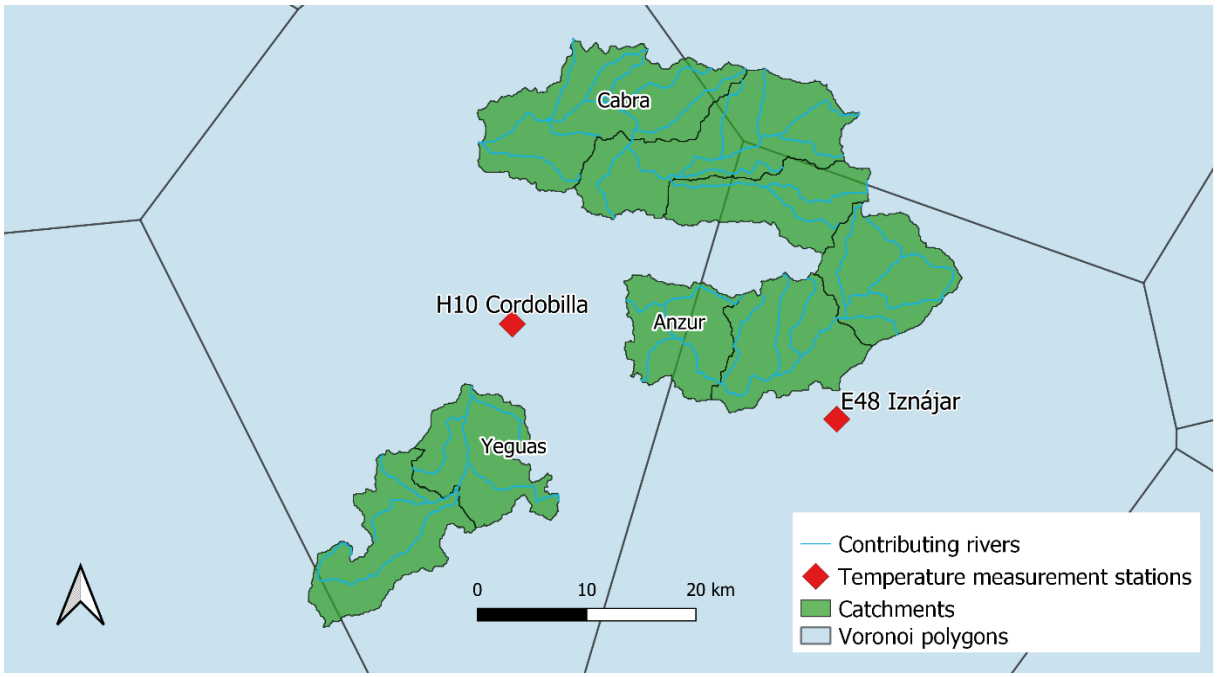

Figure 15: Voronoi polygons based on temperature measurement stations.

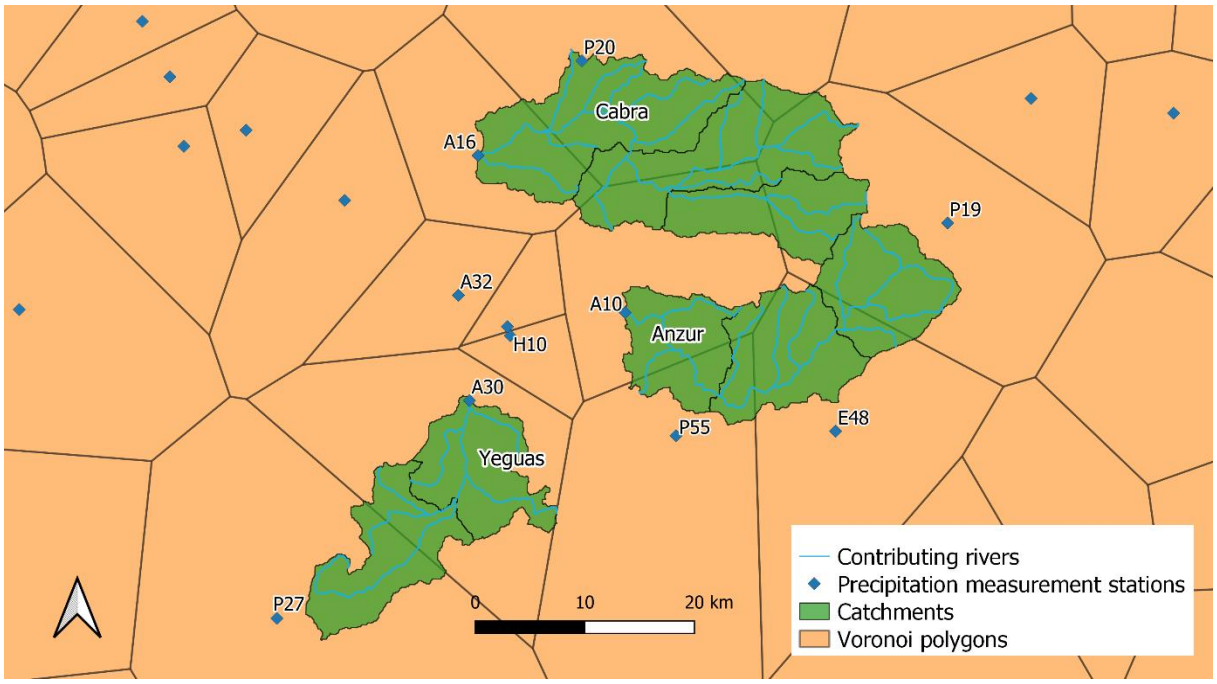

Figure 16: Voronoi polygons based on precipitation measurement stations.

Simple weighting coefficients for the different measuring stations regarding each of the basins are chosen based on visual evaluation of the Voronoi polygons. For the temperature measurement, a simplification is done using only one station per basin as there are few available stations. The selection of measurement stations for temperature data is presented in Table 4. For the precipitation, visual weighting is chosen as a more accurate simplification than for the precipitation, resulting in the values presented in Table 5.

Table 4: The chosen temperature measurement stations for the calibration catchments.

Basin	Temperature station
Anzur	E48
Yeguas	H10
Cabra	H10

Table 5: The chosen precipitation measurement stations and corresponding weighting factors for the calibration catchments.

Basin/station	P27	P20	P19	E48	P55	A10	A16	A30
Anzur	-	-	0.25	0.25	0.25	0.25	-	-
Yeguas	0.50	-	-	-	-	-	-	0.50
Cabra	-	0.25	0.25	-	-	0.25	0.25	-

An adiabatic lapse rate is applied to the historical temperature data to account for the topographic differences within the basins. This is done by adjusting the measured temperatures at the elevation of the measurement stations to correspond to the temperature at the average elevations of the catchments. The adiabatic lapse rate in Spain is found in literature to be on average -5.28 ˚c/km (Navarro-Serrano et al., 2018). By using the AQUASTAT data regarding the three calibration catchments, the average adiabatic lapse rate is found to be -4.2 ˚C/km. Since the data from AQUASTAT is solemnly based on the geographic area of the calibration catchments, the adiabatic lapse rate deduced from AQUASTAT is chosen for this model.

The coordinates of the measurement stations H10, A16, A10, E48 and A30 from CHG are extracted and used to find corresponding monthly averages for the wind speed and the relative humidity from AQUASTAT. The average of the five values per month is calculated and used as input in WEAP.

Some of the observed discharge values are considered highly unlikely and suspected to be the result of measurement errors. For the Anzur catchment, a recorded extreme discharge value of 26.11 m^3/s for six consecutive days is considered unlikely given no precipitation in the catchment the days before. The discharge values for the period 20.-27. of August 2017 are therefore replaced by the discharge value before the extreme values, being of 0.001 m^3/s. For the Cabra catchment, an extreme value on the 2nd of November 2018 is changed to the discharge value of the fore coming day of 0.003 m^3/s, the reason also being no record of extreme precipitation.

The parameters chosen for calibration are:

- Soil Water Capacity (SWC)
- Deep Water Capacity (DWC)
- Initial soil moisture (Z1 and Z2)
- Preferred Flow Direction (PFD)
- Runoff Resistance Factor (RRF)
- Deep Conductivity (DC)
- Root Zone Conductivity (RZC)

A sensitivity analysis of the calibration parameters is performed before the calibration in order to find which parameters have the biggest influence on the model. The sensitivity is calculated as the relative change in water volume divided by the relative change in the tested parameter

values compared to the initial water volume and parameter. Initial soil moisture is excluded from the sensitivity analysis, as their influence on the model is chosen to only be evaluated for the first months of the calibration. The analysis is performed on the three calibration catchments as one field. The default values in WEAP are used as the initial parameters to be varied by +/- 50%, and the resulting water volume changes in the total water balance are registered. Then, the sensitivity of the parameter is expressed as the relative change in water volume they cause with modified values. The analysis shows that the model is most sensitive to changes in root zone conductivity and least sensitive to changes in preferred flow direction. The results are presented in Table 6.

Table 6: Parameters included in the sensitivity analysis and their corresponding effects on the water balance.

Parameter	Default value	Test value		Change water volume	
		-50%	+50%	-50%	+50%
DWC	1000	500	1500	-15%	12%
SWC	1000	500	1500	18%	-2%
RRF	2	1	3	14%	-2%
DC	20	10	30	9%	-5%
RZC	20	10	30	-41%	22%
PFD	0.15	0.075	0.225	1%	-2%

As the three catchments have to some extent different physical properties, a general calibration is thought to fit better to the whole of the Guadalquivir basin that a calibration fit more specifically to just one of the catchments. The three individual catchments are therefore calibrated as one field by using the same parameters for each of the fields. The results of the parameter modifications are exported to Excel from WEAP, enabling mathematical comparisons of the different calibrations and thus to find the parameter set giving the best fit. Finally, the calibrated parameters from the calibration field are inserted into the main model of the whole Guadalquivir basin.

For the evaluation of the simulation results for the model covering the whole Guadalquivir basin, simulated streamflow values are compared with observed values. This is done by including measurement data from the river discharge measurement stations Alcála del Río and Peñaflor. Alcála del Río is the most downstream measuring station in the river basin and is therefore the most important indication of the overall simulation performance. In addition, observed monthly reservoir storages for all the NPDs and the other dams with available data records are included in the model to allow for an evaluation of the reservoir modelling of each of the dams individually, and all the reservoirs seen as one big reservoir.

3.2.5 Model evaluation criteria

One common way to evaluate the goodness of fit of a calibration of water balance is the percent bias (PBIAS). The PBIAS represents the deviation of the simulated flow values from the observed flow values in percentage, and is calculated using the following equation:

$$PBIAS = \frac{\sum_{i=1}^{n}(Q_{i,obs} - Q_{i,sim}) \cdot 100\%}{\sum_{i=1}^{n} Q_{i,obs}}, \quad (11)$$

where $Q_{i,obs}$ is the observed flow [m^3/s] and $Q_{i,sim}$ is the simulated flow [m^3/s], both at timestep *i*. As we wish to minimize the difference between $Q_{i,obs}$ and $Q_{i,sim}$, we seek to minimize the absolute value of PBIAS with the ideal value being 0%.

A satisfying model calibration is needed to ensure representable results. The chosen evaluation criteria are based on the work of Moriasi (Moriasi, 2007) and are presented in Table 7. These criteria are meant for application on monthly timesteps but are in this study applied to evaluate both the water balance of the monthly averages, the annual totals values, and the overall total values for the whole simulation period.

Table 7: Model evaluation criteria as a function of PBIAS in absolute values.

Performance	Very Good	Good	Satisfactory	Unsatisfactory
PBIAS [%]	[0;10]	[10;15]	[15;25]	[25;∞)

3.2.6 Scenario definition

Three scenarios are considered in this study. Their main difference is the different amounts of water considered available for hydropower production. This can be described briefly by the following points:

- Scenario 1: Considers the potential of all the water released from the dams
- Scenario 2: Considers the potential of the water flowing through turbines designed according to historical discharge observations
- Scenario 3: Considers the potential of the water flowing through the turbines from Scenario 2, with water demands reduced by 10, 20, 30, 40, and 50%

For all the scenarios, the following assumptions apply to all the NPDs and the currently powered dams implemented in the model:

- The hydraulic head is calculated based on the given tailwater elevations and reservoir elevations for each timestep. The maximum gross head equals therefore the highest regulated water level (HRWL) minus the tailwater elevation. If the water level in the reservoir is below the HRWL at the end of the last timestep, the gross head is reduced accordingly.
- WEAP is set to calculate the potential hydropower generated by the water released from the dam to serve existing water uses, not optimizing its releases for hydropower production.
- The possibility of constructing new pipelines or tunnels with the aim of increasing the hydraulic head is excluded from this study. Such constructions will have to be evaluated with respect to their environmental impacts, in addition to increasing the span of the possible solutions that need individual and thorough consideration for each specific dam.
- The generation efficiency, η, is set to 85%, as this is considered a normal value for hydropower when considering head losses and variable turbine efficiencies (Hadjerioua et al., 2012).
- The plant factor is set to 100% all year, thus not implementing any additional seasonal limitations.

For the NPDs, new intakes are dimensioned based on the known releases from the dam. The existing intake capacities for the individual intakes are therefore not limiting the hydropower potential. The choice of assuming the need for new intakes is made since the specific existing capacities are unknown and an analysis of the hydraulic conditions by using equation 4 is impossible. In addition, new intakes will allow for an ensemble of the different releases which is considered more practical and economic than several smaller intakes.

An overview of the similarities and differences of the three scenarios is presented in Table 8. More detailed descriptions follow below the table.

Table 8: Description of the scenarios.

Scenario	**1**	**2**	**3**	
Spillway capacity	Equal official capacity when water level surpasses the spillway level, assumed to comprise the capacity of the other outlets.			
Outlet capacity	Equal to the maximum observed daily streamflow downstream the dam for the NPDs. The remaining dams follow official capacities.			
Turbine capacity	Same as outlet capacity	2 x observed average daily outflow	2 x observed average daily outflow	
Internal water withdrawals	6282.5 hm^3/yr	6282.5 hm^3/yr	Reduction: -10% -20% -30% -40% -50%	New value: 5654.3 hm^3/yr 5026.0 hm^3/yr 4397.8 hm^3/yr 3769.5 hm^3/yr 3141.3 hm^3/yr
External water withdrawals	57.51 hm^3/year			
Economic analysis	Not considered	Calculated NPV and LCOE for each of the NPDs	Not considered	

In Scenario 1, the maximum turbine capacity is set equal to the total current outlet capacity of the reservoir excluding the spillway capacity. The method is explained in 3.2.2. As the total capacity in most cases is a sum of the capacities of several pipes or similar hydraulic constructions possibly directing the water to other destinations than the downstream river, this capacity is meant to represent the gross potential and does not consider economic factors.

In Scenario 2, turbine capacities are found by analyzing observed daily average values for historical flow downstream the dams covering the simulation period. A method of choosing the turbine capacity to 2 x the average inflow to a hydropower plant is proposed by the Norwegian Water Resources and Energy Directorate for the early development phase of hydropower projects (SWECO Norge et al., 2010). In this study, the values are chosen as 2 x the daily average values of outflow from the dams during the given period since not all the inflow to the reservoir will be released to the downstream river. It is assumed that the current outflows from the dam can be collected upstream the dam in a new pipe serving the turbine, before being released the same place as the initial outflows from the dam. The economic analysis is based on this scenario and includes therefore the construction of new intake structures and waterways in the cost estimations.

Scenario 3 consist of 5 different cases considering decreased internal water demands. External transfers are thus kept at the initial values, as these are not necessarily dependent on the water management in Guadalquivir. The five cases consist of reductions of -10%, -20%, -30%, -40%, and -50%, all having turbine capacities equal to the capacities in scenario 2. The decrease in water demand is implemented as a general reduction factor to all the included withdrawals in the model. Such a decrease may be the result of future water recycling, improved irrigation efficiencies or alteration of land cover to less water intensive covers. Water recycling decreases the water demand from the natural sources as the same water used can serve several purposes,

whereas improved irrigation systems can decrease the amount of water being evaporated from the soil back into the atmosphere.

The turbine capacities and the resulting installed capacities for all the scenarios are presented in Table 9. Seasonal maximum releases apply to four of the NPDs during the months May-October and are included in the table. The installed capacities are based on the gross head, the turbine capacity, and the assumed generation efficiency of 85%. These are in turn used for the calculations of the simulated capacity factors. This is done by using equation 3, estimating the actual energy production by the annual average energy production from the WEAP simulations.

*Table 9: Selected turbine capacities [m^3/s] and the resulting installed capacity [MW] for the NPDs. The dams market with * have seasonal limited turbine capacities due to maximum discharge allowances downstream the dam. The limits for May-Oct are in brackets.*

	Scenario 1		**Scenarios 2&3**	
Unit	**m^3/s**	**MW**	**m^3/s**	**MW**
Dam	**Turbine capacity**	**Installed capacity**	**Turbine capacity**	**Installed capacity**
Agrio	72.62	18.52	3.74	0.95
Colomera	28.47	13.06	1.84	0.84
Francisco Abellán	12.28	7.47	1.42	0.87
Fresneda	10.69	2.94	1.07	0.29
Gergal*	49.00 (38.40)	17.16	13.83	4.84
José Torán	63.91	34.77	3.86	2.10
La Bolera	8.53	2.59	5.05	1.53
Los Melonares*	54.50 (22.90)	18.18	13.61	4.54
Martín Gonzalo*	4.70 (1.70)	1.90	0.68	0.27
Montoro III	98.21	23.75	4.48	1.08
Quiebrajano*	8.50 (2.30)	4.82	1.12	0.64
Retortillo	8.5	2.48	3.07	0.90
San Clemente	15.1	10.19	2.27	1.53

3.3 Economic analysis

Only tangible, direct costs and benefits are considered in this economic analysis. All costs and benefits are calculated to real 2018 EUR by adjusting values from other years with consumer price indexes and discounting future values. The economic parameters and the sources for the cost estimations of the different elements are presented in Table 10. The following elements are included in the cost estimations:

- New waterway, including intake structure, entrance gate, pipe foundation and a pipeline 2 x the length of the gross head
- Complete electromechanical installation, including a Francis turbine
- Operation and maintenance costs (O&M)

The following costs are excluded from the cost estimations:

- Cost of grid connection and transmission lines
- Engineering work
- Transport and access to the site

- Taxes and subsidies
- Unforeseen costs
- Cost of decommissioning or salvage value

Table 10: Sources, values, and assumptions for the included parameters and elements in the economic analysis.

	Source	Value	Assumptions
Lifetime	IRENA	30 years	
WACC	IRENA	7,5%	
CPI, NOK 2015 to NOK 2018	SSB	1.084	
HICP, xEUR to 2018 EUR	European Union		
Exchange rate, 2018 NOK to 2018 EUR	The Norwegian Bank	9.596	
Electricity price	OMIE		Price representative for power suppliers
Intake	NVE	Fig. 2.3.1	Small regulation height
Entrance gate	NVE	Fig. 4.4.1	Max water pressure 10m
Power station	NVE	2.4.1	Head between 10-100m
Pipe foundations	NVE	Fig. 2.5.1	Good soil foundations and moderate slope
Cast iron pipes	NVE	Fig. 4.6.4	C25

Approximate costs for the civil work and technical installations are calculated using the cost guide for small hydropower published by the Norwegian Water Resources and Energy Directorate (Norconsult, 2016). Prices on electromechanical equipment are assumed to be the same in Spain as in Norway, as the equipment is sold internationally, and taxes are excluded from the economic analysis. None of the costs are optimized to the individual NPDs and common values and assumptions are therefore used for the cost estimates. The required installation and construction work are assumed to be completed in one year, resulting in all the investments being made the first year and revenues starting from the second year. The estimations of the different costs are included in Appendix E and an example of the discounting of costs, revenues, and energy is included in Appendix F.

The turbine costs are simplified in means of turbine type and available head. When comparing with the figure of working areas of different turbine types as function of flow and head (IRENA, 2012), Francis is the optimal turbine for most of the NPDs. As there only exist cost estimation curves for Francis turbines for the given characteristics of the NPDs in the chosen cost guidelines, it is assumed that Francis turbines are suitable for all the NPDs. The cost functions are dependent on the effective head, thus including the different head losses. In the cost estimations, the effective head is set equal to the gross head for simplification. Interpolation between the different cost functions for the different heads are done by linear interpolation.

The cost of new intakes and pipelines for water supply to the turbines are included, as the chosen turbine capacities for retrofitting do not correspond to the existing outlets of the NPDs. The lengths of the pipelines are assumed to be twice the length of the gross head, assuming that it is possible to transport the water from the dam to a powerhouse with the turbine in close proximity to the existing outlet. In order to design the diameter of the pipes, equation 5 is used with an assumed maximum flow velocity of 3 m/s. For the entrance gate, the gross inflow

velocity for small power plants is recommended to be between 0.5-0.8 m/s (SWECO Norge et al., 2010). The necessary cross section of the entrance gates for the different NPDs are thus calculated with the continuity equation using the individual turbine capacity and an assumed inflow velocity of 0.7 m/s.

All the costs are aggregated and discounted for a design period chosen to be 30 years with a WACC set to 7,5%. O&M costs are calculated as 2,5% of the investment costs. These assumptions correspond to the IRENA Renewable Power Generation Cost 2018 report (IRENA, 2019). Using the same values allows for a comparison of the LCOE between the retrofitting projects and the other renewable energy projects in the report. As the original NPDs require maintenance independently of possible retrofitting, the maintenance costs of the dam structure are not included in the retrofitting cost.

The revenues in this analysis are only based on the energy production and the electricity prices. The energy production for each individual NPD is estimated to their corresponding average energy production during the simulation period in Scenario 2. The average energy generation is used for all the years in the project lifetime. The electricity prices on the day-ahead market in Spain and Portugal are obtained from OMIE, the company managing the spot market (Marín and García-Marín, 2019). These prices represent the arithmetic average price of the electricity generated from all the different energy sources on the market. It is assumed that these prices do not include taxes, and rather represent the price received by the power producer excluded subsidies. The electricity prices in Spain in the simulation period from October 2010 to October 2018 increased from 49.93 euros/MWh to 57.29 euros/MWh, with an average value over the years of 48.25 euros/MWh (OMIE, 2020a). These prices are assumed to be nominal prices, and are therefore adjusted to 2018 EUR real prices by using the Harmonized Indices of Consumer Prices (HICP) for Spain (European Union, 1995-2020). Despite the starting month of the hydrological year and the calendar year not being identical, the electricity prices for 2011 are accorded to the hydrological year 2010/2011 and so on. The electricity prices for the simulation period are presented in Table 11.

Table 11: Electricity prices in nominal and real 2018 EUR/MWh.

Year	2011	2012	2013	2014	2015	2016	2017	2018
Nominal price	49.93	47.23	44.26	42.13	50.32	39.67	52.24	57.29
Real price	53.29	49.20	45.41	43.31	52.06	41.18	53.15	57.29

For the remaining years of the lifetime after the simulation period, a fixed electricity rate is applied. Instead of using the electricity price in 2018, the average value from the simulated years is used. This is done both in order to correspond to the chosen future energy generation which also is set equal to the average value for the simulation period, and to choose a more conservative price estimate. In real 2018 EUR, the average price of electricity is calculated to 49.36 EUR/MWh. The expected revenues are calculated as the energy output from the retrofitted NPDs multiplied with the electricity prices, and discounted for the lifetime of the projects. An analysis of the sensitivity to the future prices for each of the NPDs is performed by increasing and decreasing the fixed rate for the years after the simulation period by 10%. The used electricity prices in the economic analysis and the prices used for the sensitivity analysis are presented in Figure 17.

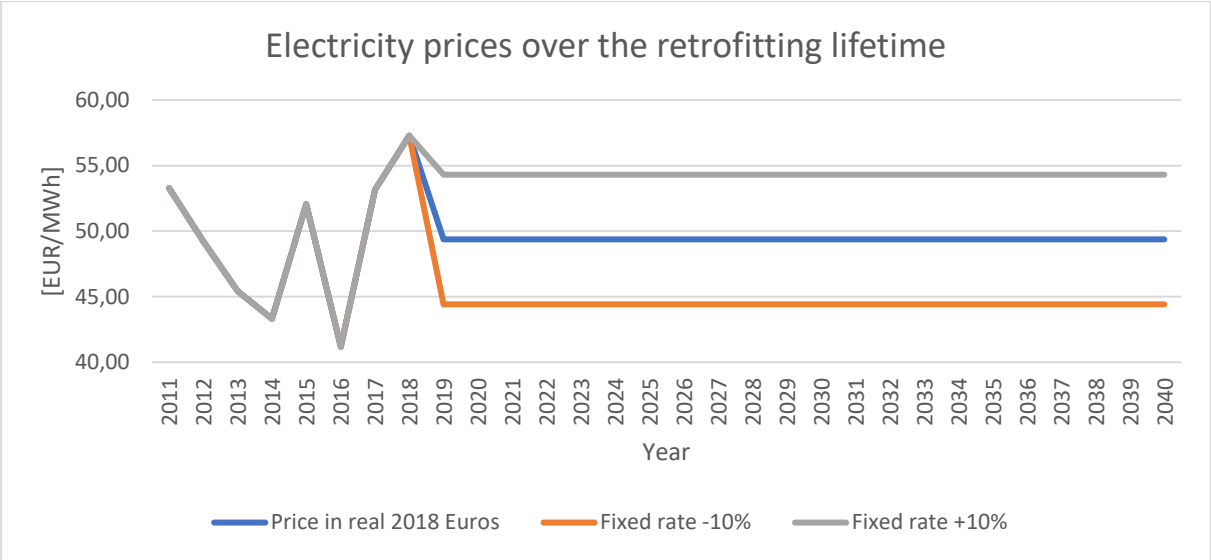

Figure 17: Electricity prices used in the economic analysis. The fixed rates +/- 10% are only used for the sensitivity analysis.

A comparison of the economic costs of retrofitting in Guadalquivir with alternative renewable energy sources is performed. This is done using the LCOE for new electricity energy projects from the IRENA report and the calculated LCOE for the different retrofitting scenarios. To allow for a direct comparison, the values for LCOE from IRENA are converted from 2018 USD to 2018 EUR. It should be highlighted that the values from IRENA are based on finished projects and include the cost of transmission lines and grid connections, which are not considered in the cases for retrofitting. The LCOE for the different renewable energy sources are presented in Table 12.

Table 12: Global Weighted Average LCOE for different renewable energy sources for electricity production (IRENA, 2019). The prices are converted to real 2018 EUR.

Technology	**Global Weighted Average LCOE [USD/kWh]**	**Global Weighted Average LCOE [EUR/kWh]**
Bioenergy	0.062	0.073
Geothermal	0.072	0.085
Hydro	0.047	0.056
Solar photovoltaics	0.085	0.100
Onshore wind	0.056	0.066

3.4 Upscaling to find global potential

In order to estimate the potential of bigger geographical areas, it is thought that a regression between the hydropower potential simulated in WEAP and common dam characteristics might be valuable. Analyses are therefore carried out to find a relation between the modelled hydropower potentials for energy and power, and selected NPD characteristics available in the ICOLD database. This is done for Scenario 1 as this scenario excludes the turbine capacity based on known outflow values and rather assumes the turbine capacity to be equal to the outlet capacity. The considered characteristics for regression development are:

- catchment area
- dam height
- reservoir capacity

The drainage area is chosen because it has an important impact on the volume of the inflow to the reservoir. The reservoir capacity may be designed to store water for periods of days to periods of several years, but nonetheless describes the regulation potential of the dam and thus the possibility to supply an even amount of water. The dam height defines the maximum water level and thus affects the potential head and in turn the potential power. For the development of the regression expressions, the input values for the NPD characteristics are chosen to equal the corresponding data in the database where these deviate from the input in WEAP.

Since the simulations of the different NPDs show variable performances, only the NPDs with a PBIAS of monthly simulated reservoir volume considered satisfactory (ref. Table 7) are included in the regression. The data analysis tool in Excel is used to find regression expressions between the calculated hydropower potentials and the chosen dam characteristics. This is an analysis tool generating a linear relationship between input and output data, automatically calculating different statistical indicators of the goodness of fit of the proposed regression function. All the regressions are specified to give zero energy and power for parameters equal to zero. Three types of combinations are tested for their regression fit. First, the regression is based on the individual parameters, thus a function of one parameter. Then, regressions are made as functions of all the different combinations of two to three characteristics, resulting in 7 regressions each for energy and power.

The regression with the best value of the adjusted R square is chosen as the resulting expression to be used for the upscaling. An estimate of the hydropower potential of the NPDs in Spain as well as an estimation of the NPDs worldwide are calculated by applying the expression to the non-powered dams in the ICOLD database. Only dams with registered data for all the three parameters are included. The resulting regression expression for power is also applied to the currently powered dams in Guadalquivir with known capacity and compared to their simulated capacity in WEAP for evaluation of the regression. Several of the currently powered dams are not included in the ICOLD register, and the official characteristics from the local water authorities (CHG) are therefore used as input to the regression expression.

4 Results

This section starts by presenting the results of the calibration of the WEAP model. Then, the simulation results regarding the reservoir volumes, unmet water demands and environmental flow requirements for Scenarios 1 and 2 are presented, followed by the hydropower output of the different scenarios. Scenario 1 and 2 have the same hydrological results due to the same outlet capacities, but different results regarding the energy output as the implemented turbine sizes are different. The results of the economic analysis are then provided, in addition to a comparison of the calculated LCOEs with the LCEOs of other renewable energy sources. Moreover, the findings in the regression analysis with corresponding global retrofitting potential are reported.

4.1 Model calibration and evaluation

The final calibration of the catchments Anzur, Yeguas and Cabra results in an overall PBIAS of -0.81%. The yearly PBIAS values for 2017, 2018 and 2019 are 14.58%, 10.41%, and -34.22% respectively. The resulting calibrated parameters are presented in Table 13.

Table 13: Calibrated parameters.

Parameter	SWC	DWC	Z1 & Z2	PFD	RRF	DC	RZC
Unit	[mm]	[mm]	[%]	[-]	[-]	[mm/month]	[mm/month]
Value	1375	1850	8	0.1	1.55	4	4

The total monthly streamflow in the three catchments are summarized into one simulated flow value and one observed flow value based on the three gauges. A comparison of monthly simulated and observed flows is presented in Figure 18.

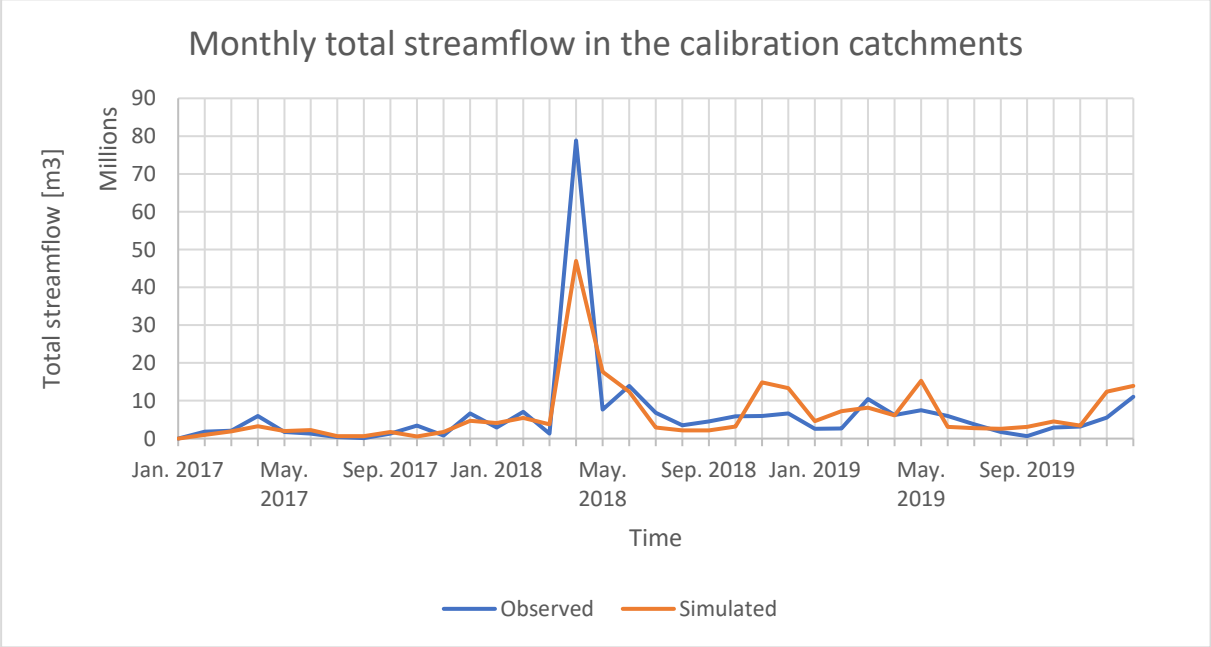

Figure 18: Monthly total streamflow for Anzur, Yeguas and Cabra.

The implementation of the calibrated parameters in the main model results in a PBIAS of 6% when considering the total water balance over the whole period at the measuring point Alcála del Río for Scenario 1 and 2. For Peñaflor, the corresponding PBIAS is 28%. This means that the

streamflow is in general underestimated in the simulations, and can thus be considered conservative.

The PBIAS values for the water balance at Alcála del Río for the individual years varies from -191% to 53% with a median value of -10% and an average of -53%. The monthly observed and simulated streamflow are presented in Figure 19 and shows that the months with high streamflow peaks are underestimated, in contrast to the months with stable, low flow. This is also further highlighted in Figure 20, representing the annual streamflow values and the corresponding PBIAS values for each.

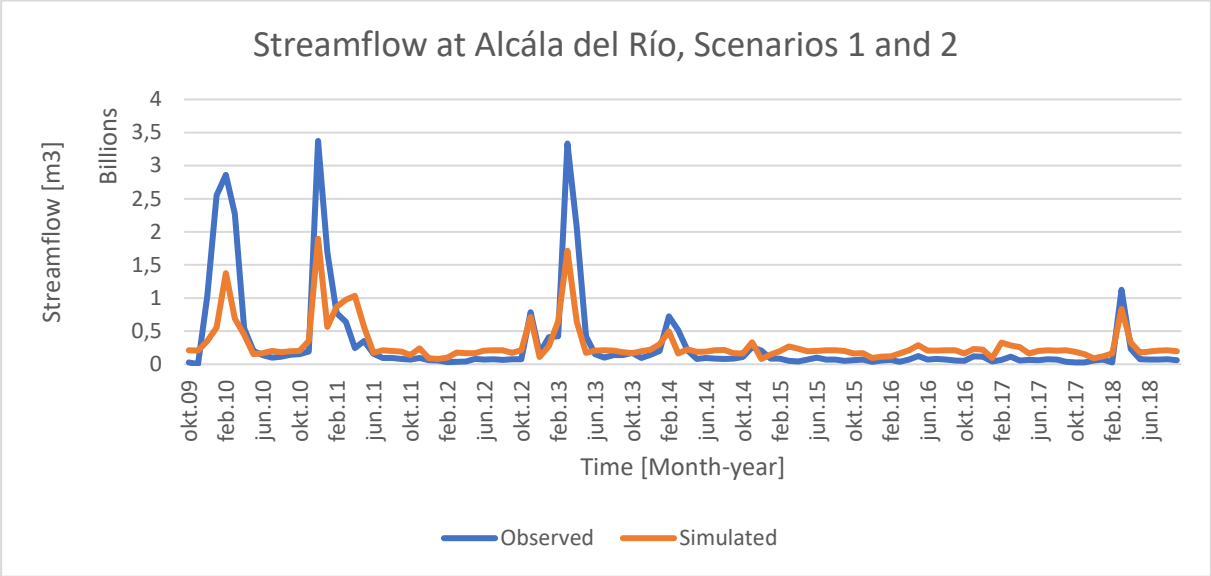

Figure 19: Monthly streamflow at Alcála del Río for Scenario 1 and 2.

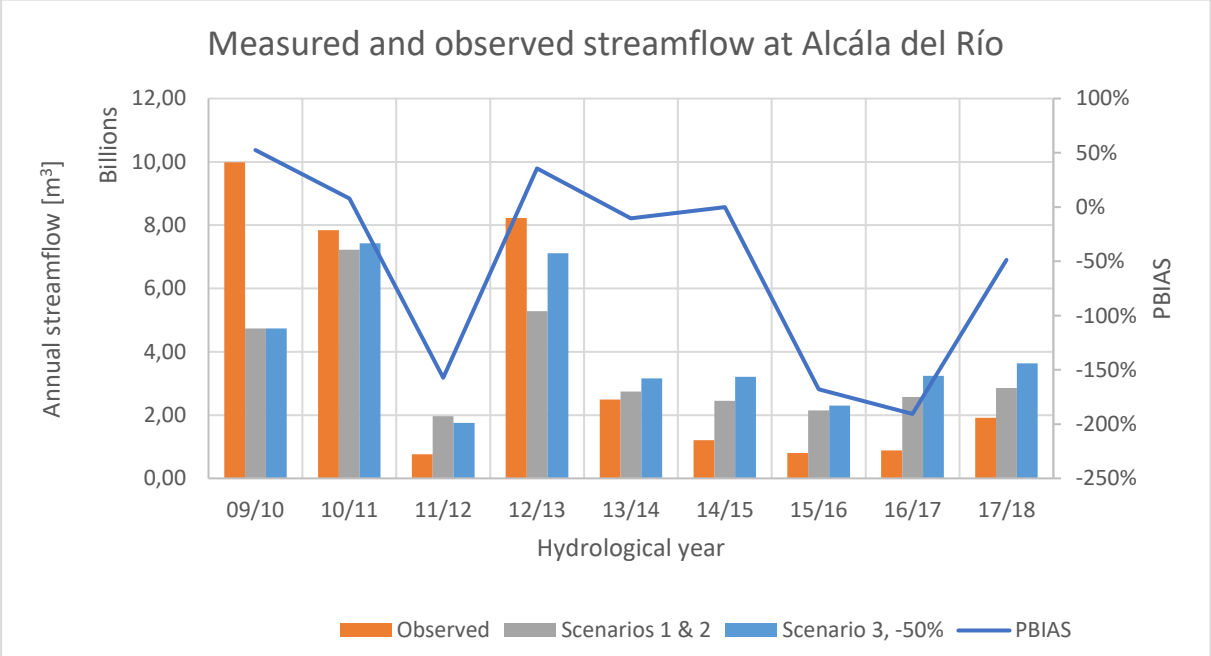

Figure 20: Measured and observed streamflow at Alcála del Río and the corresponding PBIAS values. The hydrological year of 09/10 start the 1st of October 2009 and end the 30th of September 2010.

The PBIAS of the simulations regarding the reservoir fillings of the NPDs varies from 2% to 94% for the different reservoirs when considering monthly timesteps. These two extreme values are obtained for Gergal and Francisco Abellán respectively. Their simulated and observed reservoir

volumes are presented in Figure 21 and Figure 22, whereas the corresponding figures for the rest of the NPDs are included in Appendix D. The simulated reservoir in Gergal is filled as many times as the observations show but tend to fill up a month earlier. Francisco Abellán's simulated reservoir volume is of a much lower magnitude than the observed values and is empty 50% of the simulated months. The small peaks tend however to happen during the same months or a month early as for Gergal.

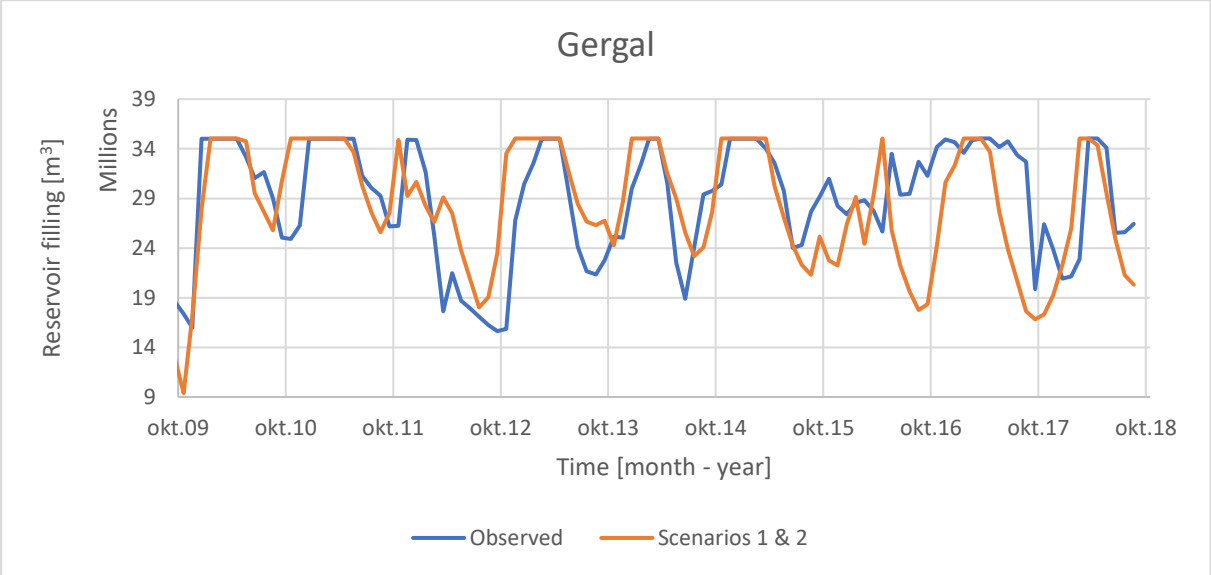

Figure 21: Observed and simulated reservoir filling for Gergal.

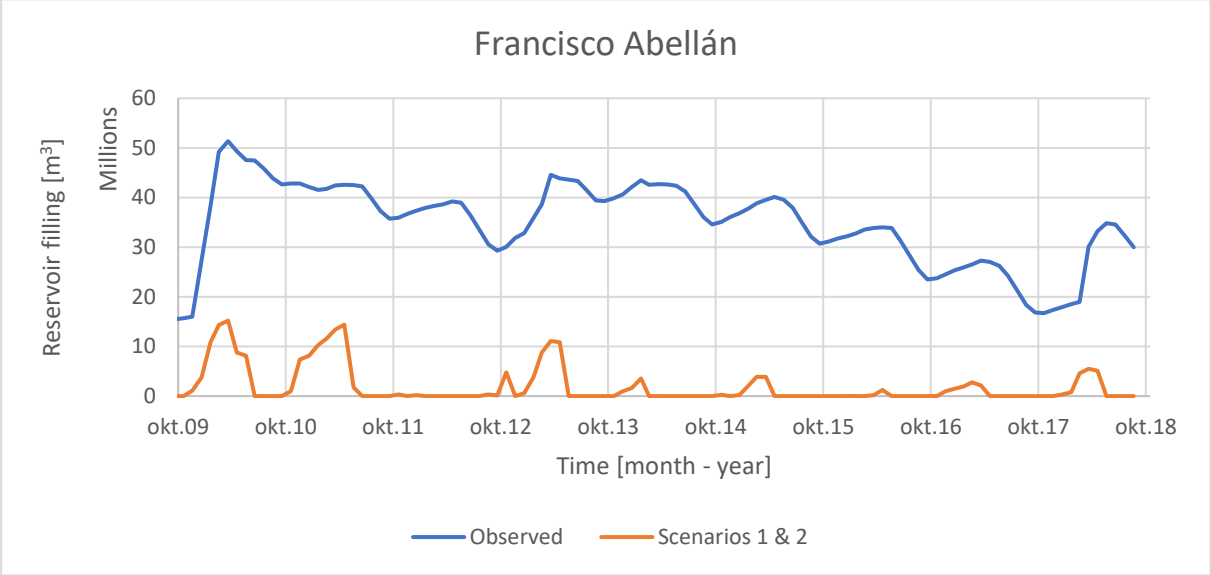

Figure 22: Observed and simulated reservoir filling for Francisco Abellán.

A geographical overview of which reservoir are considered to be satisfactory modelled is presented in Figure 23. The unsatisfactory modelled reservoir volumes are all underestimated. When comparing the geographical placement of the unsatisfactory modelled reservoirs with the placement of the unmet water demands and environmental flow requirements, they are found to lay in proximity to each other. The annually averaged unmet water demands are presented in Figure 24 and the percentage of unmet environmental flow requirements are presented in Figure 25.

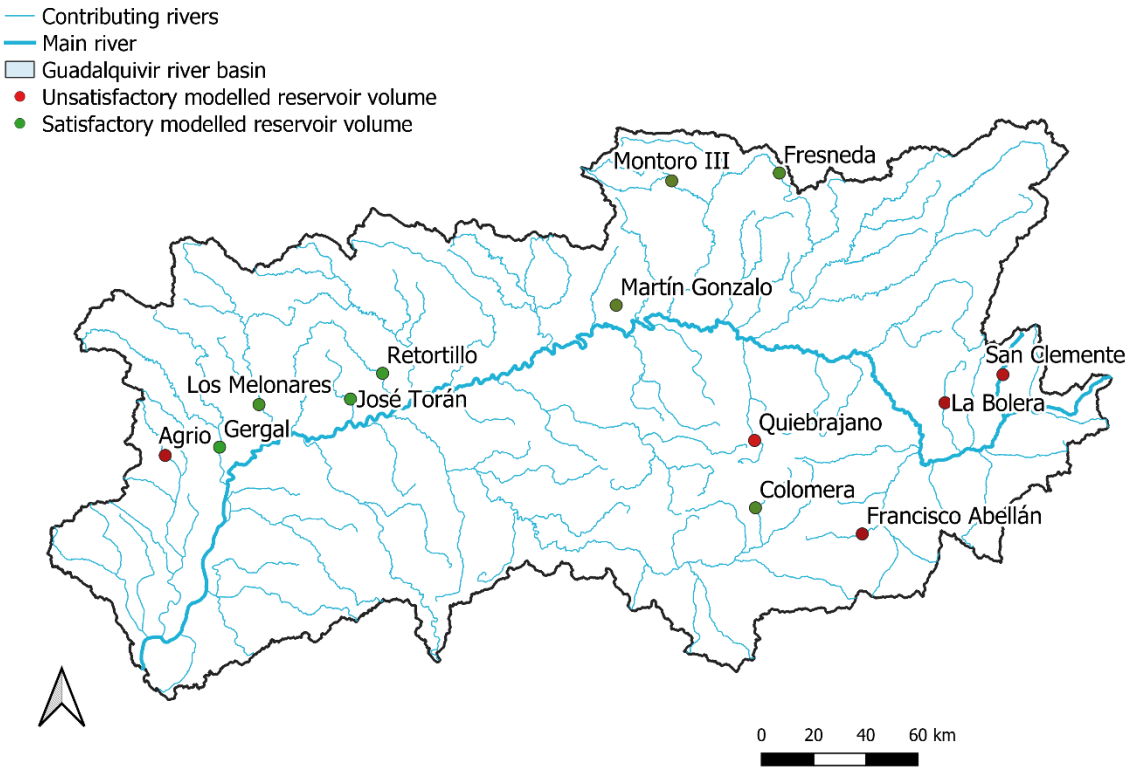

Figure 23: Overview of the reservoir simulation performance for the NPDs. The results are grouped into satisfactory (green) and unsatisfactory (red) based on the corresponding PBIAS values.

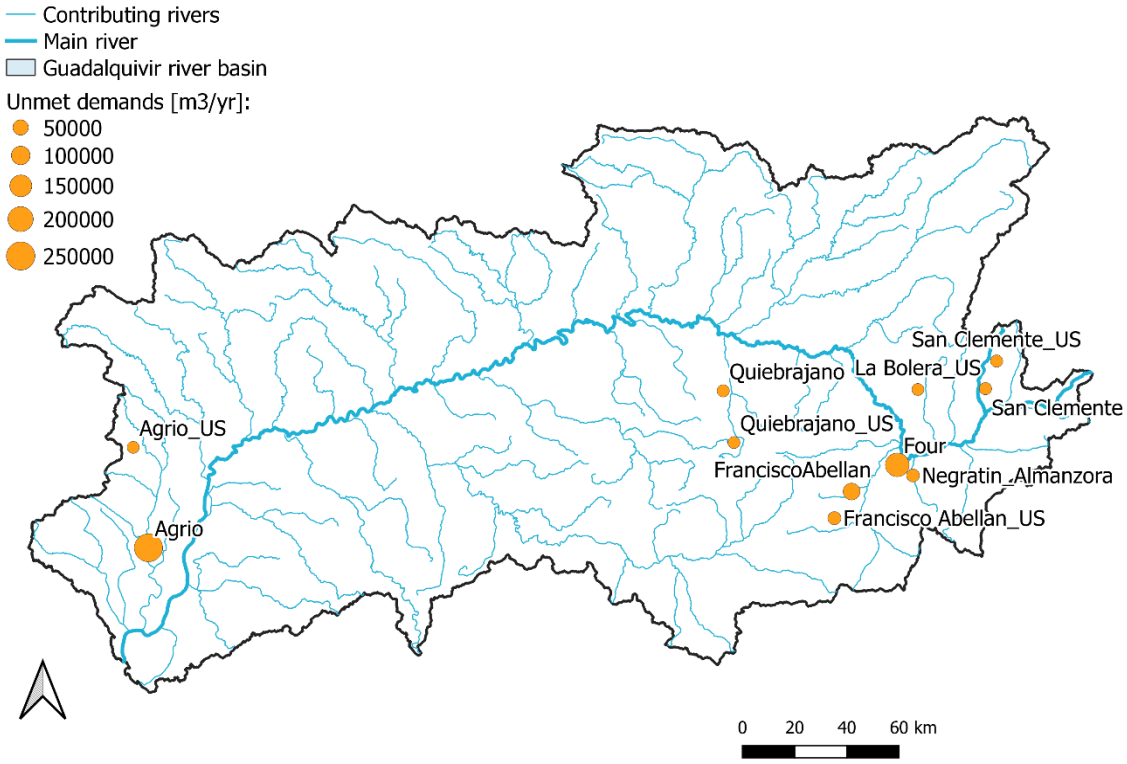

Figure 24: Annually averaged unmet water demand in m³/year. The radiuses of the markers are proportional to the values. The demands indicated as "_US" represent the demands upstream of the dam.

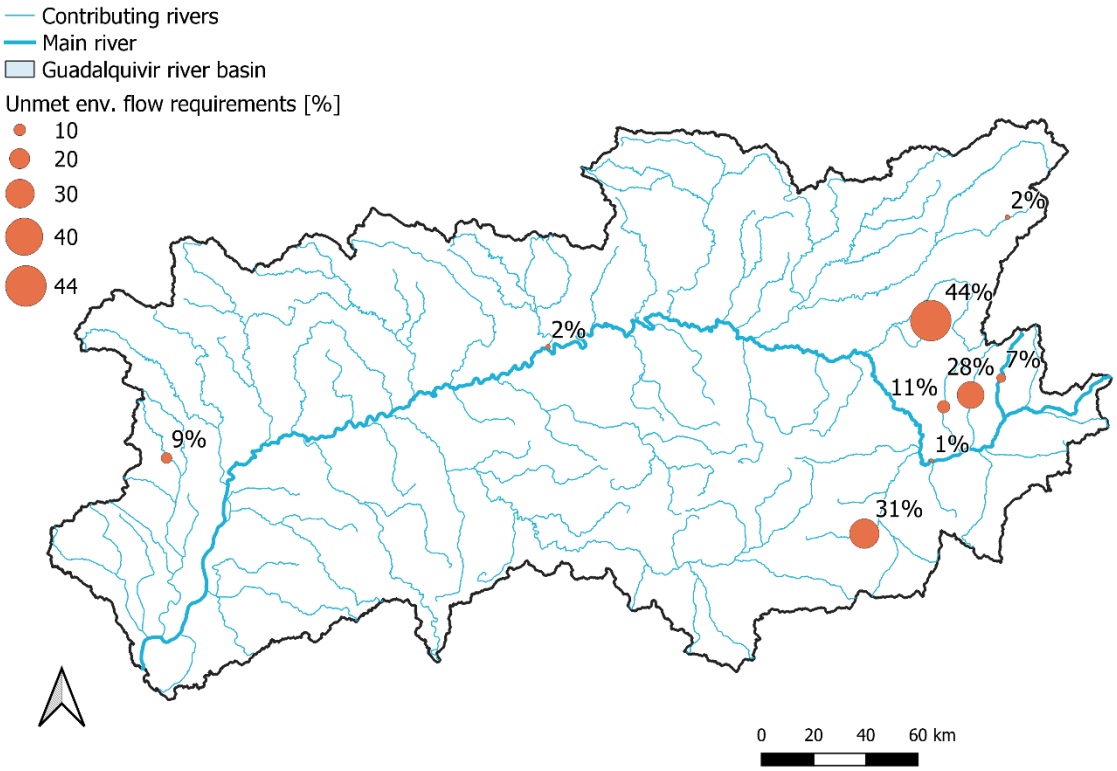

Figure 25: Unmet environmental flow requirements in %. The radiuses of the markers are proportional to the values.

The model performance is also evaluated based on the reservoir filling of all the reservoirs in the basin considered as one reservoir. When only including the 50 reservoirs with available time series of observed reservoir filling for the complete simulation period, the PBIAS is 13% in Scenarios 1 & 2. This value lays between the PBIAS values for the streamflow at the measuring gauges at Alcála del Río and Peñaflor and is considered satisfactory. The total reservoir fillings during the simulation period is presented in Figure 26. The officially estimated total capacity of the river basin is 8 500 hm^3, which corresponds well to the observations when knowing that not all the reservoirs are included in the model.

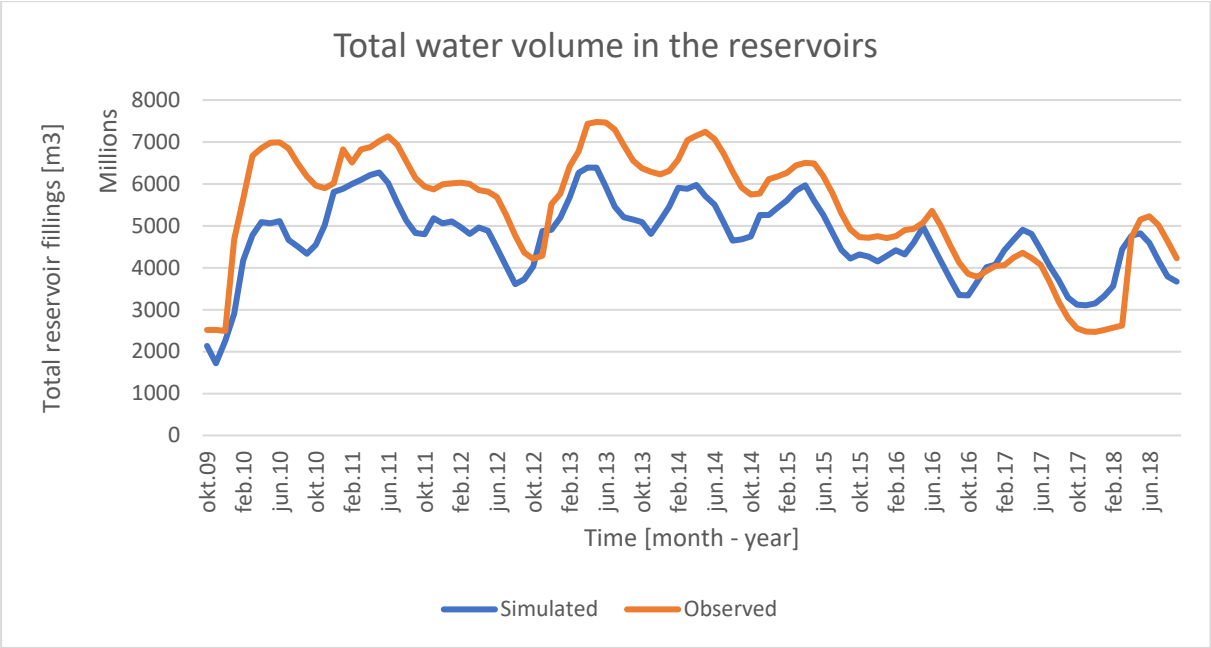

Figure 26: Total simulated and observed water volumes stored in reservoirs in the Guadalquivir basin during the simulation period.

4.2 Hydropower generation

Scenario 1 and 2 result in an average annual hydropower generation of 64.61 GWh and 57.79 GWh respectively for the 13 NPDs in total. The three NPDs with the biggest potentials are Gergal, Los Melonares, and José Torán. The limited turbine capacities in Scenario 2 results in a reduced power generation of 8.82 GWh. In percentage, the reduction ranges from 0% to 35.8% for the individual dams with a total average reduction of 13.7%. The NPDs with the worst simulation performance are found to have the lowest capacity factors, whereas the satisfactory simulated NPDs have capacity factors ranging from 0.2 to 0.48. The corresponding PBIAS values for the reservoir volume simulations and the calculated capacity factors are presented in Table 14. An average household in Spain uses 10 500 kWh per year (IDAE, 2011), and the hydropower potential of the considered NPDs in Scenario 2 can therefore be estimated to serve 5313 households on an average year. Average values for the yearly power generation for the different NPDs are shown in Figure 27.

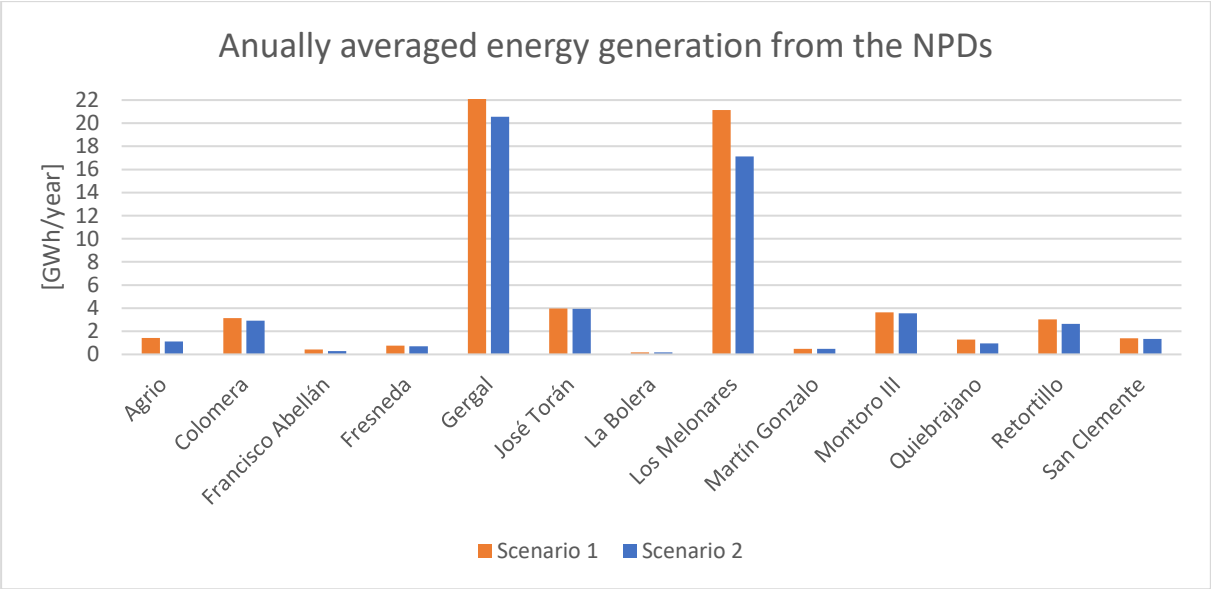

Figure 27: Annually averaged energy production.

Table 14: Annually averaged energy production, capacity factor, and reservoir simulation performance of Scenario 2 compared to the observed reservoir volumes.

NPD	PBIAS	Performance evaluation	Potential [GWh/year]	Capacity factor
Agrio	79%	Unsatisfactory	1.119	0.13
Colomera	9%	Very Good	2.910	0.39
Francisco Abellán	94%	Unsatisfactory	0.276	0.04
Fresneda	-8%	Very Good	0.714	0.28
Gergal	2%	Very Good	20.546	0.48
José Torán	4%	Very Good	3.950	0.21
La Bolera	85%	Unsatisfactory	0.175	0.01
Los Melonares	6%	Very Good	17.121	0.43
Martín Gonzalo	14%	Good	0.471	0.20
Montoro III	12%	Good	3.567	0.38
Quiebrajano	45%	Unsatisfactory	0.948	0.17
Retortillo	-4%	Very Good	2.647	0.34
San Clemente	72%	Unsatisfactory	1.346	0.10

The maximum and average power generated by the NPDs in Scenario 1 and 2 are presented in Figure 28. Summarizing the maximum values for the 13 NPDs results in a total power potential of 45.33 MW and 18.86 MW for Scenario 1 and 2 respectively. In Scenario 2, Gergal is the NPD delivering the highest power of 4.95 MW, whereas La Bolera only can generate 0.18 MW. The results show that there is a significant gap between the maximum power and the average. The average power expressed as a percentage of the maximum power range from 6% to 47% for Francisco Abellán and Gergal respectively. This should be seen in correspondence with the reservoir simulation results, as the simulated reservoir of Francisco Abellán is empty half of the time whereas the Gergal reservoir is never empty, but full 31% of the time.

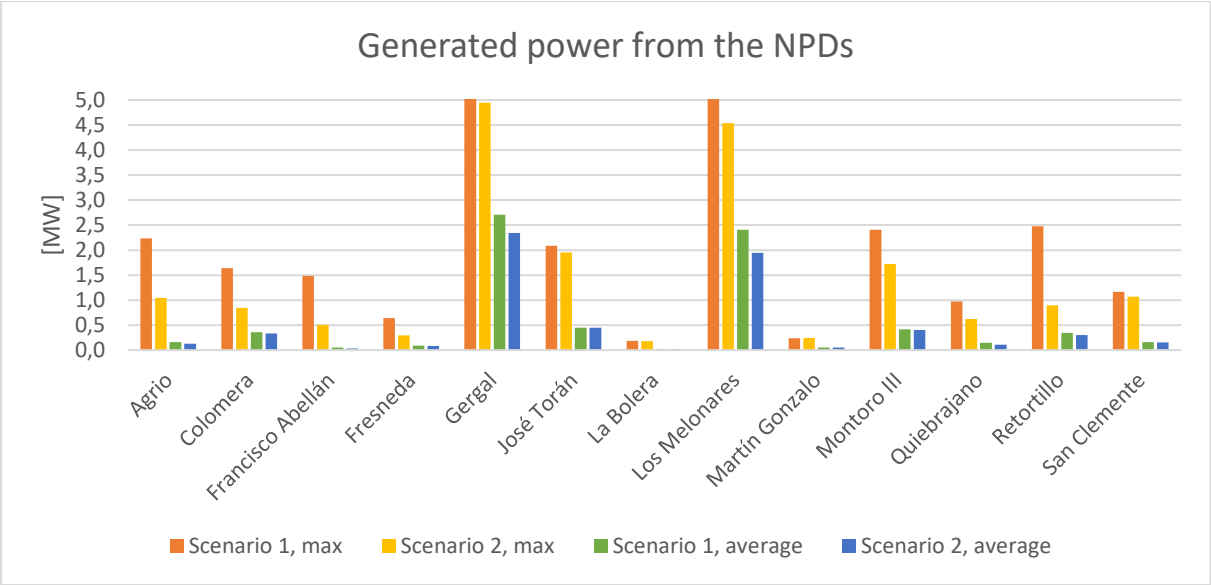

Figure 28: Maximum and average generated power from the NPDs for Scenarios 1 and 2.

The monthly averages of precipitation, water supply from the dams, and hydropower generation from the NPDs are presented in Figure 29. A pronounced seasonal variation in the hydropower generation can be observed when looking at the monthly average generation, with a clear increase in production during June-August. October is the least productive month with an average production of 2.11 GWh, whereas July is the most productive month with a production of 7.93 GWh.

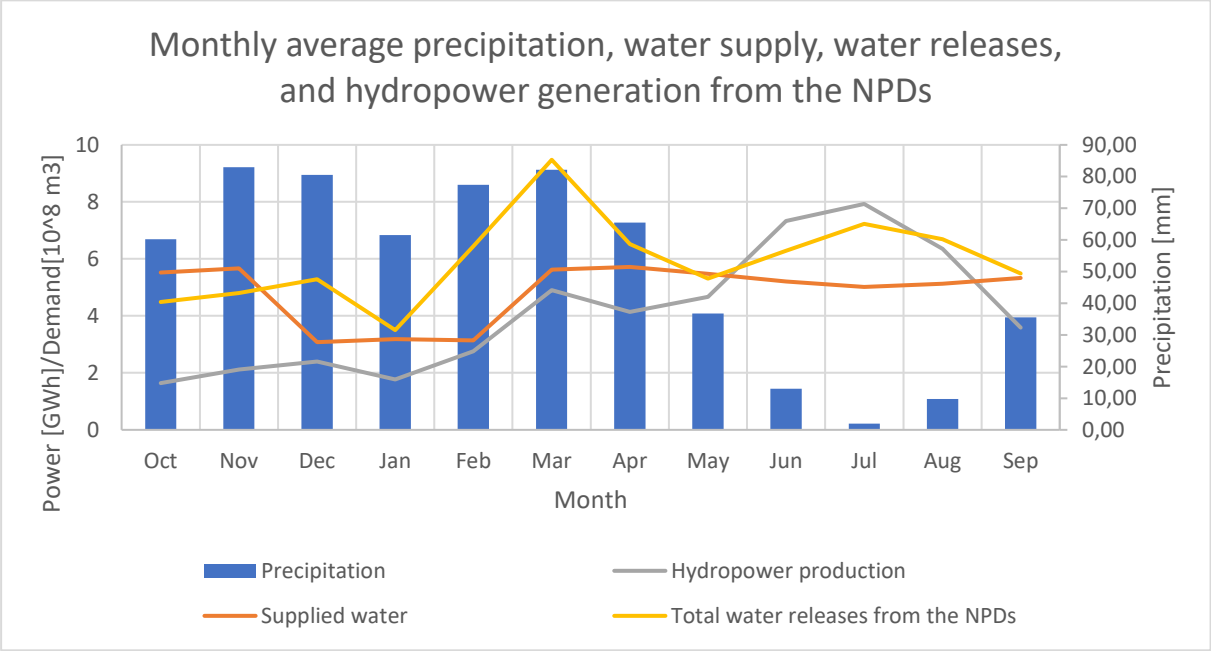

Figure 29: Monthly averaged precipitation, delivered supply, water releases, and total hydropower production of the NPDs.

Annual total hydropower generation for the different cases in Scenario 3 are presented in Figure 30. The total hydropower generation in Scenario 3 for the simulation period decreases with decreased withdrawal volumes, though the relationship is not proportional.

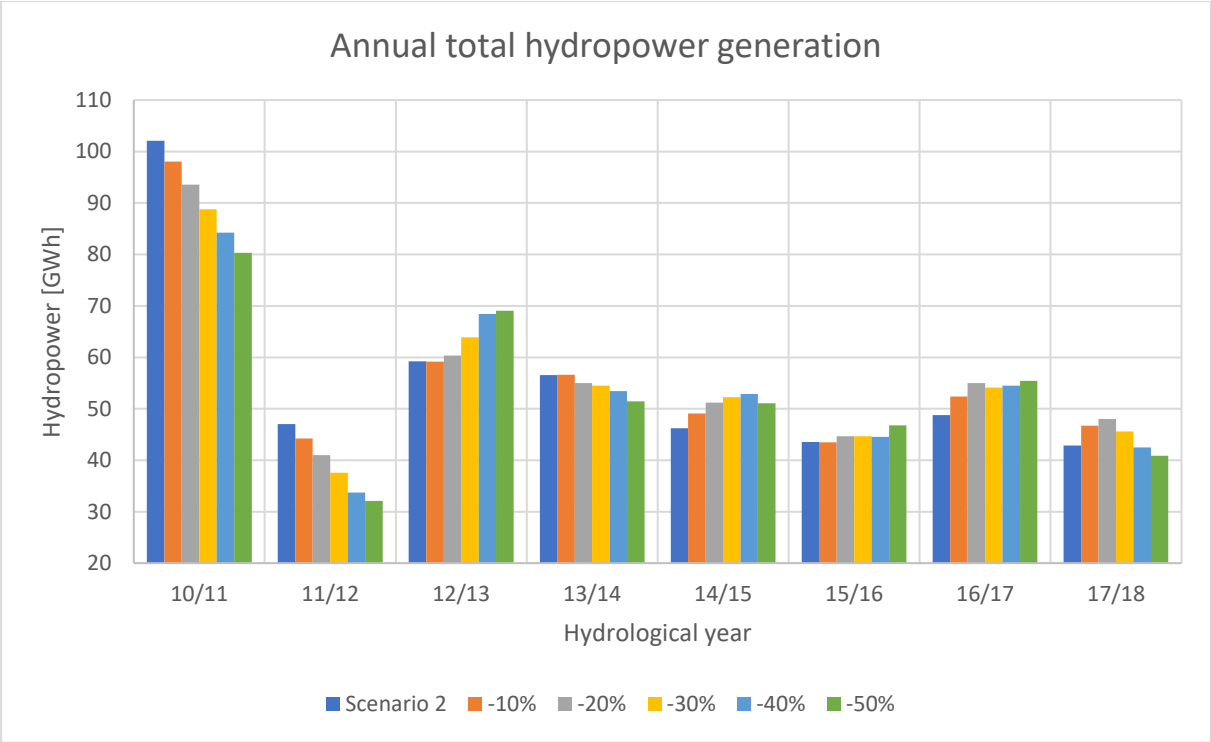

Figure 30: Annual total hydropower production of Scenario 2 and the different cases with reduced withdrawal in Scenario 3.

4.3 Economic analysis

The estimated total investment costs of the retrofitting projects span from 0.62 million EUR to 3.1 million EUR. In total, the retrofitting of all the 13 NPDs have an NPV of 6.62 million 2018 EUR. Six of the 13 NPDs have positive NPVs, and their retrofitting potentials are thus considered economically viable. Gergal and Los Melonares are the two NPDs with the biggest economic potentials with NPVs of 7.39 and 5.68 mill 2018 EUR respectively, whereas La Bolera, San Clemente and Francisco Abellán are the least economically viable projects with negative NPVs of respectively -2.03, -1.17 and -1.10 million 2018 EUR. The NPDs' sensitivity to future changes in electricity price range from 26% for Martín Gonzalo to 1741% for Retortillo. The estimated economic key numbers including capital cost, annual operation and maintenance cost, NPV, LCOE, and the absolute value of sensitivity to future electricity prices are presented per dam in Table 15.

Table 15: Economic key numbers for the retrofitting of the NPDs.

NPD	Investment cost	Annual O&M	NPV	LCOE	Sensitivity to electricity price
	[10^3 EUR]	[10^3 EUR]	[10^3 EUR]	[EUR/MWh]	-
Agrio	1260	31	-912	124	34%
Colomera	1112	28	236	42	338%
Francisco Abellán	1042	26	-1107	414	7%
Fresneda	802	20	-580	123	34%
Gergal	3102	78	7388	17	76%
José Torán	1856	46	-97	52	1110%
La Bolera	1766	44	-2033	1107	2%
Los Melonares	2984	75	5676	19	82%
Martín Gonzalo	615	15	-486	143	26%
Montoro III	1331	33	328	41	297%
Quiebrajano	971	24	-657	112	39%
Retortillo	1155	29	42	48	1741%
San Clemente	1579	39	-1174	129	31%

4.3.1 Competitiveness with other renewable energy sources

The calculated LCOE for the retrofitting of the NPDs is compared to the LCOE of other renewable energy sources (RES) from the IRENA report *Renewable power generation costs in 2018* (IRENA, 2019). A graphical comparison of the LCOE of the renewable energy sources and the 11 most profitable retrofitting projects is presented in Figure 31. From the figure, it can be seen that all the included renewable energy sources have higher LCOE than the assumed future electricity price, and thus higher than the LCOE of the NPDs calculated to be economically viable.

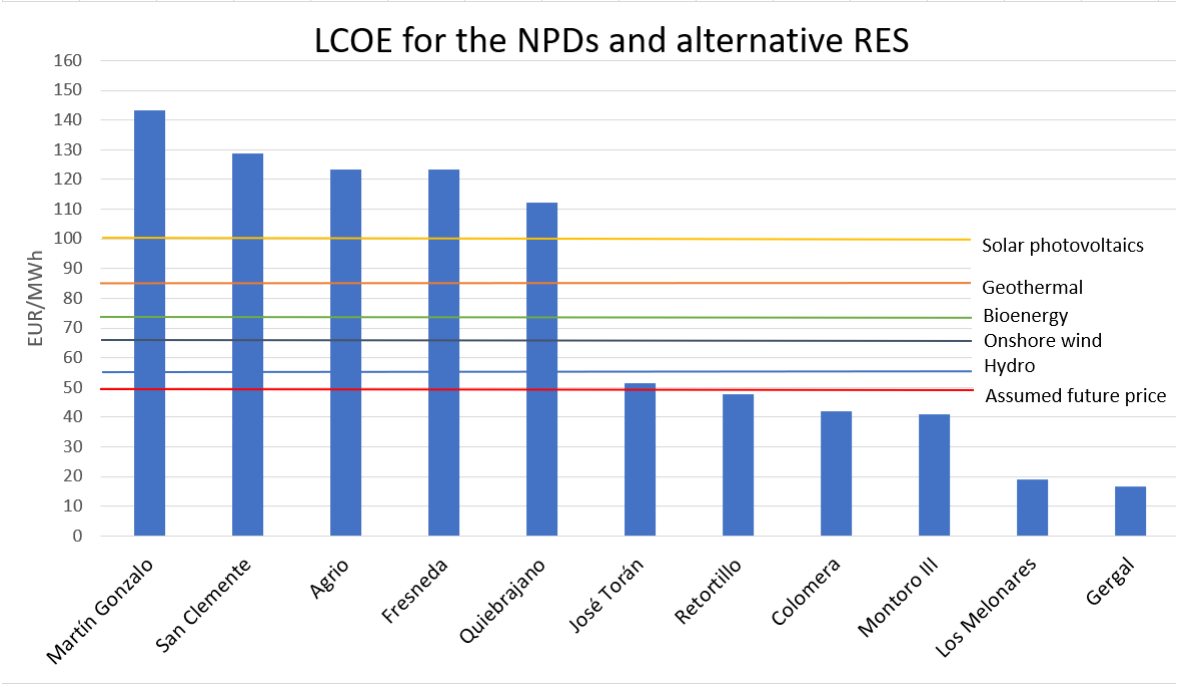

Figure 31: LCOE for the NPDs, the assumed fixed rate for the future electricity prices, and the LCOE of alternative renewable energy sources (IRENA, 2019).

4.4 Global potential

4.4.1 Resulting function

For the energy potential, the best regression is a function of the drainage area and the reservoir volume, with a corresponding adjusted R Squared value of 0.69. For the power potential, the best regression is a function of all the three characteristics with an adjusted R Squared value of 0.67. The regression analysis shows a clear relation between the hydropower potential and the drainage area. This is because the drainage area is included in both the resulting regression for the energy potential and the power potential, and is the characteristic giving the best regression fit when considered as the only parameter. Surprisingly, there was no direct relation between the dam height and the output energy or power with resulting adjusted R Squared values of 0.28 and 0.25 respectively. The resulting expressions are:

$$Energy\ potential = 11978.6 \cdot catchment\ area\ + 39.5563 \cdot reservoir\ capacity$$

$$Power\ potential = 8.79144 \cdot catchment\ area\ + 0.05882 \cdot reservoir\ capacity\ - 63.677 \cdot dam\ height,$$

where the energy potential is given in kWh, the power in kW, the drainage area in km^2, the reservoir volume in 10^3 m^3 and the dam height in m. The units correspond to the units in the ICOLD register.

The simulated potentials in WEAP for the satisfactory simulated NPDs are presented in Figure 32 beside the potentials calculated by the chosen regression expressions from the regression analysis. It can be seen that the power potentials from the regression become negative for the dams simulated to low power potentials in WEAP. Compared to the WEAP simulations of the eight satisfactory modelled NPDs, the estimates based on the regression expressions cause a 15% bigger potential regarding the energy and a 3% smaller potential for the power.

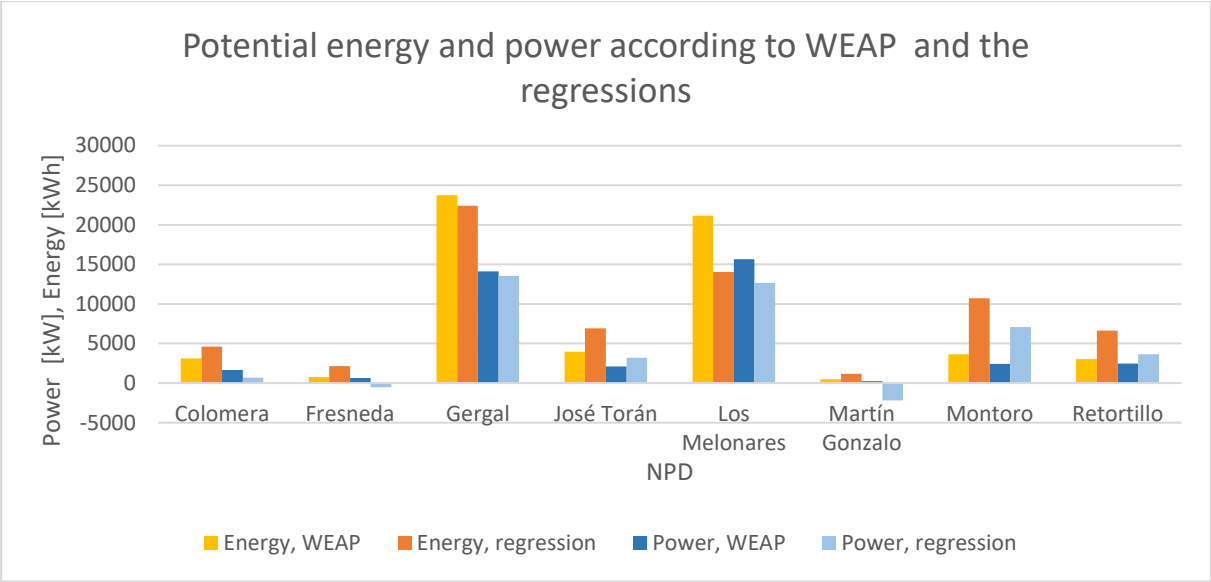

Figure 32: Potential energy and power as simulated by WEAP and as calculated by the regression.

4.4.2 Resulting potential

The potential of retrofitting the NPDs in Spain from the ICOLD database is calculated to 4 623 GWh and 2 413 MW when using the regressions and excluding the negative power potentials. Based on the average electricity consumption of a Spanish household, the estimated potential is enough to supply 440 293 households. Out of 29 163 registered NPDs in the global ICOLD database, 10 914 dams are registered with dam height, reservoir capacity, and catchment area, and thus included in the estimation of global retrofitting potential. This results in a global retrofitting potential of 233.77 TWh and 170.23 GW.

For evaluation of the regressions and the resulting potentials from the model simulations, these values are compared to the official installed capacity and the regression results of the currently powered dams. The maximum produced power for the seven dams, their official capacity, their capacity estimated by the regression, and the simulation performance of the fillings of their corresponding reservoirs over the total simulation period are presented in Figure 33. The modelling results are independent of scenario, as the currently powered dams are implemented in the model with the same official characteristics in all scenarios. It can be read from the results that the simulated potentials for some of the dams are very close to the official capacities, whereas others are clearly overestimated or underestimated. The potentials based on the regression overestimate all the power potentials. The overestimations range from 18% for Iznajar to 247% for Guadalén, supporting that the dams with lower installed capacity are more prone to overestimation than the dams with higher installed capacity.

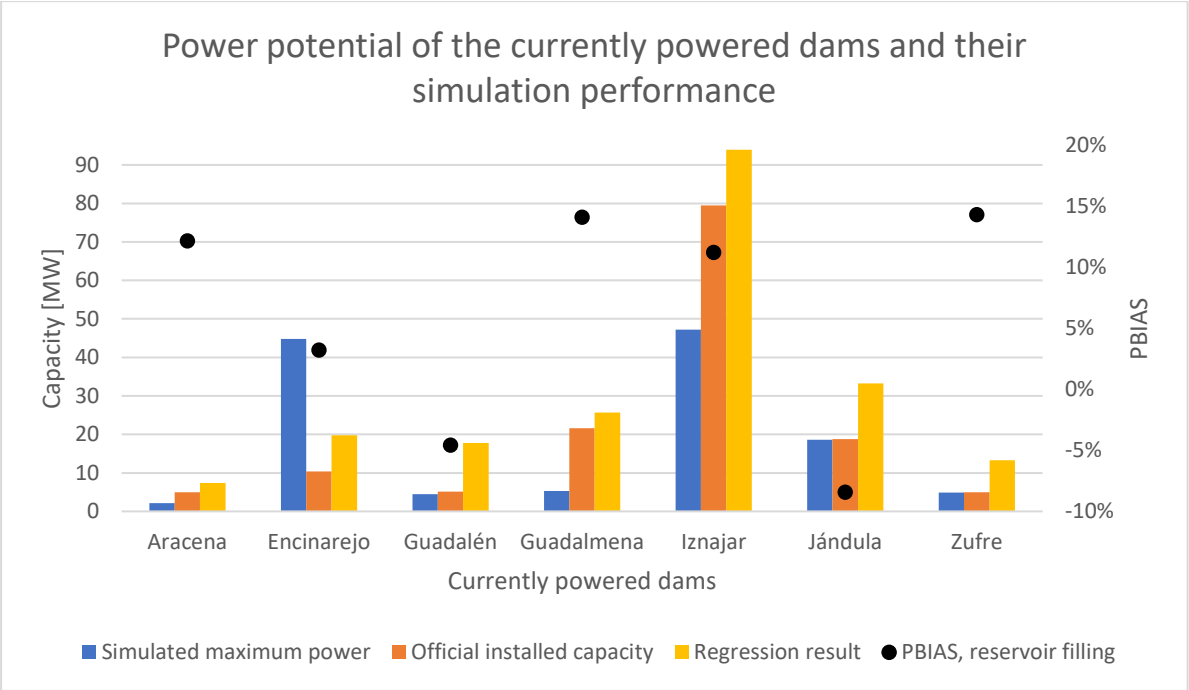

Figure 33: Simulated maximum capacity, regression based capacity and official capacity of currently powered dams in addition to the simulation performance of their corresponding reservoir fillings over the total simulation period.

5 Discussion

This section serves to clarify and discuss the assumptions, limitations and uncertainties in this study. It first assesses the quality and the interpretation of the input data before highlighting simplifications and assumptions made in the method, and how verifications of the results can be performed. Then, the results and possible effects of future changes that can affect the results are discussed. Last is a discussion of the upscaling of the retrofitting potential and other possible methods with corresponding requirements of input data and suggested topics for further research.

5.1 Limitations and uncertainties

5.1.1 Input data

The temporal resolution is set to monthly timesteps, despite WEAP allowing for a daily resolution. The monthly timestep is chosen in order to fit the resolution of wind and humidity data and the uncertain water demand pattern given an estimated monthly variation. A monthly resolution allows for taking seasonal variation into account but is not sufficient to consider the daily- or hourly variations in water and electricity demand. With the calculation method in WEAP, the monthly resolution results in the assumption that the discharge from the dams can flow constantly at the required rate to satisfy the demands and that all the inflow to the dams is available from the beginning of the month. A constant flow is better than a highly variable flow with regard to the flow rate dependent efficiency of the turbines. Since it is unsure whether monthly constant flows are realistic or not, this might be a contributing factor to overestimated potentials.

The electricity grid may require power input at different times than the existing water demands which drive the power generation. A mismatch between demand patterns have been proven in other studies to cause load rejections depending on the grid size and other energy sources on the grid (Patsialis et al., 2016). If the grid network has a relatively big capacity, as it can be assumed for an area as populated as Guadalquivir, load rejections are assumed to be unlikely. This is however impossible to model with WEAP as an hourly resolution would be necessary, and this issue is therefore not assessed in this study. In cases with a need for more detailed energy system analyses, the LEAP energy model can be coupled with the WEAP model.

The spatial resolution of the gridded data from CRU implies limited accuracy due to the grid size of 56 x 56 km. The WEAP model is a semi-distributed model, which in this case means that input data and calculations are distributed between the catchments but averaged within each catchment. The spatial resolution of the climate data is therefore considered suitable for this WEAP model, as the accuracy is further limited by the WEAP model itself when aggregating climate data to represent each of the catchments with average values. This eliminates the effect of topographic variations and local weather phenomena inside the catchments. However, the choice of using a monthly resolution instead of a daily resolution is assumed to reduce these possible effects and thus represent the catchment response with a suitable accuracy for this model.

Measurement errors can affect the fit between simulated and observed values and thus affect the model performance evaluation. Measurement errors might more frequently impact the evaluation of streamflow than reservoir volumes, as errors such as sudden peaks in reservoir volumes may be easier to detect and correct than erroneous peaks in streamflow. In this study, observed streamflow values for the calibration are checked for obvious errors and modified, and

further errors are considered negligible. The overall error at Alcála del Río is assumed be minimized due to the inclusion of the large number of reservoirs in the model upstream of the streamflow measuring point. With regard to measurement errors, the total reservoir filling is considered a more reliable indicator than the individual reservoir fillings. This is because the total reservoir filling represents all the 50 monitored reservoirs with continuous time series of measurement, and the measurement errors are therefore assumed to be balanced out.

The included volume of water withdrawals in the model is uncertain despite being based on the dataset covering all the licensed withdrawals from the official authorities. This is supported by the observation that the value of the total water withdrawals is bigger than the official values of total water consumption in Guadalquivir even when considering the assumed consumption rate. In total, the water withdrawals included in the model sum up to 6282.5 hm^3, which results in a consumption of 4397.8 hm^3 when accounting for the fixed consumption rate of 70%. For comparison, the water consumption was of 3350.2 hm^3 in 2016/2017 according to MITECO (Ministerio para la Transición Ecológica, 2018), and of 3356.8 hm^3 in 2015 according to the local water authorities (CHG, 2015). The difference may be caused by several reasons; authorized withdrawal allowances may not be used to their full potential or has been misinterpreted by the author, water restrictions may have been applied for specific uses due to periodically less available water as shown in Figure 26, or the consumption rate may be lower than what is assumed.

From the results of Scenario 3 shown in Figure 30, it is uncertain what the impact of overestimated water demands may be on the hydropower generation. It is however likely that reduced withdrawals may cause a bigger flexibility to the water regulations, as more water can be stored for use during optimal periods for hydropower production. In the model setup for Scenario 3, the withdrawals are reduced incrementally by 10% starting at 10% and ending at 50%. Official numbers state that the water consumption is foreseen to slightly decrease from 3356.8 hm^3 in 2015 to 3225.9 hm^3 in 2027 (CHG, 2015). This corresponds to a decrease of almost 4%, thus significantly less than the reductions simulated in Scenario 3. Reductions of the scales simulated in Scenario 3 can therefore be seen as unrealistic for normal hydrological years but may be more representative for years of drought and water restrictions.

The essential dam characteristics are included in the model after interpretation of the official information, but some simplifications have been done due lack of data. Dead volumes and flood protection volumes, defined as inactive zone and flood control zone in Figure 4, are not included in the model as this information was lacking for several of the dams. On the one hand, water demands may therefore cause the reservoirs in the model to completely empty. On the other hand, lower water demands can result in the reservoirs being kept at full capacity and thus represent a bigger risk of flooding. The implementation of dead volumes will cause less water availability, whereas the implementation of flood protection volumes will cause less spill of water via the spillways. The effect on the hydropower potential of merging the different reservoir zones into one therefore needs to be analyzed for each specific case.

Internal transfers are also excluded from the model since no complete information about the subject has been found. This simplification may possibly alter which geographical areas that experience water shortages as available water in the modelled reservoirs only can serve the demands situated downstream of the reservoirs. Due to the same reason, the catchment's ability to balance the underestimated and overestimated reservoir volumes is limited. Information regarding the internal transfers could possibly have been collected from the local water authorities but were not collected for this study. This is seen as one of the advised improvements of the model for further studies.

5.1.2 Method

WEAP is chosen as modelling tool for this study due to its strength of including different water uses into a hydrological model. WEAP can include different water demands such as water for hydropower generation, water for environmental flow requirements, water for refilling of the reservoirs and other water uses implemented as individual withdrawal nodes. The possibility of assigning priorities to the different water uses is especially useful for this study. This is because the hydropower generation at NPDs then can be given a lower priority than the existing water demands, and thus be modelled as a function of these. The division into different water demands has also allowed for the analysis of the scenario concerning reduced withdrawals, without having to modify the water demands from the neighboring basins and the environmental flow requirements.

The choice of using WEAP is done despite knowledge of its weaknesses considering the lacking complexity of the hydropower calculations. The hydropower calculations do not account for varying turbine efficiency with varying discharges and do not allow for the implementation of several turbine units in one hydropower plant. In addition, the choice of using monthly timesteps causes the head and the available flow at the start of the month to be modelled as constants for the whole timestep without considering possible time-specific demands and changes in water elevation. In more detailed studies, a more complex hydropower routine should be sought after, but WEAP is found to be suitable for the rough estimates resulting from this study.

Several other studies have been carried out to estimate the hydropower potential of NPDs in different regions, at different scales, and with different strengths and weaknesses. One of these studies developed a model considering the technical, legislative, financial, social and environmental aspects of retrofitting for the evaluation of the feasibility of retrofitting at existing dam sites in South Africa (van Vuuren et al., 2011). A significant part of the feasibility evaluation is based on the legislative considerations, both including the probability of getting an allowance for the projects and the costs of getting this allowance. Ratings are given to the different aspects of the feasibility based on developed tables of criteria, and the scores for the different aspects are combined to an overall evaluation. The biggest strength of this model is considered to be this combined focus on the different aspects of retrofitting, ensuring that the estimated potential is realistic. Applying this model to the Guadalquivir basin would require a deeper insight in the local legislative regulations, social acceptance, and environmental vulnerability than what was considered the scope of this study.

Another study has estimated the nationwide potential for retrofitting in the U.S. to 12 GW and 45 TWh (Hadjerioua et al., 2012). Similar to this case study, the American study used a monthly timestep for the hydropower calculations but chose to let the gross head be constant and thus independent of the upstream water level. Furthermore, the available flow was estimated equal to the monthly average flow for the different dam sites. To account for these unrealistic estimations, regional capacity factors were developed from data for existing hydropower plants and applied to the NPDs. By using GIS coupled with national dam registers, more than 54 000 NPDs were assessed. The main improvement suggested by the study is the inclusion of economic constraints to the possible retrofitting in order to find a more realistic potential. A WEAP model would be too extensive if it was to cover areas close to the size of the U.S including such big numbers of dams, but the advice of including economic considerations has been followed up in this study.

The calibration method is based on the calibration results of three smaller, unregulated catchments within the Guadalquivir basin. Their size is limited to only include unregulated areas

of the catchment and thus avoid possible detention of water flow due to regulated reservoirs. Small areas situated as close to each other as these calibration catchments are likely to include less variation in topography and climate than bigger areas covering different parts of the basin. Based on a GIS analysis of the topography and land cover in the basin, the three catchments are found to be representative of the middle part of the basin. The calibration catchments do not cover the low flat lands nor the high mountain ranges. The highest mountain ranges are known to be snow covered part of the year, and the exclusion of similar altitude for the calibration might oversee the adjustments needed for a better modelling of the snow processes in the river basin. The share of olive groves in the calibration catchments is also found to be bigger than for the Guadalquivir basin, which is likely to result in a calibration causing a different response to precipitation than what is representative for the rest of the basin. A calibration of a more representative area or several areas with different characteristics would likely improve the fit of the calibrated parameters with the more diverse basin.

The time period for the simulation is from October 2009 to September 2018, whereas the calibration period for the calibration catchment is set from 1st of January 2017 to 31st of December 2019. From the observed streamflow at the measurement gauge at Alcála del Río presented in Figure 19, it can be seen that the observed streamflow peak in December 2010 is approximately 3 times bigger than the observed streamflow peak in March 2018 which is the biggest peak in the calibration period. Furthermore, it can be seen that the calibration model in general performs best during the periods of moderate stream flows and tend to underestimate the peaks and overestimate the lower flows. A longer calibration period covering the peaks in 2009 and 2013 could possibly result in a better fit for the extreme values, even though the overall performance is considered satisfactory.

In addition to the uncertainties linked to water withdrawals as described under *Input data*, the placement and seasonal variations of the water withdrawals also represent a noticeable uncertainty. Despite the geographical placement of the withdrawals being given in the dataset, they are aggregated for the implementation in the WEAP model and placed upstream or downstream of the NPDs. The aggregation is based on their location, and not on information about which sources they are actually taken from. This can contribute to a geographical alteration of water shortages as for the exclusion of internal transfer.

The seasonal variations in the withdrawal demands are chosen to follow the assumed pattern for crop water need since agriculture stands for more than 80% of the total water consumption. The selected crop coefficient causes the water demands to be almost double the amount during the summer months than during the winter months. The pattern seems however to fit well with the results of the reservoir simulations presented in Figure 21 and Figure 26. The simulated peaks and lows of the total reservoir fillings fit month by month with the observed volumes, being consistently one to two months ahead of the observations. This supports the assumed seasonal variation, but also suggests that the pattern should be considered delayed one month compared to the consumption pattern of olives according to the FAO report 56.

Snow and groundwater processes are highly simplified in the model. There is no initial snow cover included in the model setup, and the melting and freezing points are not calibrated to the catchment characteristics. In the results of the model simulations, there is no stored snow on a monthly basis. A delay in available water due to snow accumulation during the winter and snow melt during the spring may thus be underestimated in the model. The snow accumulation and melting processes are however considered negligible in this study as they are assumed to balance each other out during the hydrological year, and are only likely to occur in the highest mountain ranges of the basin. The temporal delay due to groundwater is also assumed to be balanced out over time. If assuming that the groundwater stays within the basin during its whole

hydrological cycle, the implementation of separate groundwater routine is likely to only result in a more accurate timing of available water.

Several simplifications are also included in the economic analysis, such as the choice of including the construction of new intakes and waterway structures. The new technologies specially developed for retrofitting projects have not been considered in the economic analysis. This is both due to a lack of information about the dam sites and how these technologies can be fitted to each site, and because the costs of these solutions have not been found. On one hand, the solution of new intakes and waterways may be more expensive than retrofitting the original outflows of the dam using traditional or new technologies. On the other hand, the solution of new intakes and waterways is assumed to generate more power, and thus revenues. The increased power generation is due to possible reduced head losses in the new waterways and the collection of several smaller outflows into one bigger. The replacement of existing valves with turbines might result in more profitable power production because of the minimal costs, but do also require better technical information about the existing structures. A proper site visit or meeting with the engineers responsible for the dam structures is considered necessary in order to develop specific technical solutions for each of the dams, and specific costs could be collected directly from suppliers for more accurate estimates.

The cost of transmission lines is excluded because of uncertainties regarding the existing grids concerning their condition and distance from the NPDs. This cost may be significant if the distance to the nearest existing grid is long (IRENA, 2012), and may turn an initially profitable project into a loss for the developer. It is important to keep this in mind when comparing the LCOE for the different renewable energy sources presented in Figure 31, as the values from IRENA are assumed to include transmission lines of unknown lengths. Developing projects of bigger power plants like solar parks and wind farms will however also require transmission lines, and the cost of transmission lines can in a direct comparison with retrofitting then be disregarded.

The included electricity prices are assumed to exclude taxes and be representable for what a power producer can count as revenue. A comparison of the electricity prices from the nominated electricity market operator (OMIE) with electricity prices from the official electrical system operator (ESIOS) (Red Eléctrica de España, 2020) show almost identical electricity prices for the simulation period. The electricity market in Spain consists of a day-ahead market, an intra-daily market, and a balancing market (OMIE, 2020b). In addition to the main part of the revenues coming from the day-ahead market, further revenues from the two other markets are available for the power suppliers that are able to balance the grid when the power supplied from other sources is fluctuating. Hydropower is considered a power source that can both provide base load and peak load with the quickest response time among the current technologies (IRENA, 2012). Realistic electricity prices for hydropower plants are therefore likely to be higher than the average electricity supply price. As a result, it is assumed that the included prices are representative estimates, and close to the most accurate values that are possible to obtain.

Future electricity prices are uncertain as they are a function of many different factors. This make them hard to predict and are in some power projects seen as the biggest source of risk in power projects (Noothout et al., 2016). A fixed rate equal to the average price during the simulation period is chosen since no official forecasts were found. Spain has also experienced a rapid growth in renewable energy sources and thus had to restructure their energy market and tariff system (Deloitte Conseil, 2015), increasing the uncertainty regarding future prices.

Several assumptions made in the model limit the possible potential of hydropower generation compared to the maximum technically feasible potentials. First, the decision of only using the

HRWL and the tailwater elevation for the estimation of available head is likely to eliminate several options where new penstocks or tunnels with outlets further downstream could have been advantageous for the power production. However, such solutions are also seen as likely to have a bigger environmental impact on the surroundings. This is because parts of the downstream river may get by-passed and dry more frequently out than when using the original outlet, in addition to the more extensive construction work. Furthermore, water demands located between the dam and the new outlet would either have to be supplied separately from the reservoir and hence reduce the available water for power production, or require the construction of waterways with pump capacity from the new outlet.

Second, it was chosen to not optimize the water regulation for hydropower generation nor increase the reservoir volume by engineering methods. Instead, the releases are based on the initial water demands and the reservoirs are modelled with their original capacities. Not altering the water regulations implicitly means that the food production and other water demands are considered more important than possible electricity production, whereas not increasing the reservoir capacity benefits the land currently used for other purposes. Despite reducing the potential, these limitations eliminate the arguments of retrofitting projects further impacting the environment and introducing another competing water demand.

Of these limitations and uncertainties, the water regulation strategy, the unknown transfer possibilities between the reservoirs, the seasonal variation of the water demands, and the calibration of the model are considered to be the most influential. The biggest limitation to the estimated feasibility of the assessed retrofitting projects is considered to be the exclusion of the legislative aspect and the cost of possible transmission lines.

The method has several strengths that can be useful for further research. Having included the entire river basin in the model allows for analyses of the dependency between the existing water demands and the hydropower generation. In turn, this enables the creation of different scenarios which can consider multiple modifications to the current situation, such as reduced withdrawals, climate change and changes in the priority given to the different water demands. There will always be a retrofitting potential at NPDs that serve downstream demands, but the economic analysis provided in this study might convince water authorities and possible hydropower developers that several of these cases also represent an economic potential.

5.1.3 Verfication strategy and possible improvement of the WEAP software

There are several ways to verify and improve the estimated retrofitting potential from this study. A verification strategy aiming to address the main uncertainties is outlined by the following points:

- A meeting with the local water authorities, the responsible engineer, dam owners and local politicians should be prioritized. This is advised to be the first step in order to clarify the technical and strategical details of the water management and unveil possible barriers.
- Second, an inspection of the dam site should be carried out. The aim of the site inspection should be to find the realistic gross head and possible technical solutions for the retrofitting based on the conditions of the dam and its surroundings.
- Third, a daily timestep should be considered. This modification is likely to result in more precise estimates of the hydropower generation and more accurately analyze the compatibility of hydropower and the existing water demands.
- Since there are such big amounts of available measurement data online provided by the local authorities, more detailed calibrations of the individual catchments within the

basin are possible yet considered to be very time consuming. This is therefore likely to only be relevant in more detailed studies.

Some suggestions for further improvement of the WEAP software have been discovered during this study. WEAP does not allow for the implementation of several turbines connected to one dam, nor a discharge dependent generation efficiency to the knowledge of the author. Replacing existing valves in intakes with turbines may in some cases be the most cost-efficient alternative for retrofitting NPDs. In such cases it might be possible to replace valves of different sizes by turbines or to install several turbines to the same dam using different solutions. Using several turbines independent of technical solution also allows for the optimization of the power generation since the generation efficiency is a function of discharge. With several turbines, it is possible to stop one or more turbines in order to obtain discharges through the running turbines as close to the optimal value as possible. With version 2019.2 of the WEAP software, it is possible to code the generation efficiency to be dependent on the reservoir level of the last timestep, as done to make the hydraulic capacity dependent on the reservoir level. This method has not been possible to adapt for a generation efficiency dependent on the discharge. The possibility to simulate several turbines per hydropower plant with discharge dependent efficiencies would be a significant improvement of the hydropower routine in WEAP.

The possibility of specifying different source files for the aggregation of gridded climate data in the automatic catchment delineation mode would simplify the data processing of the input data. The chosen climate data sets from CRU provides the different variables in separate NetCDF files, and modification of these files requires third party software. The self-developed method used for merging the precipitation, temperature, and cloud cover data from CRU in this study requires a manipulation of the automatic catchment delineation mode to generate csv files that can be merged manually using Excel. To avoid the mode from overwriting the aggregated climate data from CRU, the mode must be deactivated, and the climate data entered as manual input files in csv format. Several of the global datasets are provided as NetCDF files, and for models requiring many variables in different NetCDF files, this is an unnecessarily time-consuming method. A possibility to specify different source files for the different input in the catchment delineation mode would therefore be a time-saving improvement.

5.2 Results of case study

The varying modelling performance for the different NPDs naturally cause varying quality of the estimations of the hydropower potential. It should however be highlighted that all the NPDs with positive NPVs are found to be satisfactorily simulated. The NPDs with high bias compared to observations are in all the cases considered to have an underestimated potential, as the reservoir volumes are clearly underestimated. The reservoir volumes are not as representative for the potential as the outflow, since the volumes of outflow that empty the reservoir can still generate power. However, the dams with underestimated reservoir volumes are empty in a considerable amount of time according to the simulations, and there is a proven amount of unmet demands downstream the corresponding dams, as presented in Figure 24.

The calculated capacity factors for Scenario 2 can be used to evaluate how realistic the chosen turbine capacities are for the different NPDs regarding economic considerations. The capacity factors from currently powered dams are assumed to represent hydropower plants with optimized production. These are expected to be higher than the resulting capacity factors from the case study, as the case study does not consider optimization of the water releases but rather follow the release pattern from the existing demands. The American study of the retrofitting potential in the U.S. calculated regional capacity factor based on the currently powered dams in the different regions. The resulting values ranged from 0.25 for the Texas-Gulf to 0.67 for the

Great Lakes (Hadjerioua et al., 2012). When comparing these values to the simulation results, the capacity factors obtained from the simulations are overlapping with the values form the American study as they range from 0.21 to 0.48. The fact that they lay a bit lower is as expected, and the comparison thus support the method used for turbine capacity selection.

The choice of turbine capacities for Scenario 2 is further supported by the simulation results regarding energy and power potential. From Figure 28, it can be seen that the power capacity is significantly reduced for several of the NPDs in Scenario 2 compared to Scenario 1. However, the annually averaged energy generations for the two scenarios presented in Figure 27 only show a slight decrease resulting from the reduced turbine capacities. This shows that the turbine capacities for Scenario 2 are sufficient to exploit the majority of the annual water releases despite not being able to generate power from the maximum discharges form the dam. As a result, the turbines in Scenario 2 generate more energy per installed MW than Scenario 1, and are therefore considered to be closer to a cost-optimized solution.

The results concerning the currently powered dams show overall satisfying simulations of the reservoir fillings. The overall performance and the individually well simulated reservoir fillings support the reliability of the estimated of retrofitting potentials. Despite this, the estimated power potentials for the currently powered dams do not represent a distinctive trend, as presented in Figure 33, and cannot be used to assume whether the hydropower potential of retrofitting the NPDs might be overestimated or underestimated. This inconsistency is most likely due to a combination of unknown water regulation strategies, generation efficiencies and effective head. Regulation strategies can optimize the water releases to generate a maximum power output, different turbine types cause different generation efficiencies, and different head losses cause varying effective head. Another important point is that the monthly resolution causes WEAP to calculate the monthly maximum power, rather than the hourly maximum which is likely to be higher. All in all, the results from the simulations of the currently powered dams can both be considered to support the estimated potential and highlight the uncertainties related to the individual differences between the dam sites.

The results from Scenario 3 show that the hydropower generation decreases with decreased water withdrawals with a non-proportional relation. This is as expected due to two settings in the model. First, the water for hydropower is limited to the water being released from the dam to supply the existing purposes. Decreased releases can therefore result in less hydropower. Second, dam releases have a lower limit set by the environmental flow requirements which will be supplied regardless of further reduced water demands as long as there is available water. As a result, the hydropower generation can decrease due to reduced withdrawals just to the point where environmental flow requirements dominate.

The inconsistency in which of the five cases in Scenario 3 that generates the most hydropower from year to year can be explained by the different evolutions of reservoir fillings from case to case. The reservoirs will supply all the demands possible based on their current storage, and they will therefore be able to store different amounts of volume from year to year dependent on the withdrawal case. In years with relatively much available water, the water supply will be sufficient to meet the demands in all of the five cases and thus produce decreasing amounts of energy for decreasing demands, which is shown for the two first years. After these two years, several of the reservoirs have less available water to meet the demands, and the hydropower production therefore varies from year to year dependent of the refills from the precipitation.

The average monthly hydropower production presented in Figure 29 is expected to follow the water demand and thus the amount of releases to a certain degree. The deviation in the pattern of power production and the water demands can however be explained by the spatial

distribution of the reservoirs and the model performance. As seen on the figure, the total water releases show two peaks that explain the hydropower production, but which do not follow the water demand. The peak in March is caused by releases of excess water from full reservoirs after the rainy months. There is also a peak in hydropower production in July that do not seem to correspond to the amount of supplied water. The dip in water supply during the summer months is contradictory to the implemented seasonal variation based on the crop coefficients, and is the result of the unsatisfactory modelled reservoirs and their unmet demands. The two NPDs producing the most power (Gergal and Los Melonares) are however satisfactory modelled and the peak in hydropower production in July is mainly due to the releases from these two NPDs. Their hydropower productions peak is in July when there is increased demands and the reservoir levels still are high, which support this explanation.

The comparison of the costs of the retrofitting projects with the costs for other renewable energy sources from IRENA cannot be directly compared. This is due to uncertainties of what costs are included in the numbers from IRENA and the uncertain costs of transmission and grid connection for the retrofitting projects. It is assumed that the cost of transmission is included in the IRENA calculations, but no details about the length of transmission or other aspects are known. It can however be seen that the six retrofitting projects with the lowest LCOEs are found to have a lower LCOE than all the included renewable energy sources. In contrast to the LCOE representing the necessary electricity price for the costs to equal the benefits, the NPV is dependent on specified future electricity prices. With the assumed fixed rate for the future electricity prices applied to the NPV calculations of the retrofitting projects, none of the renewable energy sources technologies presented in the IRENA report are profitable in Spain. This both shows that renewable energy sources may be dependent on political support and the accounting of additional benefits to compete with other energy sources, and that retrofitting of NPDs possibly can compete with other renewable energy sources.

The sensitivity analysis of the retrofitting potentials of the NPVs regarding future electricity prices shows that there is no clear relation between the magnitude of the investment costs or the NPVs, and the resulting sensitivity. Both the two most sensitive NPDs and the two least sensitive NPDs are found to be economically unviable. Gergal and Los Melonares are the NPDs with the highest NPVs and highest investment costs, and show a sensitivity to changes in future electricity price of about 80%. Due to the uncertainty regarding the future electricity prices, the NPD considered safest to retrofit may be Gergal since it has the highest NPV and the lowest sensitivity to future electricity prices of the economically viable NPDs.

5.3 Future opportunities and challenges

Projected climate change is expected to cause a global increase in hydropower production due to bigger annual volumes of precipitation and runoff (Kumar et al., 2011). However, climate change is foreseen to cause alterations of the precipitation distributions with significant geographical differences rather than an increase in all regions. In Southern Europe, the precipitation in semi-arid areas is expected to decrease (Kovats et al., 2014), comprising the area of the Guadalquivir basin. This means that less water might be available for exploitation and consequently cause more frequent water shortages of longer durations. An example of the effects of decreased rainfall was observed in 2017 when several hydropower plants had to be closed and the hydropower production in Spain decreased by 33% from the year before (Marín and García-Marín, 2019).

On the other side, improved irrigation techniques may cause more available water in the basin. This water can be used in several ways, including the optimization of surplus water to fit hydropower generation. In periods with more available water than needed to supply the

reduced demand, the water can be stored in the reservoirs in order to increase the water level and thus gain a bigger head. This must however be evaluated with regard to flood risk, as higher reservoir levels might cause a higher risk of flooding in cases of extreme precipitation events. For the case of Guadalquivir, a further improvement might however be limited, as the local water authorities already have invested heavily in water saving technologies and strategies (Berbel et al., 2015) and the agricultural activity must be considered to remain somewhat stable in terms of total water volume needed in the future.

A growing population must also be considered, as this will increase the water demand if the water consumption per capita does not decrease proportionally. Even if the estimated person equivalent of 230 liters per day per person is kept stable, the domestic water demand is foreseen to increase from 379 hm^3 per year in 2015 to 416.4 hm^3 per year in 2027 (CHG, 2015) due to population growth. In the Guadalquivir basin, the domestic water demand is small compared to the agricultural water demand and the growth only represents a 0.85% increase compared to the total annual consumption of 4397.8 hm^3 included in the case study. A possible population growth is therefore considered to have a minimal impact on the overall water demands.

The economic aspect of renewable energy sources such as hydropower depend in many cases on political decisions regarding taxes and subsidies, in addition to the traditional competition with conventional energy technologies. Which energy sources that are considered renewable and get supported with subsidies vary from country to country, but small hydro (<10MW) are generally more accepted than large hydropower projects (Khare et al., 2019). Studies have shown that retrofitting projects might depend on getting the same economic support as other renewable energy sources in order to be financially viable for the developer (Sandt and Doyle, 2013). Even though taxes and subsidies are important for project profitability, they do not affect the economic viability i.e. the profitability for the society as a whole.

CO_2 certificates and other additional benefits to the direct revenues from electricity sales are excluded from both the calculations in this study and the calculations in the IRENA report. Future subsidies are however more uncertain with the current situation in Spain (Bianco et al., 2019). One of the main reasons for this is that Spain has been struggling to provide promised subsidies due to an unexpectedly rapid growth in renewable energy sources (Deloitte Conseil, 2015). When including the additional benefits of renewable energy sources such as hydropower retrofitting and accounting for the decreasing trend in their commissioning costs (IRENA, 2019), the economic competitiveness with conventional energy sources is likely to be stronger than presented in this study. A more thorough evaluation of the future additional benefits is however beyond the considered scope.

The retrofitting potential of the U.S has been assessed and the country has several retrofitting projects under development. The Red Rock Hydroelectric Project is of special interest because it demonstrates the possibility of drilling a new waterway through the existing dam structure and is planned to operate on what they call a “run-of-release” mode (Missouri River Energy Services, 2019). This mode corresponds to the main assumption made in this study of only using the releases made for existing water uses. The retrofitting potential in the U.S. is estimated to 12 GW (Hadjerioua et al., 2012), and the American Office of Energy Efficiency & Renewable Energy published in May 2020 a “New Round of Hydroelectric Incentive Funding (…)” of 7 million U.S. dollars from the Water Power Technologies Office, also available for retrofitting projects (Office of Energy Efficiency and Renewable Energy, 2020). This supports the idea of retrofitting being a realistic hidden resource, and the projects in the U.S. may serve as useful examples for the technical planning of future retrofitting projects in Europe.

An ongoing study is being carried out by the IEA Hydropower (International Energy Agency). The study had official start date in 2018, but no published results have yet been found. The topic of retrofitting is to be covered under the subtask 3 "*Adding Power to "Non-power Dams" and Water Management Facilities*". The potential of retrofitting is also listed as an untapped potential of special interest by Hydropower Europe (Hydropower Europe, 2020). This demonstrates the actuality of the topic and the need for further research.

When studying the potential of retrofitting the NPDs, it must be questioned why these NPDs initially were built without a hydropower generating unit and why retrofitting may not be realistic today. Political concerns such as environmental restrictions (Punys et al., 2019) and social acceptance from the population close to the NPDs (Murray, 2012) are found to significantly influence whether the retrofitting projects may be realized or not. The selection of NPDs included in this case study is only based on the fact that they are non-powered and controlled by the CHG, not considering other limitation factor such as possible areas of conservation or formerly performed feasibility studies. This choice was made since the hydropower potential in this study is based on the criteria of not altering the current water regulation and thus avoid common conflicts. The case study is therefore meant to estimate a technical potential without any influence of political concerns.

The dam "El Portillo" in the Guadalquivir river basin was excluded from the selected NPDs due to official plans to install a hydroelectric generation unit at the foot of the current dam structure (Departamento Hidroeléctrico y Geotermia, 2010). It is unclear whether the retrofitting has been completed or not, but the construction work is confirmed to have started. A lawsuit against the concession was filed in 2018 by the City Council of Castril due to the environmental risks related to the planned regulation of the river downstream the dam (European Press, 2018). The water regulation after retrofitting the dam was said not to respect the hydrological plan for the river basin from an environmental point of view, which demonstrates the importance of avoiding further negative impacts on the surrounding environment when conducting retrofitting of NPDs.

5.4 Assessment of a global retrofitting potential

The global retrofitting potentials found by using the regression based on the WEAP results are highly uncertain and should not be used for other purposes than method evaluation before being further improved. First of all, the potentials simulated in WEAP are based on the Guadalquivir river basin and adapted to its unique climate, water demands and reservoirs. The available water for hydropower generation from this basin is likely to be different from the available water in other basins of the same size. Second of all, the regressions are not perfectly fitted to the WEAP results with an overestimation of 14% of the energy potential and an underestimation of 3% for the power potential. Third of all, the estimated global potential only accounts for 37% of the NPDs in the ICOLD register due to limited information about the remaining NPDs. Last, the included parameters in the regression functions only describe the physical characteristics of the reservoir, the catchment, and the dam since these are the most common details about the dams in the ICOLD database. Parameters describing hydrological parameters and regulation strategy such as average inflow, average releases, and degree of regulation are probable to result in more accurate regression expression but are difficult to obtain for all the NPDs.

Interestingly, the resulting regression for the power potential estimates decreasing potentials with increasing dam heights. Theoretically, the power potential is positively proportional to the head and the discharge capacity, and it is therefore considered ideal to maximize the two variables. The regression expression does however not account for the discharge capacity of the turbine, as this parameter is designed for the WEAP model and not included in the ICOLD database. From the results presented in Figure 28 and the NPDs' gross heads presented in Figure

2, it can be seen that the NPD Los Melonares have the biggest power potential, but has the third lowest gross head. If comparing this to the installed turbine capacities presented in Table 9, the large power potential is explained by the fact that Los Melonares has the second highest turbine capacity of the NPDs. The negative effect of increased dam height on the power potential from the resulting regression is therefore found to be caused by the non-linear relation between the dam height and the installed turbine capacities of the NPDs included in the regression analysis.

The data considered strictly necessary for estimations of hydropower potentials depend on the wanted accuracy. For simple calculations of rough estimates, drainage area is found to be the most representative single parameter for the hydropower potential of an NPD within the modelled catchment. Hydrological parameters representing the available water volumes directly or indirectly are expected to improve the representability. If one aims at setting up a water balance model, much more input data should be included, also covering the strategic characteristics of the dams. The "Global Earth Observation for Integrated Water Resources Assessment" project have recently released two new, freely available datasets for water resources analysis covering the period 1979-2012 (Sterk et al., 2020). The datasets contain both input data such as precipitation, radiation, and heat flux, and output data such as soil moisture, evapotranspiration, snow depth, and streamflow. This, and similar datasets, allows for more detailed water balance models independent on local water management and monitoring.

The climate in Guadalquivir is defined as a Mediterranean climate (Csa) according the Köppen-Geiger climate classification (Beck et al., 2018). Similar climates are likely to experience similar precipitation patterns and the retrofitting potential in these areas may be more similar to the potential in Guadalquivir than other climate types. Spain as a country is classified as one of the most climate diverse countries in the world with 13 different Köppen-Geiger climate zones (AEMET, 2011), and a case study of one river basin is not considered sufficient for upscaling to a national or a global scale. To highlight the possible hydrological differences between climate types, the city of Santiago de Compostela in North-Western part of Spain receives approximately 2.8 times more precipitation during a year than the city of Sevilla in the Guadalquivir (FAO, 2016). It is therefore likely that two catchments of the same area in each of the regions will have very different hydropower potentials. Since this study is based on climate input data specific to Guadalquivir which is not available in the ICOLD register nor in the GRanD database, it is assumed that similar studies covering basins with different climates should be performed. This will possibly allow for a better understanding of the importance of the different variables on the available water.

Other studies have been carried out to estimate regional hydropower potentials based on different variables. The estimated potential for the U.S. of 12 GW used data on monthly mean inflow to the reservoirs, available head and regional capacity factors for currently operating hydropower plants (Hadjerioua et al., 2012). The existing water demands were only accounted for by the calculated capacity factor for the region, as water demands are assumed to be among the affecting factor for the current hydropower generation. Applying the regression based on the case study to the NPDs in the ICOLD database registered in the U.S. results in a potential of 107 GW, equal to 8.9 times the potential from the American study. Even though the estimated potential of 12 GW also contains uncertainties, this further supports the upscaled potential to be unsuited for the estimation of a global potential.

5.5 Topics for further studies

Future studies are suggested to address the potential barriers and to further improve the accuracy of the estimates of the retrofitting potentials. Very few studies considering only the current reservoir regulation estimation of the retrofitting potential have been found. It is

believed that additional studies proving a realistic potential without further impacting the environment can draw more attention to this hidden hydropower potential. Moreover, the legislative aspect of the potential should be given more attention as the project feasibilities highly depend on being given the necessary allowances. In the case of Spain, there is even a current difficulty of obtaining renewal of the existing water concessions (Marín and García-Marín, 2019), which highlights the impacts of political influence.

The development of standardized retrofitting solutions based on the existing dam structure is believed to be useful for both technical and economic planning, as well as for the evaluation of retrofitting potentials. Such solutions should take into consideration the dam type, the dam size, and the existing intake structures. The surrounding geologic conditions might be set as an additional criterion for the solutions that are not possible to integrate in or around the dam body. If new technologies specially developed for retrofitting are integrated into these standardized solutions, they may become easier and more appealing to the developers and engineers to take advantage of the new possibilities and improvements the new technologies provide.

In addition to the obvious advantage of using existing reservoirs for multiple purposes, indirect and intangible benefits of retrofitting should be included in the calculations for a more holistic evaluation. There are several studies that have already addressed the additional benefits of hydropower, and the CO_2 certificates is an example of an additional benefit that has been monetized and implemented in today's society. A study considering the Bahkra dam system reported the benefits of the synergy between agriculture and hydropower generation to be almost three times bigger than the individual benefits of the two individual uses summed up (Bhatia et al., 2007). The IPCC report on hydropower highlights this interconnected relation between water, energy, and food, also called the water, energy and food nexus. Even though the big advantage of being able to store and regulate water already exist before retrofitting the current dams, the retrofitting of NPDs for hydropower can also cause positive effects on the existing uses due to the increased amount of available electricity. "*On the one hand, water availability is crucial for many energy technologies, including hydropower, and on the other hand, energy is needed to secure water supply for agriculture, industries and households*" (Kumar et al., 2011). Accurate monetary values of additional benefits of retrofitting are case specific and may be complex to calculate, but will strengthen the decision-making.

Despite desktop studies being able to estimate a potential based on extensive data concerning hydrology, water demands, environmental aspects and existing dam structure, a site visit and meeting with the relevant parties is seen as necessary to state whether the potential is realistic or not. The dam owner or the responsible engineers should know if there are existing intakes that are suited to be retrofitted or if there are alternative places to construct a new waterway for the hydropower generation. In addition, local authorities may be aware of special environmental requirements or ownerships of the dams to avoid conflicts from stopping possible retrofit projects. All in all, a cooperation between the involved parties is seen as a necessity in order to estimate a completely realistic potential.

6 Conclusion

This study has found the annual average hydropower potential for the selected non-powered dams in the Guadalquivir river basin to be 64.61 GWh with a corresponding capacity of 45.33 MW. When turbine capacities are adapted to the releases from the dams to represent more realistic dimensions and reduce costs, the potentials are reduced to 57.79 GWh and 18.86 MW. Out of 13 dams, five are found to be economically viable given the assumed future electricity price of 49.36 2018 EUR/MWh. For these five dams, the estimated hydropower potential with adapted turbine capacities is 46.79 GWh annually, with a corresponding net present value of 13.67 million 2018 EUR. For these results, the present water regulations serving the existing purposes of the non-powered dams have been kept unchanged.

The main strength of this study is the consideration of the existing water uses on a full basin scale and the economic constraints for the evaluation of the technical retrofitting potentials. Modelling the entire basin also enables the analysis of future scenarios regarding change in water management strategy, climate change, or other changes in the basin. By limiting the potential to the current water regulation, the main arguments against hydropower developments are avoided. The quantified economic viability of retrofitting can also attract investors and authorities to look further into retrofitting projects. The promising results of this study can hopefully draw more attention to the hidden hydropower potential of existing infrastructure and thus promote a cost-efficient source of renewable energy.

The main uncertainties in the model setup are considered to be the unknown water regulation strategy, the possible transfer lines between the reservoirs, the seasonal patterns of the different water demands, and the limited calibration area of the model. Despite these uncertainties, the model simulates the streamflow of the most downstream gauge in the basin with an overall percent bias of 6%, and the reservoir volumes for the economically viable non-powered dams with percent bias between -4% and 12%. For the estimated potentials from the case study, the exclusion of the legislative aspect and the cost of possible transmission lines represent the uncertainties with the highest risk concerning the feasibility of the projects. Site visits and meetings with the local water authorities and dam owners should minimize these uncertainties and are believed to be the best way to improve this study.

Finally, an upscaling of the simulated potentials was performed based on the ICOLD database. The resulting linear regression between the results and selected parameters in the ICOLD database estimates the global retrofitting potential to 277.33 TWh and a corresponding capacity 170.23 GW. From the regression, the global retrofitting potential may have an uncertainty of at least 15% and 3% respectively, and an improvement of the method is strongly advised.

The following four topics for future studies have been identified:

- Analysis of the effect of the different climate dependent variables on the retrofitting potential. This can be achieved by performing water balance studies in different climates and may result in more accurate estimates on the global retrofitting potential.
- Technical guidelines for retrofitting based on dam type and dam size for more robust pre-feasibility studies. These should include new technologies specially developed for retrofitting.
- Investigation of local barriers to retrofitting considering the legislative aspect.
- Valuation of the direct and indirect benefits of retrofitting. The indirect benefits should also include the benefits from the synergy effects of the retrofitting.

References

AEMET, I. 2011. Atlas climático ibérico/Iberian climate atlas.

AGENCIA ESTATAL BOLETIN OFICIAL DEL ESTADO 2016. Anexo VII. Plan Hidrológico de la DH del GUADALQUIVIR (2015-2021). Agencia Estatal Boletin Oficial del Estado.

AL-SHNYNAT, N. 2018. Challenges of integrating a small hydropower plant at existing Mujib dam. *European Journal of Electrical Engineering,* 20**,** pp. 181-191.

ALEASOFT ENERGY FORECASTING. 2019. *The 2018-2019 hydrological year classified as dry and the same is forseen for the start of Q1-2020* [Online]. Alea Business Software S.L. Available: https://aleasoft.com/2018-2019-hydrological-year-classified-dry-same-forecasting-start-q1-2020/ [Accessed 03/06/20].

ALLEN, R., PEREIRA, L., RAES, D. & SMITH, M. 1998. FAO Irrigation and Drainage Paper No. 56. *Rome: Food and Agriculture Organization of the United Nations,* 56**,** pp. 26-40.

BAKKEN, T. H., MODAHL, I. S., ENGELAND, K., RAADAL, H. L. & ARNØY, S. 2016. The life-cycle water footprint of two hydropower projects in Norway. *Journal of Cleaner Production,* 113**,** pp. 241-250.

BECK, H. E., ZIMMERMANN, N. E., MCVICAR, T. R., VERGOPOLAN, N., BERG, A. & WOOD, E. F. 2018. Present and future Köppen-Geiger climate classification maps at 1-km resolution. *Scientific Data,* 5.

BERBEL, J., BORREGO-MARÍN, M. M. & GUTIÉRREZ, C. 2015. System of Water Accounting in Guadalquivir River Basin (SYWAG) Final Report.

BHATIA, R., MALIK, R. P. S. & BHATIA, M. 2007. Direct and indirect economic impacts of the Bhakra multipurpose dam, India. *Irrigation and Drainage,* 56**,** pp. 195-206.

BIANCO, V., DRIHA, O. M. & SEVILLA-JIMÉNEZ, M. 2019. Effects of renewables deployment in the Spanish electricity generation sector. *Utilities Policy,* 56**,** pp. 72-81.

CHG. *Infraestructuras Hidráulicas* [Online]. Confederación Hidrográfica del Guadalquivir. Available: https://www.chguadalquivir.es/la-gestion-del-agua#Infraestructurashidr%C3%A1ulicas [Accessed 21/05/20].

CHG. 2011. *Historia* [Online]. Confederación Hidrográfica del Guadalquivir. Available: https://www.chguadalquivir.es/historia [Accessed 10/05/20].

CHG 2015. Memoria. *Plan Hidrológico de la demarcación del Guadalquivir Segundo Ciclo de Planificación: 2015-2021.*

CHG 2016. Documento Resumen, Plan hidrológico de la demarcación hidrográfica del Guadalquivir 2016-2021. Ministerio de Agricultura, Alimentación y Medio Ambiente,.

CHG 2019a. Captaciones de agua autorizadas en la demarcación del Guadalquivir. Confederación Hidrográfica del Guadalquivir

CHG 2019b. Informe Pluviométrico Mensual Mayo 2019. Sevilla.

CORÀ, E. 2020. Hydropower Technologies: the state-of-the-art.

DELOITTE CONSEIL 2015. Country profile: Spain. *European energy market reform.* Deloitte Conseil.

DEPARTAMENTO HIDROELÉCTRICO Y GEOTERMIA 2010. Central Hidroeléctrica de El Portillo T/M Castril de La Peña (Granada). IDAE (Instituto para la Diversidicación y ahorro de la Energía).

EUROPEAN ENVIRONMENT AGENCY 2019. Corine Land Cover (CLC) 2018. *In:* COPERNICUS LAND MONITORING SERVICE (ed.) 20 ed.

EUROPEAN PRESS. 2018. Castril lleva al TSJA la explotación de la central hidroeléctrica del Portillo. *Granada Digital*, 04/10/18.

EUROPEAN UNION 1995-2020. HICP (2015=100) - annual data (average index and rate of change). 22/04/20 ed.: Eurostat.

FAO 2016. AQUASTAT Main Database. Food and Agriculture Organization of the United Nations (FAO).

FJOESNE, N. R. 2019. *Assessment of the retrofitting potential of dams and reservoir without hydropower.* Non-degree Project Thesis, Norwegian University of Science and Technology.
HADJERIOUA, B., WEI, Y. & KAO, S.-C. 2012. An Assessment of Energy Potential at Non-Powered Dams in the United States. Oak Ridge National Laboratory.
HARRIS, I. C. & JONES, P. D. 2020. Climatic Research Unit (CRU) Times Series (TS) version 4.03 of high -resolution gridded data of month-by-month variation in climate (Jan.1901-Dec.2018). *In:* UNIVERSITY OF EAST ANGLIA CLIMATIC RESEARCH UNIT (ed.).
HYDROPOWER EQUIPMENT ASSOCIATION 2015. Global Technology Roadmap.
HYDROPOWER EUROPE. 2020. *Hydropower in Europe* [Online]. Author. Available: https://hydropower-europe.eu/about-hydropower-europe/hydropower-energy/ [Accessed 24/05/20].
ICOLD 2019. World Register of Dams. *In:* INTERNATIONAL COMMISSION ON LARGE DAMS (ed.). ICOLD-CIGB.
IDAE 2011. Analyses of the energy consumption of the household sector in Spain. *SECH Project - SPAHOUSEC.*
IEA 2019. Electricity generation by source, World 1990-2017. International Energy Agency.
IHA. 2019. *A brief history of hydropower* [Online]. International Hydropower Association,. Available: https://www.hydropower.org/a-brief-history-of-hydropower [Accessed 05/05/20].
IRENA 2012. Hydropower. *Renewable Energy Technologies: Cost Analysis Series.* Abu Dhabi: International Renewable Energy Agency.
IRENA 2019. Renewable Power Generation Costs in 2018. Abu Dhabi: International Renewable Energy Agency.
JENSSEN, L., TESAKER, E., LUND, S. & HUBER, D. 2006. Inntakshåndboken - Rettledning for utforming av inntak til små kraftverk. Oslo: Norges vassdrags- og energidirektorat.
KAO, D. T., ZHONG, T. & MAHAR, J. R. 2009. A cost effective and environmentally sustainable approach to retrofitting existing dams for hydroelectric power generation. *Waterpower XVI.* PennWell Corporation.
KHARE, V., KHARE, C., NEMA, S. & BAREDAR, P. 2019. Chapter 1 - Introduction to Energy Sources. *Tidal Energy Systems.* Elsevier.
KOVATS, R. S., VALENTINI, R., BOUWER, L. M., GEORGOPOULOU, E., JACOB, D., MARTIN, E., ROUNSEVELL, M. & SOUSSANA, J.-F. 2014. Part B: Regional Aspects. Contribution of Working Group II to the Fifth Assessment Report of the International Panel on Climate Change. *In:* BARROS, V. R., FIELD, C. B., DOKKEN, D. J., MASTRANDREA, M. D., MACH, K. J., BILIR, T. E., CHATTERJEE, M., EBI, K. L., ESTRADA, Y. O., R.C., G., GIRMA, B., KISSEL, E. S., LEVY, A. N., MACCRACKEN, S., MASTRANDREA, P. R. & WHITE, L. L. (eds.) *Climate Change 2014.* Cambridge, United Kingdom and New York, NY, USA.
KUCUKALI, S. 2010. Hydropower potential of municipal water supply dams in Turkey: A case study in Ulutan Dam. *Energy Policy,* 38**,** pp. 6534-6539.
KUMAR, A., SCHEI, T., CACERES RODRIGUEZ, R., DEVERNAY, J.-M., FREITAS, M., HALL, D., KILLINGTVEIT, Å. & LIU, Z. 2011. Hydropower. *In:* EDENHOFER, O., PICHS-MADRUGA, R., SOKONA, Y., SEYBOTH, K., MATSCHOSS, P., KADNER, P., ZWICKEL, T., EICKEMER, P., HANSEN, G., SCHLÖMER, S. & VON STECHOW, C. (eds.) *IPCC Special Report on Renewable Energy Sources and Climate Change Mitigation.* Cambridge, United Kingdom and New York, NY, USA.
LEHNER, B., LIERMANN, C., REVENGA, C., VÖRÖSMARTY, C., FEKETE, B., CROUZET, P., DÖLL, P., ENDEJAN, M., FRENKEN, K., MEGOME, J., NILSSON, C., ROBERTSON, J., RÖDEL, R., SINDORF, N. & WISSER, D. 2011. High-resolution mapping of the world's reservoirs and dams for sustainable river-flow management. *Frontiers in Ecology and the Environment 9,* 9**,** pp. 494-502.

LOOTS, I., VAN DIJK, M., BARTA, B., VAN VUUREN, S. J. & BHAGWAN, J. N. 2015. A review of low head hydropower technologies and applications in a South African context. *Renewable and Sustainable Energy Reviews,* 50**,** pp. 1254-1268.
LOOTS, I., VAN DIJK, M., VAN VUUREN, S. J., BHANGWAN, J. N. & KURTZ, A. 2014. Conduit-hydropower potential in the City of Tshwane water distribution system : A discussion of potential applications, financial and other benefits. *Journal of the South African Institution of Civil Engineering,* 56**,** pp. 2-13.
MARÍN, C. & GARCÍA-MARÍN, R. 2019. World Small Hydropower Development Report 2019- Europe Region (Spain). United Nations Industrial Development Organization and International Center on Small Hydro Power.
MARTINEZ, J., DENG, Z., KLOPRIES, E.-M., MUELLER, R., TITZLER, P., ZHOU, D., BEIRÃO, B. & HANSTEN, A. 2019. Characterization of a Siphon Turbine to Accelerate Low-Head Hydropower Deployment. *Journal of Cleaner Production,* 210**,** pp. 35-42.
MINISTERIO PARA LA TRANSICIÓN ECOLÓGICA 2018. Apéndice 1.8 Información correspondiente a la Demarcación Hidrográfica del Guadalquivir. *Informe de seguimiento de Planes Hidrológicos y Recursos Hídricos - 2018.* Ministerio para la Transición Ecológica.
MISSOURI RIVER ENERGY SERVICES. 2019. *Red Rock Hydroelectric Project* [Online]. Available: https://www.redrockhydroproject.com/project-overview/ [Accessed 02/06/20].
MITECO. 2020. *Embalses de Guadalquivir* [Online]. iAgua. Available: https://www.iagua.es/data/infraestructuras/demarcaciones-hidrograficas/guadalquivir [Accessed March 2020].
MORIASI, D. N. 2007. Model evaluation guidelines for systematic quantification of accuracy in watershed simulations. *Transactions of the ASABE,* 50**,** pp. 885-900.
MURRAY, M. 2012. *Investigation of New Hampshire hydropower potential.* Senior Honor Thesis, University of New Hampshire - Main Campus.
NAVARRO-SERRANO, F., LÓPEZ-MORENO, J. I., AZORIN-MOLINA, C., ALONSO-GONZÁLEZ, E., TOMÁS-BURGUERA, M., SANMIGUEL-VALLELADO, A., REVUELTO, J. & VICENTE-SERRANO, S. M. 2018. Estimation of near-surface air temperature lapse rates over continental Spain and its mountain areas. *International Journal of Climatology,* 38**,** pp. 3233-3249.
NOOTHOUT, P., DE JAGER, D., TESNIÈRE, L., VAN ROOIJEN, S., KARYPIDIS, N., BRÜCKMANN, R., JIROUS, F., BREITSCHOPF, B., ANGELOPOULOS, D., DOUKAS, H., KONSTANTINAVICIUTE, I. & RESCH, G. 2016. The impact of risks in renewable energy investments and the role of smart policies. ECOFYS.
NORCONSULT 2016. Kostnadsgrunnlag for små vannkraftanlegg (<10MW). Oslo: Norges vassdrags- og energidirektorat.
OFFICE OF ENERGY EFFICIENCY AND RENEWABLE ENERGY 2020. New Round of Hydroelectric Incentive Funding Now Available. Washington D.C., U.S.: Author.
OMIE 2020a. Day-ahead minimum, average and maximum price: Spain. Madrid: OMI, Polo Español S.A. (OMIE).
OMIE. 2020b. *Electricity market* [Online]. OMI, Polo Español S.A. (OMIE). Available: https://www.omie.es/en/mercado-de-electricidad [Accessed 05/05/20].
PATSIALIS, T., KOUGIAS, I., KAZAKIS, N., THEODOSSIOU, N. & DROEGE, P. 2016. Supporting Renewables' Penetration in Remote Areas through the Transformation of Non-Powered Dams. *Energies,* 9**,** 1054.
PUNYS, P., KVARACIEJUS, A., DUMBRAUSKAS, A., ŠILINIS, L. & POPA, B. 2019. An assessment of micro-hydropower potential at historic watermill, weir, and non-powered dam sites in selected EU countries. *Renewable Energy,* 133**,** pp. 1108-1123.
QGIS DEVELOPMENT TEAM 2020. QGIS Geographic Information System. 3.10.2-A Coruña ed.: Open Source Geospatial Foundation Project.
RED ELÉCTRICA DE ESPAÑA 2020. Precio Mercado Spot Diario España. Red Eléctrica de España.

SAIH 2020a. Datos Históricos. Sistema Automático de Información Hidrológica de la Cuenca del Guadalquivir.
SAIH 2020b. Red de Control S.A.I.H.: Sistema Automático de Información Hidrológica de la Cuenca del Guadalquivir.
SANDT, C. J. & DOYLE, M. W. 2013. The hydrologic and economic feasibility of micro hydropower upfitting and integration of existing low-head dams in the United States. *Energy Policy,* 63**,** pp. 261-271.
SCHUMANN, A. H. 1998. Thiessen Polygon. *Encyclopedia of Hydrology and Lakes.* Dordrecht: Springer Netherlands.
SIEBER, J. 2019. Water Evaluation And Planning (WEAP) System. Somerville, MA, USA: Stockholm Environmental Institute.
SIEBER, J. & PURKEY, D. 2015. User Guide for WEAP 2015. Somerville, MA, USA: Stockholm Environmental Institute.
STERK, G., SPERNA-WEILAND, F. & BIERKENS, M. 2020. Guest Editorial: Special Issue on Global Hydrological Datasets for Local Water Management Applications. *Water Resources Management,* 34**,** pp. 2111-2116.
STOCKHOLM ENVIRONMENT INSTITUTE. 2020. *Selected Publications* [Online]. Stockholm Environment Institute. Available: https://www.weap21.org/index.asp?action=216 [Accessed 04/06/20].
SWECO NORGE, FLADEN, B., HOLMQVIST, E. & BACHKE, D. 2010. Veileder i planlegging, bygging og drift av små kraftverk. Oslo: Norges vassdrag- og energidirektorat.
TRABUCCO, A. & ZOMER, R. J. 2019. Global Aridity and Potential Evapotranspiration (ET0) Climate Database v2. *In:* CGIAR CONSORTUM FOR SPATIAL INFORMATION (CGIAR-CSI) (ed.). figshare.
VAN VUUREN, S. J., BLERSCH, C. L. & VAN DIJK, M. 2011. Modelling the feasibility of retrofitting hydropower to existing South African dams. *In:* COMMISSION, W. R. (ed.) *Water Research Commission 40-Year Celebration Conference,.* Kempton Park.
YEGGINA, S., TEEGAVARAPU, R. S. V. & MUDDU, S. 2020. Evaluation and bias corrections of gridded precipitation data for hydrologic modelling support in Kabini River basin, India. *Theoretical and Applied Climatology*.
YUGUNDA, T. K., LI, Y., XIONG, W. & ZHANG, W. 2020. Life cycle assessment of options for retrofitting an existing dam to generate hydro-electricity. *International Journal of Life Cycle Assessment,* 25**,** pp. 57-72.
ZHOU, D., GUI, J., DENG, Z. D., CHEN, H., YU, Y., YU, A. & YANG, C. 2019. Development of an ultra-low head siphon hydro turbine using computational fluid dynamics. *Energy,* 181**,** pp. 43-50.

Appendices

APPENDIX A: DESCRIPTION OF THE MASTER THESIS

APPENDIX B: INCLUDED DAMS WITH CORRESPONDING STORAGE CAPACITIES

APPENDIX C: ENVIRONMENTAL FLOW REQUIREMENTS AND ALLOWANCES

APPENDIX D: OBSERVED AND SIMULATED RESERVOIR FILLING OF THE NON-POWERED DAMS

APPENDIX E: COST ESTIMATIONS

APPENDIX F: EXAMPLE OF THE DISCOUNTING OF THE COSTS, REVENUES, AND ENERGY FOR GERGAL

APPENDIX G: DISTRIBUTION OF WATER WITHDRAWALS

APPENDIX H: VOLUME-ELEVATION CURVES FOR THE NPDs INCLUDED IN THE WEAP MODEL

APPENDIX I: SCREEN DUMPS FROM THE WEAP MODEL

DIGITAL APPENDIX:

- The WEAP model with necessary input files integrated
- A separate version of the input climate data
- A separate version of the input data for the observed streamflow and reservoir fillings

NTNU Faculty of Engineering

Norwegian University of Science and Technology

Department of Civil and Environmental Engineering

M.Sc. Thesis in

Water Resources Modelling and Engineering

Candidate: Nora Rydland Fjøsne

Title: Demonstrating the retrofitting potential of non-powered dams for hydropower production

1 BACKGROUND

A large number of the world's large dams and reservoirs are built for other types of use than hydropower production. According to the statistics derived from the ICOLD database (by 2019), being the most complete inventory of large dams and reservoirs, close to 90% of the dams in Africa, around 75% of the dams in Asia and close 60% of the European large dams are presently not used for hydropower production. Retrofitting describes the addition or expansion of an existing dam not used for hydropower with hydroelectric power generation capabilities.

Compared to the construction of a new dam, retrofitting could pose a cost-effective way to increase electricity production. Impacts on the environment are less severe as most substantial impacts have already been caused. The mere addition of turbines and other electromechanical equipment usually requires little additional construction and limited degradation of an already impacted river basin. The project aims at developing and demonstrating a methodology assessing the potential of such a retrofitting in a river basin, with the focus on analysing the availability of water resources for hydropower production. Furthermore, the projects aim at assessing the potential of upscaling the methodology for the calculation of regional, national or global numbers.

2 MAIN QUESTIONS FOR THE THESIS

Key questions to be addressed in the thesis are;

1. Develop a method to calculate the retrofitting potential in a basin with non-hydropower dams/reservoir (e.g. based on a regulated basin in Spain).
2. Demonstrate the proposed methodology for instance with use of WEAP or any other suitable tool for the purpose.
3. Provide a rough estimate of costs of retrofitting, the revenue of the possible hydropower production, and compare to other sources of (new) renewable energy production.
4. Assess the assumptions, limitation and uncertainties in the methodology and

calculations

5. Outline an approach to calculate the regional / global retrofitting potential for retrofitting, and the data and research needs, in order to further refine the calculations of the hidden hydropower potential.

3 SUPERVISION, DATA AND INFORMATION INPUT

Professor Tor Haakon Bakken will be the main supervisor of the thesis work. Discussion with and input from colleagues and other research or engineering staff at NTNU, power companies or consultants are recommended, if considered relevant. Significant inputs from others shall, however, be referenced in a convenient manner.

The research and engineering work carried out by the candidate in connection with this thesis shall remain within an educational context. The candidate and the supervisors are therefore free to introduce assumptions and limitations, which may be considered unrealistic or inappropriate in a contract research or a professional engineering context.

4 REPORT FORMAT AND REFERENCE STATEMENT

The report shall be typed by a standard word processor and figures, tables, photos etc. shall be of good report quality, following the NTNU style. The report shall include a summary, a table of content, lists of figures and tables, a list of literature and other relevant references. All figures, maps and other included graphical elements shall have a legend, have axis clearly labelled and generally be of good quality.

The report shall have a professional structure and aimed at professional senior engineers and decision makers as the main target group, alternatively written as a scientific article. The decision regarding report or scientific article shall be agreed upon with the supervisor.

The thesis shall include a signed statement where the candidate states that the presented work is his/her own and that significant outside input is identified.

This text shall be included in the report submitted. Data that is collected during the work with the thesis, as well as results and models setups, shall be documented and submitted in electronic format together with the thesis.

The thesis shall be submitted no later than 11th of June, 2020.

Trondheim 15th of January 2020

Tor Haakon Bakken

Tor Haakon Bakken, Professor

APPENDIX B: INCLUDED DAMS WITH CORRESPONDING STORAGE CAPACITIES

Table 16: Included dams in the WEAP model and their corresponding reservoirs' storage capacities.

Dam	Storage capacity [hm^3]	Dam	Storage capacity [hm^3]
Agrio	20	La Bolera	53
Aguascebas	6	La Breña	823
Aracena	129	La Minilla	58
Arenoso	167	Los Melonares	186
Bembezar	342	Martín Gonzalo	18
Bermejales	103	Montoro III	105
Cala	60	Negratin	567
Canales	71	Peñaflor	3
Colomera	43	Portillo	34
Cubillas	19	Puebla de Cazalla	74
Danador	4	Puente Nuevo	282
Derivacion Retortillo	4	Quentar	14
El Pintado	213	Quiebrajano	32
Encinarejo	15	Retortillo	61
Fernandina	245	Rumblar	126
Francisco Abellán	58	Salto del Molino	1
Fresneda	13	San Clemente	117
Gergal	35	San Rafael de Navallana	157
Giriballe	475	Sierra Boyera	41
Guadalen	163	Siles	31
Guadalmellato	155	Torre del Aguila	70
Guadalmena	347	Tranco de Beas	498
Guadanuño	2	Vadomojon	163
Huesna	135	Viboras	19
Iznajar	981	Yeguas	229
Jandula	322	Zocueca	5
José Torán	114	Zufre	175

Reference:

CHG. Infraestructuras Hidráulicas [Online]. Confederación Hidrográfica del Guadalquivir. Available: https://www.chguadalquivir.es/la-gestion-del-agua#Infraestructurashidr%C3%A1ulicas [Accessed 21/05/20].

APPENDIX B: INCLUDED DAMS WITH CORRESPONDING STORAGE CAPACITIES

Table 17: Seasonal minimal flow requirements [l/s] for the dams included in the WEAP model.

Dam	Oct-Nov	Dec-Apr	May-Sep
Arenoso	100	190	100
Negratin	300	320	290
Canales	115	145	110
Quentar	50	50	50
Encinarejo, Jandula	50	100	50
Martín Gonzalo	-	70	-
Retortillo	100	190	100
Rumblar	120	220	110
José Torán	90	170	80
Quiebrajano	-	60	-
Colomera	70	80	70
Cubillas	120	160	140
Iznajar	790	830	750
Francisco Abellán	50	70	60
La Bolera	100	130	110
San Clemente	50	70	60
Los Melonares	140	140	140
Pintado	310	620	250
Gergal	200	200	200
Zufre	160	300	140
Aracena	150	290	140
Agrio	50	100	60
Montoro III	50	90	60
Fresneda	8	16	9
Giribaile	590	630	550
Siles	220	260	220
Cala	120	220	110
Guadalmena	370	740	300
Fernandina	90	170	80
Portillo	350	380	380
Tranco de Beas	270	280	260
Yeguas	230	420	200
Torre del Aguila	160	180	160
Puebla de Cazalla	190	210	190
Huesna	130	250	120
Bembezar	280	530	250
Sierra Boyera	70	140	60
Puente Nuevo	310	620	250
Viboras	90	120	100
Vadomojon	210	220	200
Bermejales	110	140	130
Guadalen	290	380	330
Minilla	210	400	190
San Rafael De Navallane	210	400	190
Brena	310	590	280
Derivacion Retrotillo	328	393	328

APPENDIX C: ENVIRONMENTAL FLOW REQUIREMENTS AND ALLOWANCES

Table 18: Monthly minimal flow requirements [l/s] for dams included in the WEAP model.

Dam	Oct	Nov	Dec	Jan	Feb	Mar	Apr	May	Jun	Jul	Aug	Sep
Guadanuno	30	30	41	51	59	53	49	33	16	12	12	12
Guadalmellato	315	319	449	529	601	539	474	333	181	127	127	127
Dañador	9	9	13	15	17	16	14	10	5	4	4	4
Aguascebas	125	125	158	201	201	174	170	133	131	118	118	118

Table 19: Seasonal maximum flow allowances [l/s].

Dam	Nov-Apr	May-Oct	Spawning (1st of April)
El Negratin	24400	20800	
Guadalmena	56900	24500	22500
La Fernandina	76500	16300	14800
Guadalen	76500	16300	14800
Canales	12400	10500	8700
Quentar	12400	10500	8700
El Pintado	44300	21600	
Cala	27500	12600	
Quiebrajano	8500	2300	
Martín Gonzalo	4700	1700	
Huesna	43800	16000	
Los Melonares	54500	22900	
La Minilla	48600	22200	
Gergal	84400	38400	

Reference:

AGENCIA ESTATAL BOLETIN OFICIAL DEL ESTADO 2016. Anexo VII. Plan Hidrológico de la DH del GUADALQUIVIR (2015-2021). Agencia Estatal Boletin Oficial del Estado.

APPENDIX D: OBSERVED AND SIMULATED RESERVOIR FILLING OF THE NPDS

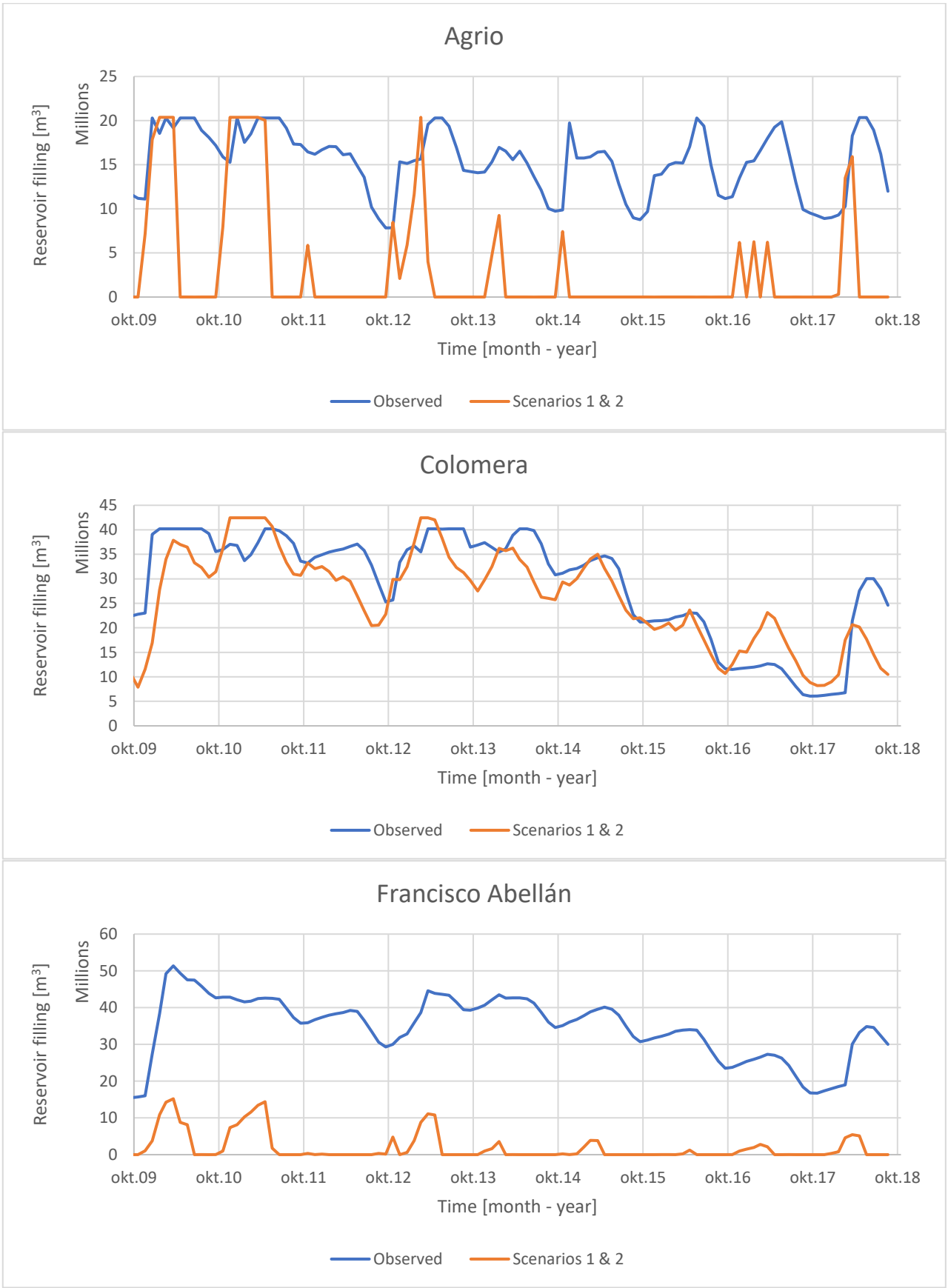

APPENDIX D: OBSERVED AND SIMULATED RESERVOIR FILLING OF THE NPDS

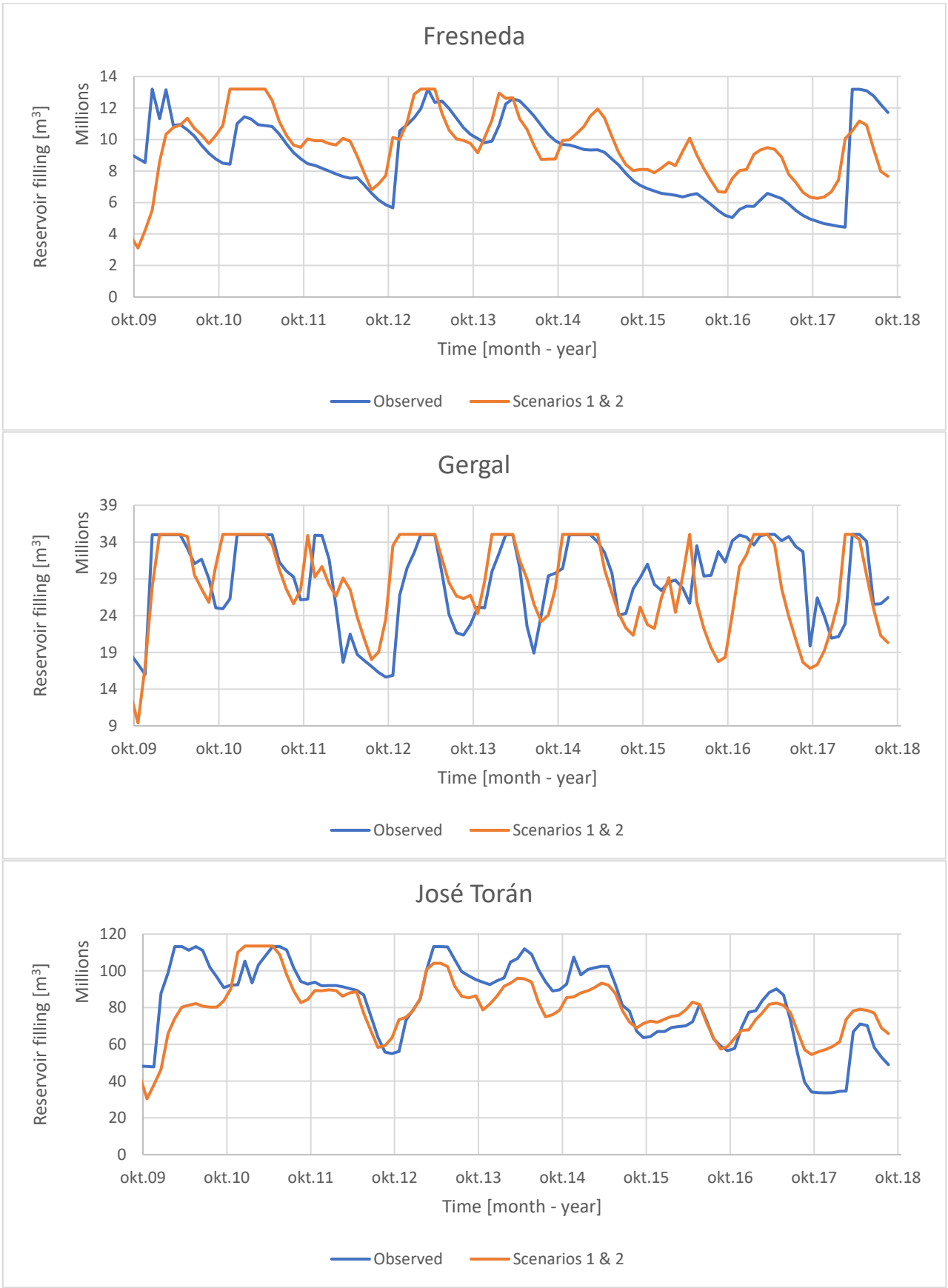

APPENDIX D: OBSERVED AND SIMULATED RESERVOIR FILLING OF THE NPDS

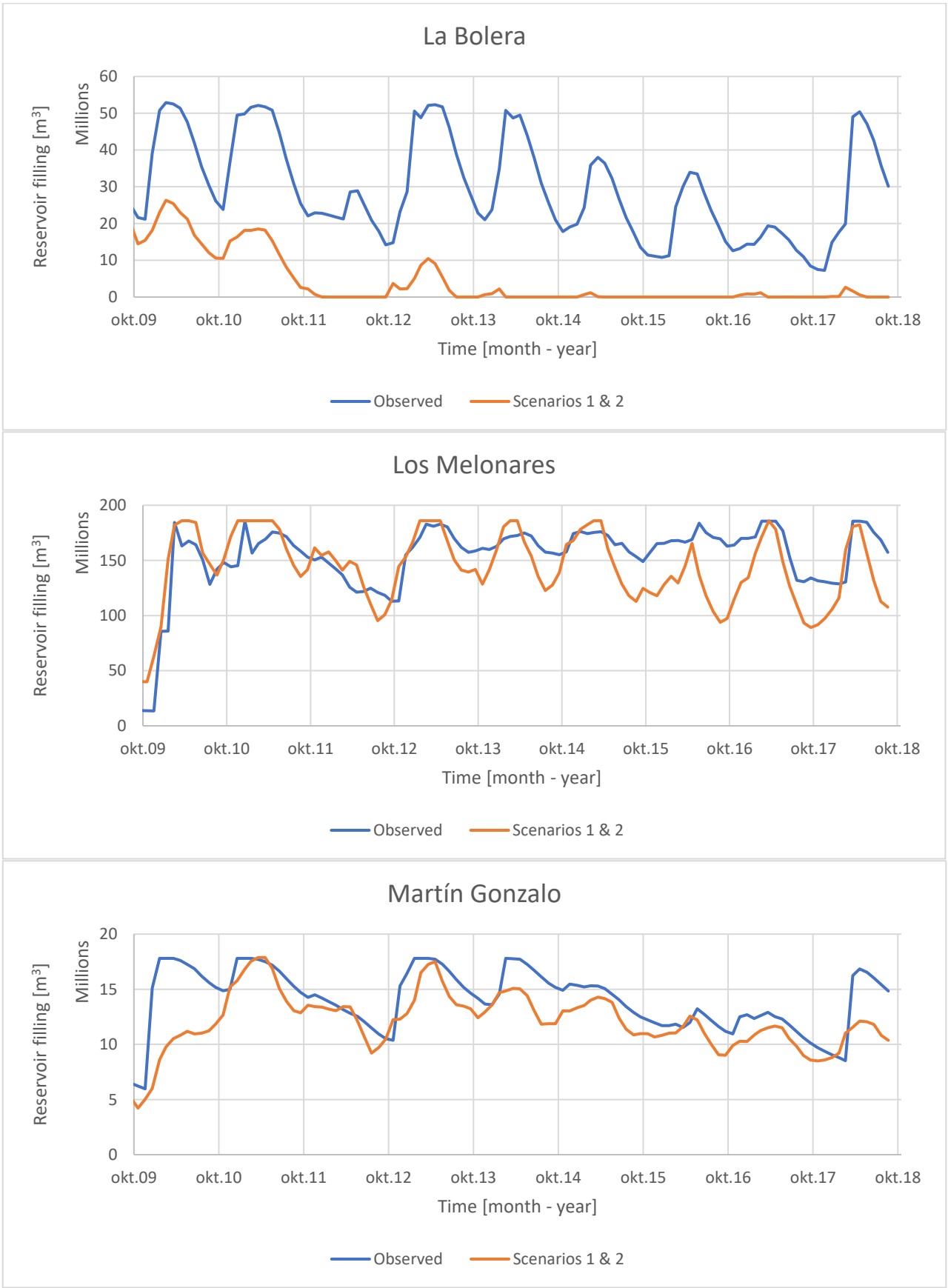

APPENDIX D: OBSERVED AND SIMULATED RESERVOIR FILLING OF THE NPDS

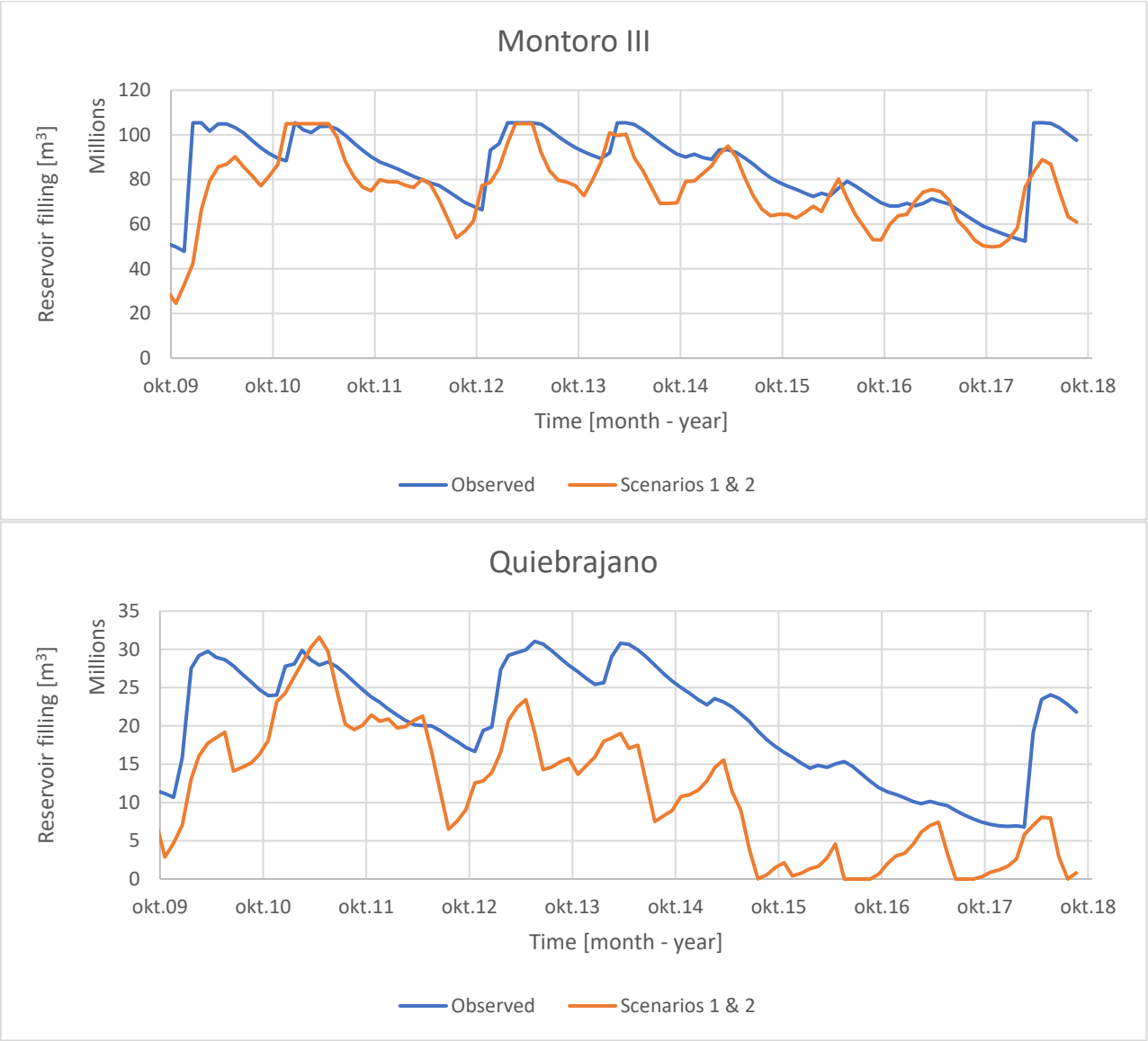

APPENDIX D: OBSERVED AND SIMULATED RESERVOIR FILLING OF THE NPDS

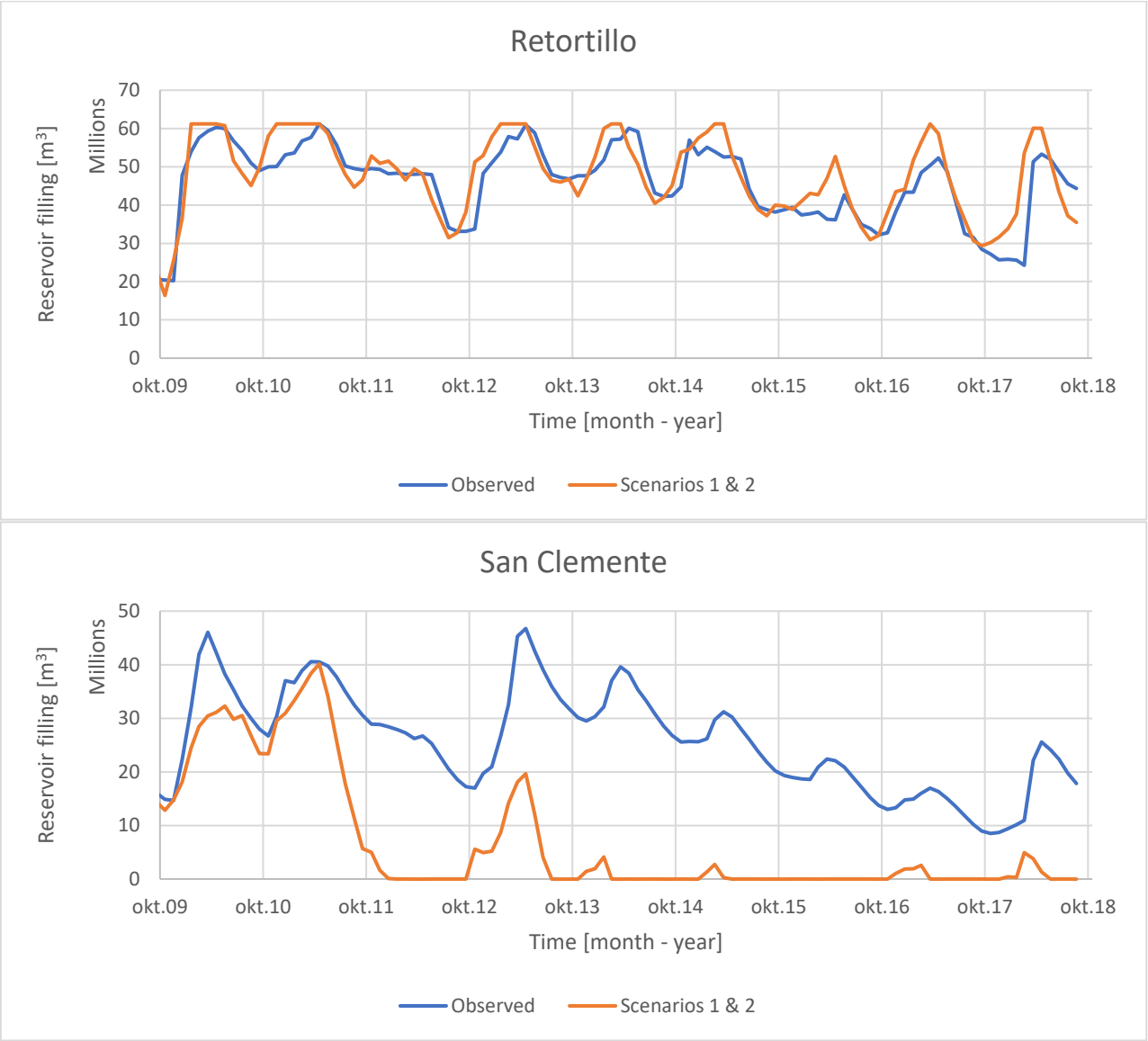

APPENDIX D: OBSERVED AND SIMULATED RESERVOIR FILLING OF THE NPDS

APPENDIX E: COST ESTIMATION FOR THE NPDs INCLUDED IN THE WEAP MODEL.

Table 20: Cost estimations for the NPDs included in the WEAP model. The yellow rows are technical input, the orange rows are cost components, the blue rows are the total investment cost (CAPEX) and the annual O&M costs. The white rows are only for calculations.

NPD / Parameter	Agrio	Colomera	Francisco Abellán	Fresneda	Gergal	José Torán	La Bolera	Los Melonares	Martín Gonzalo	Montoro III	Quiebrajano	Retortillo	San Clemente
Installed power [MW]	0.95	0.84	0.87	0.29	4.84	2.10	1.53	4.54	0.27	1.08	0.64	0.90	1.53
Avg. simulated energy prod. [MWh/yr]	1118.73	2909.61	275.80	713.66	20545.90	3950.06	174.95	17120.84	470.87	3567.38	947.96	2646.66	1345.64
Qinst. [m^3/s]	3.74	1.84	1.42	1.07	13.83	3.86	5.05	13.61	0.68	4.48	1.12	3.07	2.27
nmn (HRWL) [m.a.s.l.]	98.1	812.0	955.0	717.0	50.0	147.3	971.4	82.0	282.4	549.0	785.0	187.0	1061.0
Tailwater elevation [m.a.s.l.]	67.5	757.0	882.0	684.0	8.0	82.0	935.0	42.0	234.0	520.0	717.0	152.0	980.0
Head (gross) [m]	30.6	55.0	73.0	33.0	42.0	65.3	36.4	40.0	48.4	29.0	68.0	35.0	81.0
Pipe diameter [m]	1.26	0.88	0.78	0.67	2.42	1.28	1.46	2.40	0.54	1.38	0.69	1.14	0.98
Areal [m2]	0.31	0.15	0.12	0.09	1.15	0.32	0.42	1.13	0.06	0.37	0.09	0.26	0.19
Intake [mill NOK]	1.55	0.65	0.60	0.55	2.06	1.56	1.02	2.04	0.50	1.59	0.56	0.80	1.48
Entrance gate area [m2]	5.34	2.62	2.03	1.53	19.76	5.51	7.22	19.44	0.97	6.41	1.60	4.39	3.24
Entrance gate [mill. NOK]	0.06	0.03	0.02	0.02	0.22	0.06	0.08	0.21	0.01	0.07	0.02	0.05	0.04
Power plant [mill. NOK]	3.26	2.85	2.79	2.17	8.89	4.43	4.08	8.54	2.09	3.50	2.52	3.11	3.57
Foundation, steel pipe [mill. NOK/m]	0.01	0.00	0.00	0.00	0.01	0.01	0.01	0.01	0.00	0.01	0.00	0.01	0.01
Foundation, steel pipe [mill. NOK]	0.38	0.53	0.65	0.27	1.00	0.83	0.52	0.94	0.35	0.39	0.56	0.41	0.84
Ductile pipes [mill. NOK]	0.40	0.38	0.40	0.14	1.77	0.88	0.62	1.66	0.14	0.45	0.30	0.38	0.68
Complete el./mech. incl. Francis [NOK/kW]	5766.75	6416.40	5511.16	13387.90	2791.98	4133.85	6071.09	2867.81	8650.40	5333.56	7294.72	6117.58	4815.29
Complete el./mech. incl. Francis [mill. NOK/kW]	0.01	0.01	0.01	0.01	0.00	0.00	0.01	0.00	0.01	0.01	0.01	0.01	0.00
Complete el./mech. incl. Francis [mill. NOK]	5.50	5.40	4.77	3.95	13.52	8.67	9.31	13.01	2.36	5.78	4.64	5.48	7.38
CAPEX [mill. NOK]	11.15	9.84	9.23	7.10	27.46	16.43	15.63	26.42	5.44	11.78	8.60	10.22	13.98
O&M [mill. NOK]	0.28	0.25	0.23	0.18	0.69	0.41	0.39	0.66	0.14	0.29	0.21	0.26	0.35

APPENDIX E: COST ESTIMATION FOR THE NPDs INCLUDED IN THE WEAP MODEL.

APPENDIX F: EXAMPLE OF THE DISCOUNTING OF THE COSTS, REVENUES, AND ENERGY FOR GERGAL.

Table 21: Example of the discounting of the costs, revenues, and energy for Gergal.

Gergal	Year	Capital [mill. EUR]	O&M	El. Prod [kWh]	El. Price [EUR/kWh]	Revenue [mill. EUR]	Total costs [mill EUR]	Disc.cost [mill EUR]	Disc.benefit [mill EUR]	Disc. Energy [kWh]
	1	3.10				0.00	3.10	2.89	0.00	0.0
2011	2		0.08	20545899.28	0.05	1.09	0.08	0.07	0.95	17779036.7
2012	3		0.08	20545899.28	0.05	1.01	0.08	0.06	0.81	16538638.8
2013	4		0.08	20545899.28	0.05	0.93	0.08	0.06	0.70	15384780.3
2014	5		0.08	20545899.28	0.04	0.89	0.08	0.05	0.62	14311423.5
2015	6		0.08	20545899.28	0.05	1.07	0.08	0.05	0.69	13312952.1
2016	7		0.08	20545899.28	0.04	0.85	0.08	0.05	0.51	12384141.5
2017	8		0.08	20545899.28	0.05	1.09	0.08	0.04	0.61	11520131.6
2018	9		0.08	20545899.28	0.06	1.18	0.08	0.04	0.61	10716401.5
2019	10		0.08	20545899.28	0.05	1.01	0.08	0.04	0.49	9968745.6
2020	11		0.08	20545899.28	0.05	1.01	0.08	0.03	0.46	9273251.7
2021	12		0.08	20545899.28	0.05	1.01	0.08	0.03	0.43	8626280.7
2022	13		0.08	20545899.28	0.05	1.01	0.08	0.03	0.40	8024447.1
2023	14		0.08	20545899.28	0.05	1.01	0.08	0.03	0.37	7464602.0
2024	15		0.08	20545899.28	0.05	1.01	0.08	0.03	0.34	6943815.8
2025	16		0.08	20545899.28	0.05	1.01	0.08	0.02	0.32	6459363.5
2026	17		0.08	20545899.28	0.05	1.01	0.08	0.02	0.30	6008710.3
2027	18		0.08	20545899.28	0.05	1.01	0.08	0.02	0.28	5589497.9
2028	19		0.08	20545899.28	0.05	1.01	0.08	0.02	0.26	5199532.9
2029	20		0.08	20545899.28	0.05	1.01	0.08	0.02	0.24	4836774.8
2030	21		0.08	20545899.28	0.05	1.01	0.08	0.02	0.22	4499325.4
2031	22		0.08	20545899.28	0.05	1.01	0.08	0.02	0.21	4185419.0
2032	23		0.08	20545899.28	0.05	1.01	0.08	0.01	0.19	3893413.0
2033	24		0.08	20545899.28	0.05	1.01	0.08	0.01	0.18	3621779.6
2034	25		0.08	20545899.28	0.05	1.01	0.08	0.01	0.17	3369097.3
2035	26		0.08	20545899.28	0.05	1.01	0.08	0.01	0.15	3134044.0
2036	27		0.08	20545899.28	0.05	1.01	0.08	0.01	0.14	2915389.7
2037	28		0.08	20545899.28	0.05	1.01	0.08	0.01	0.13	2711990.4
2038	29		0.08	20545899.28	0.05	1.01	0.08	0.01	0.12	2522781.8
2039	30		0.08	20545899.28	0.05	1.01	0.08	0.01	0.12	2346773.8
2040	31		0.08	20545899.28	0.05	1.01	0.08	0.01	0.11	2183045.4
SUM								3.74	11.13	225725587.6

APPENDIX F: EXAMPLE OF THE DISCOUNTING OF THE COSTS, REVENUES, AND ENERGY FOR GERGAL.

APPENDIX G: DISTRIBUTION OF WATER WITHDRAWALS

Table 22: Distribution of water withdrawal volumes between the different withdrawal points.

Withdrawal point	Withdrawal volume [m^3/yr]	% of total withdrawal
Agrio	447632968.8	7.13%
Agrio_US	58554.0	0.00%
Colomera	890266448.3	14.17%
Colomera_US	4462470.1	0.07%
Four	468538447.9	7.46%
Francisco Abellan	201464265.2	3.21%
Francisco Abellan_US	38898053.6	0.62%
Fresneda_US	220092.9	0.00%
Gergal	22170984.5	0.35%
Gergal_US	9108365.5	0.14%
Jose Toran	848155.6	0.01%
JoseToran_US	3632606.6	0.06%
La Bolera_US	65352.0	0.00%
Los Melonares	9076587.3	0.14%
MartinGonzalo_US	201596.5	0.00%
Melonares_US	9415973.3	0.15%
Montoro e Fresneda	17455944.0	0.28%
Montoro_US	22172663.9	0.35%
One	2299899618.0	36.61%
Quiebrajano	75364276.2	1.20%
Quiebrajano_US	112902.1	0.00%
Retortillo	3373293.3	0.05%
Retortillo_US	569751.9	0.01%
San Clemente	9867792.4	0.16%
San Clemente_US	10692380.5	0.17%
Three	618617726.0	9.85%
Two	1118336603.5	17.80%
Sum	**6282523873.8**	
Sum [hm^3]	**6282.5**	

APPENDIX G: DISTRIBUTION OF WATER WITHDRAWALS

APPENDIX H: VOLUME-ELEVATION CURVES FOR THE NPDs INCLUDED IN THE WEAP MODEL

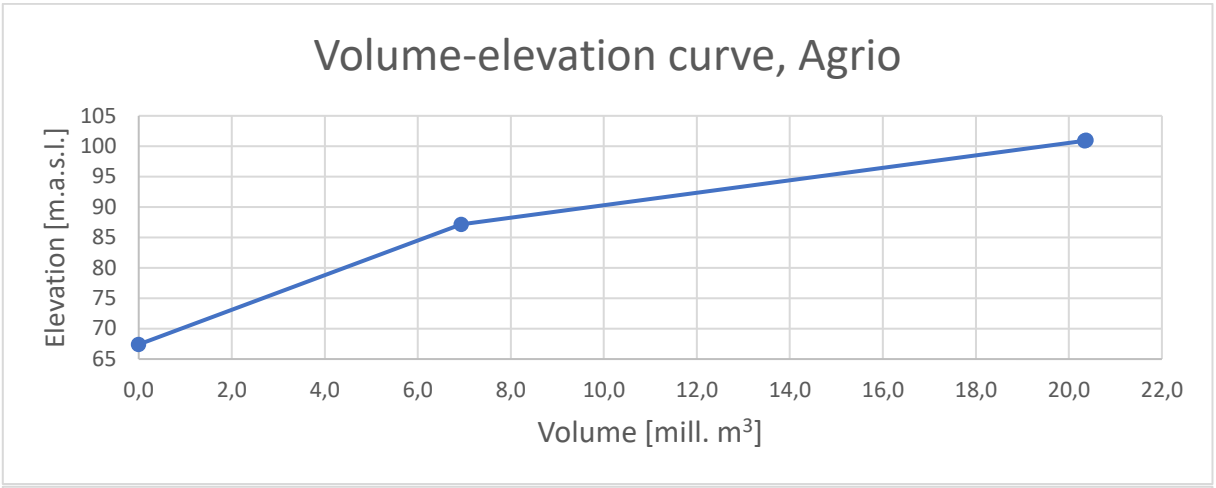

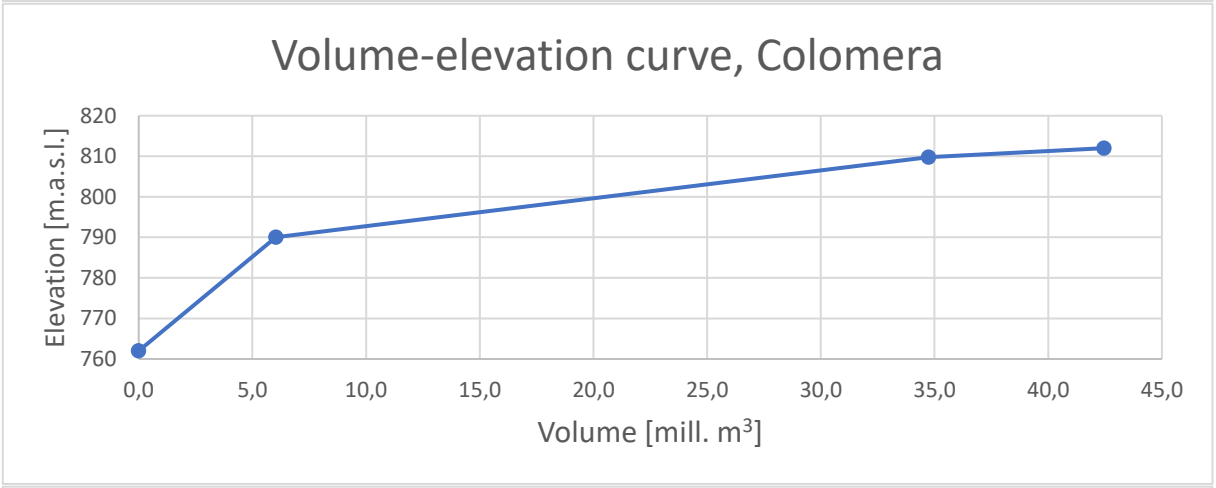

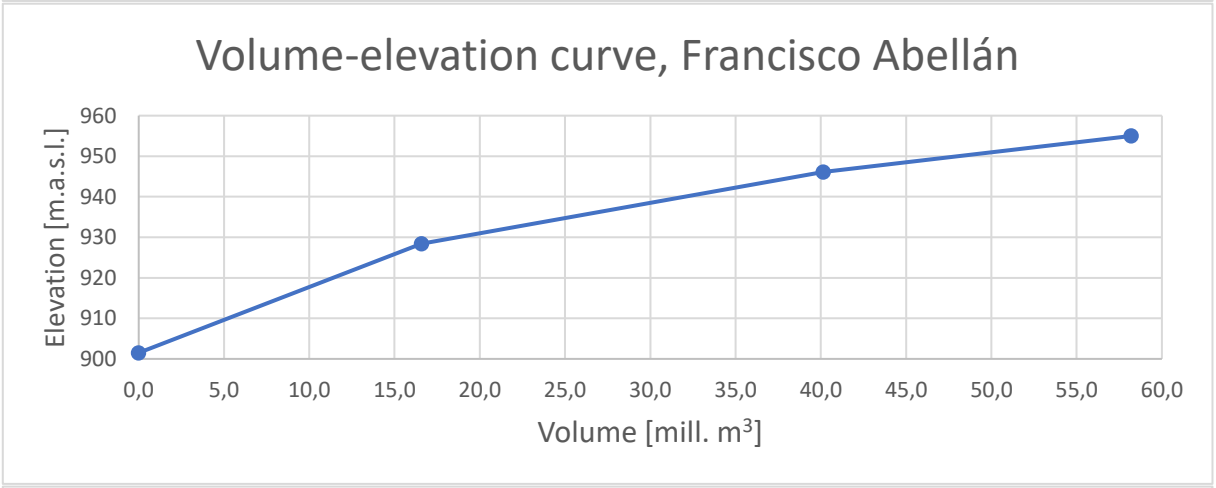

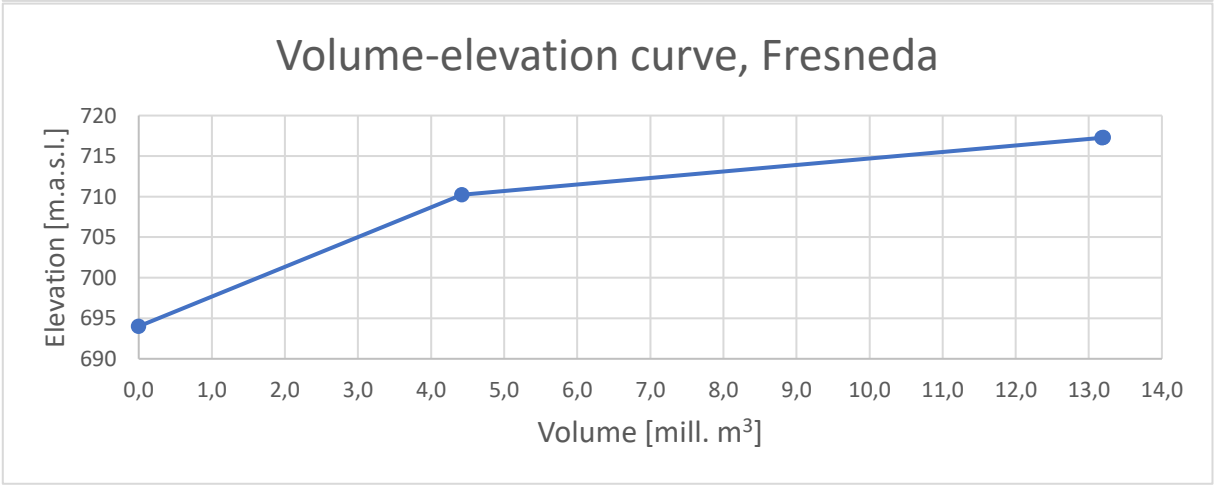

APPENDIX H: VOLUME-ELEVATION CURVES FOR THE NPDs INCLUDED IN THE WEAP MODEL

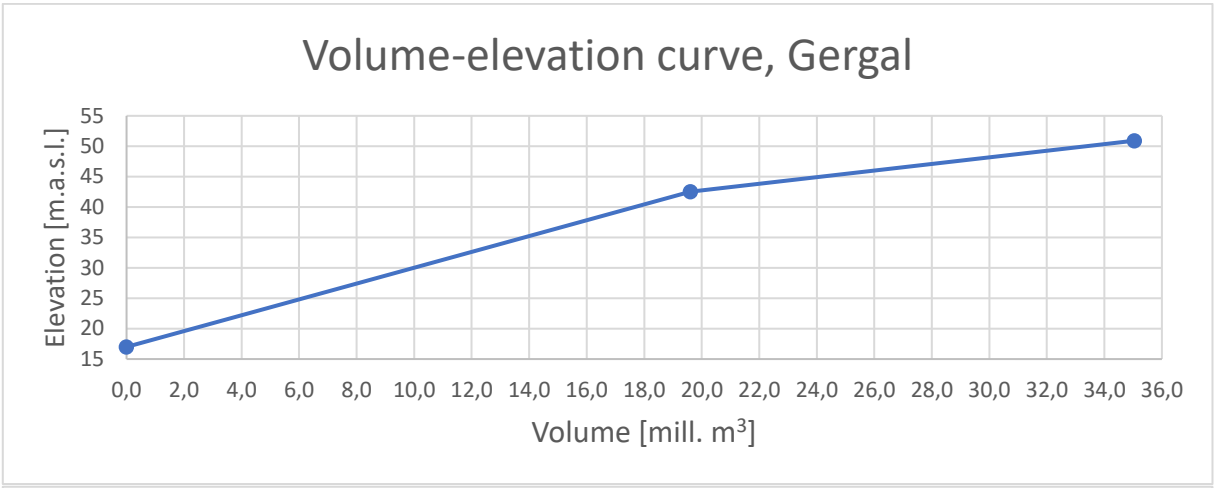

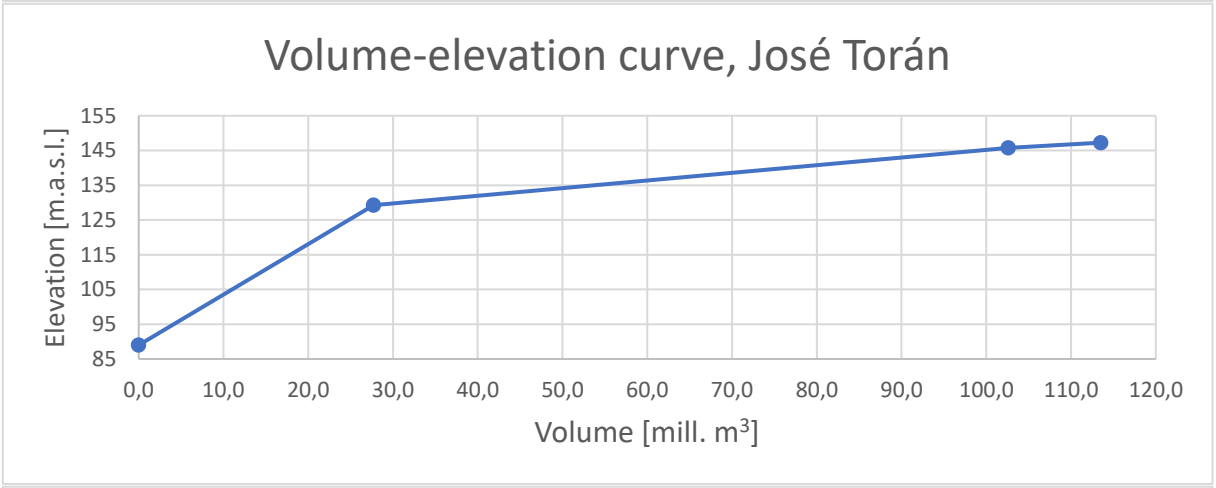

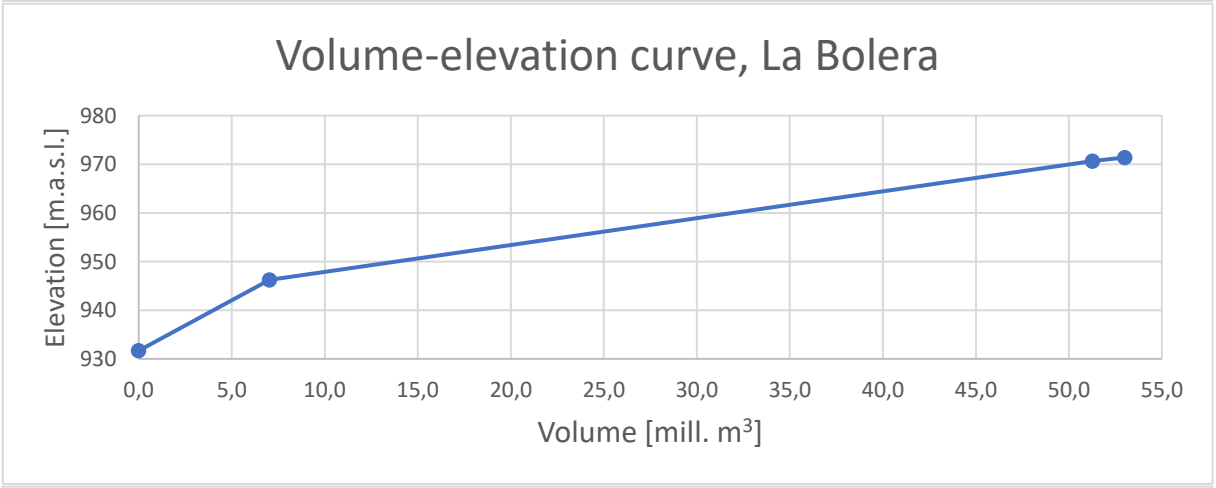

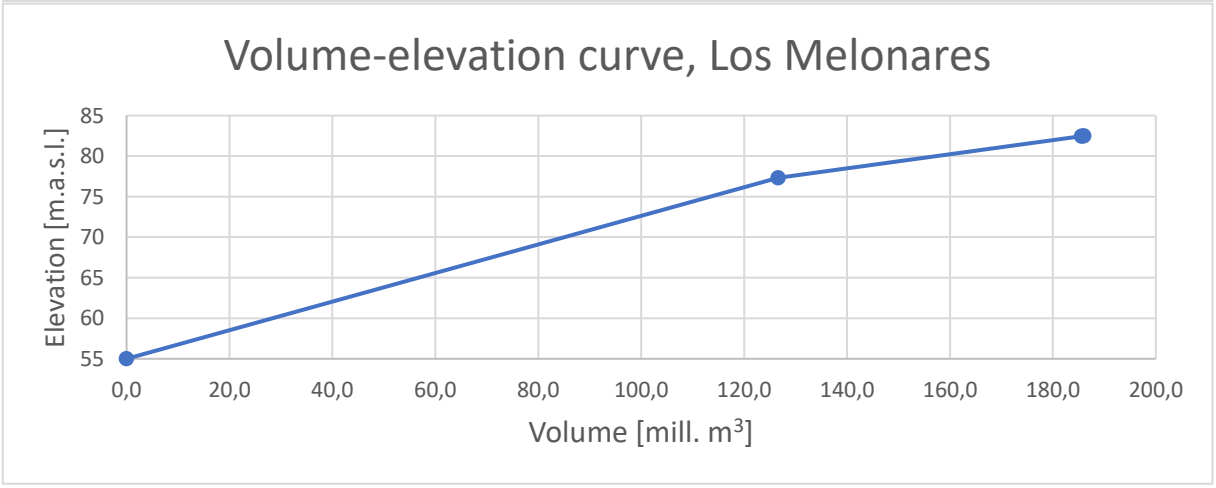

APPENDIX H: VOLUME-ELEVATION CURVES FOR THE NPDs INCLUDED IN THE WEAP MODEL

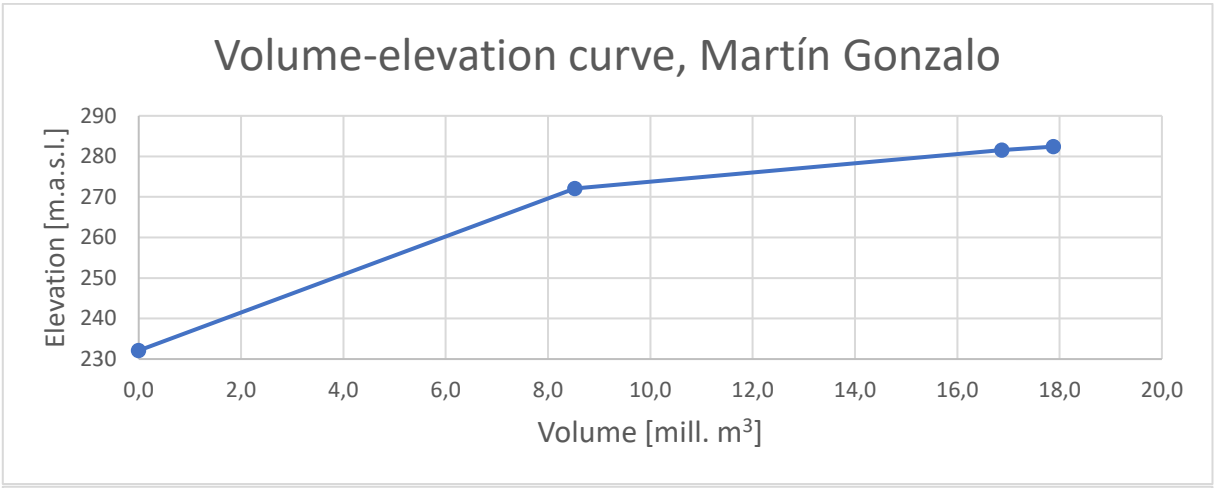

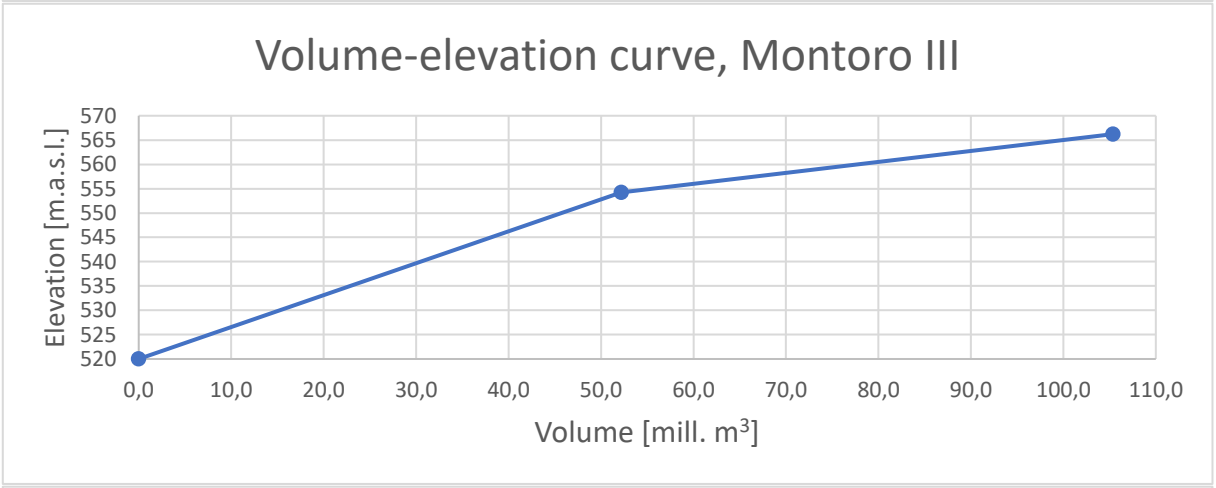

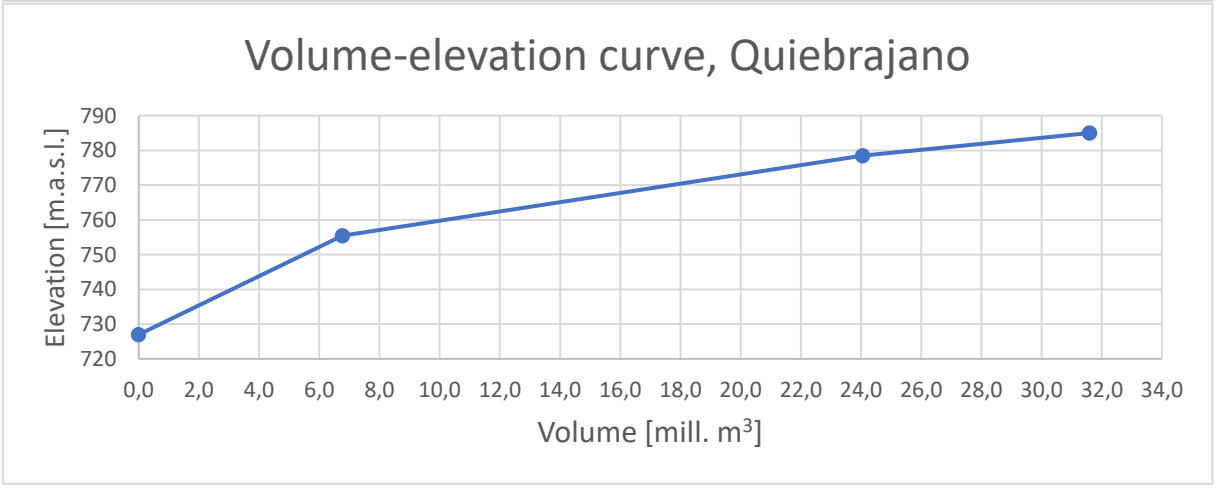

APPENDIX H: VOLUME-ELEVATION CURVES FOR THE NPDs INCLUDED IN THE WEAP MODEL

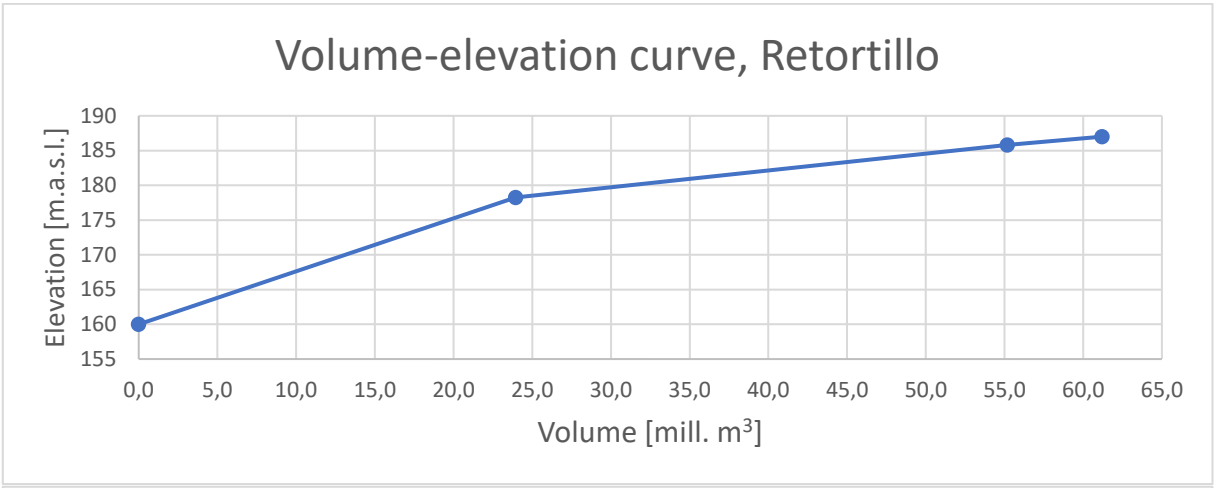

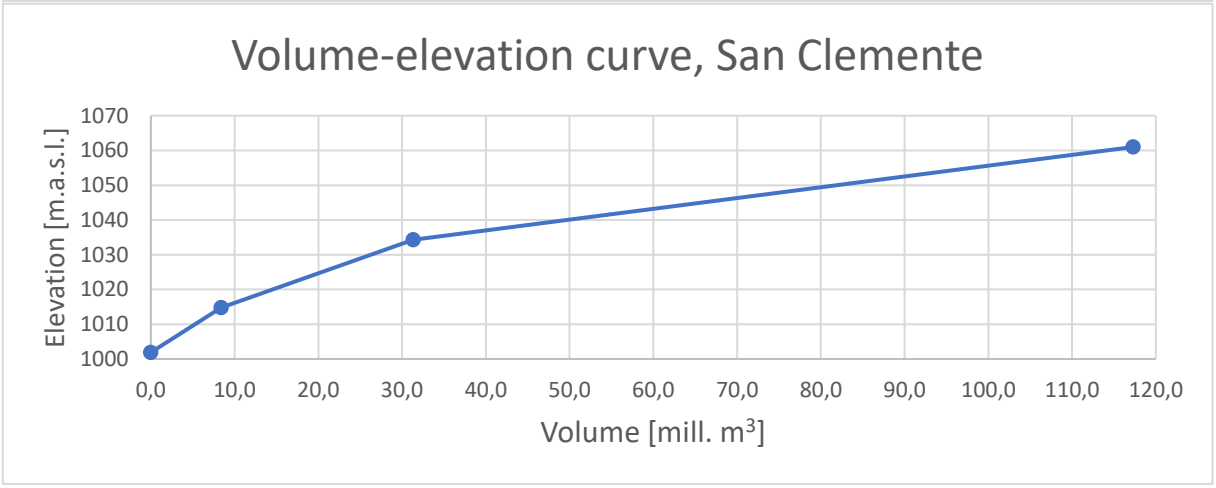

APPENDIX I: SCREEN DUMPS FROM THE WEAP MODEL

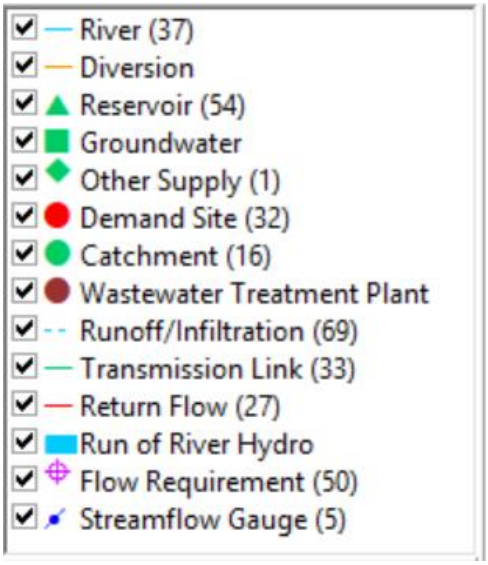

Figure 34: Legend of the WEAP Schematic view.

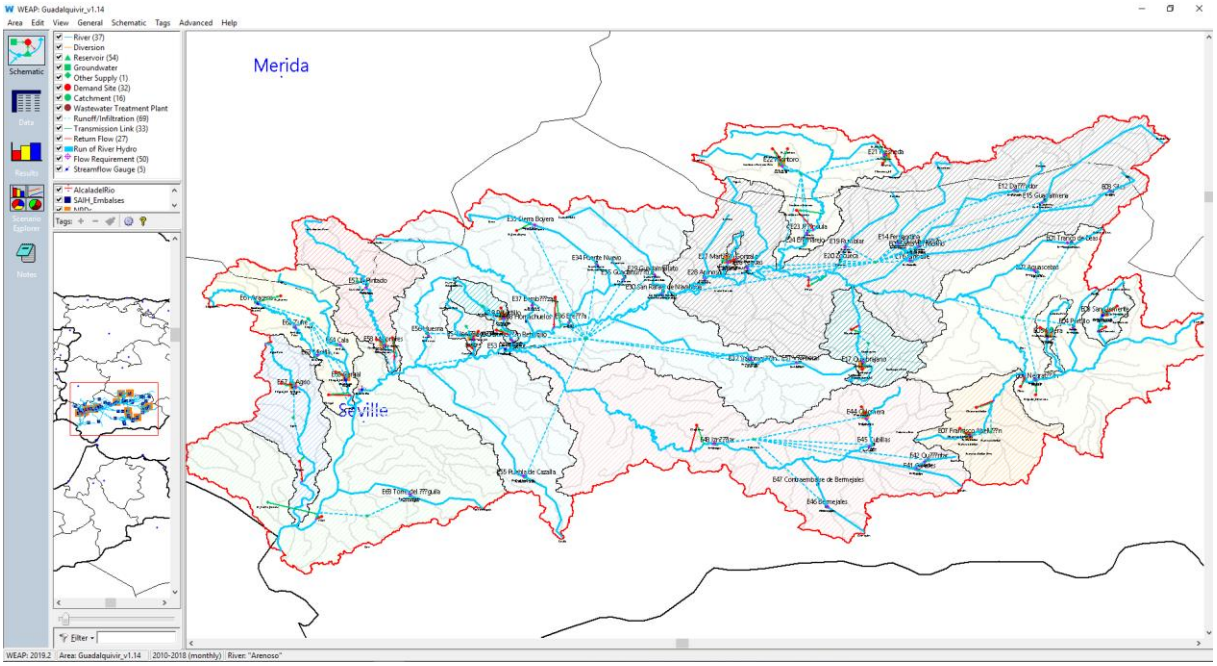

Figure 35: Overview of the whole basin with all the nodes, links and rivers in the Schematic view.

APPENDIX I: SCREEN DUMPS FROM THE WEAP MODEL

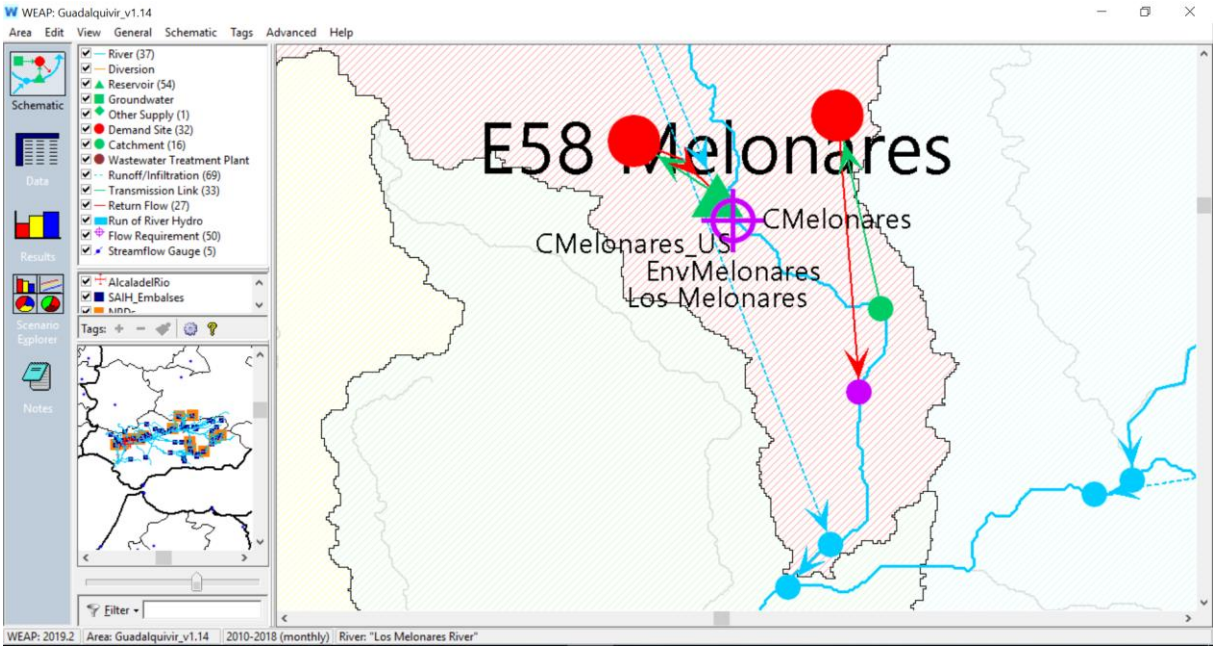

Figure 36: Example of how the water withdrawals and environmental flow requirements are implemented. The water withdrawals upstream the dam "Melonares" and their return point are connected to the reservoir, whereas the water withdrawals and their return points downstream the dam are connected between the dam and the node connecting the Melonares catchment with the downstream catchment. The environmental minimum flow requirement is implemented as a node directly downstream the dam.

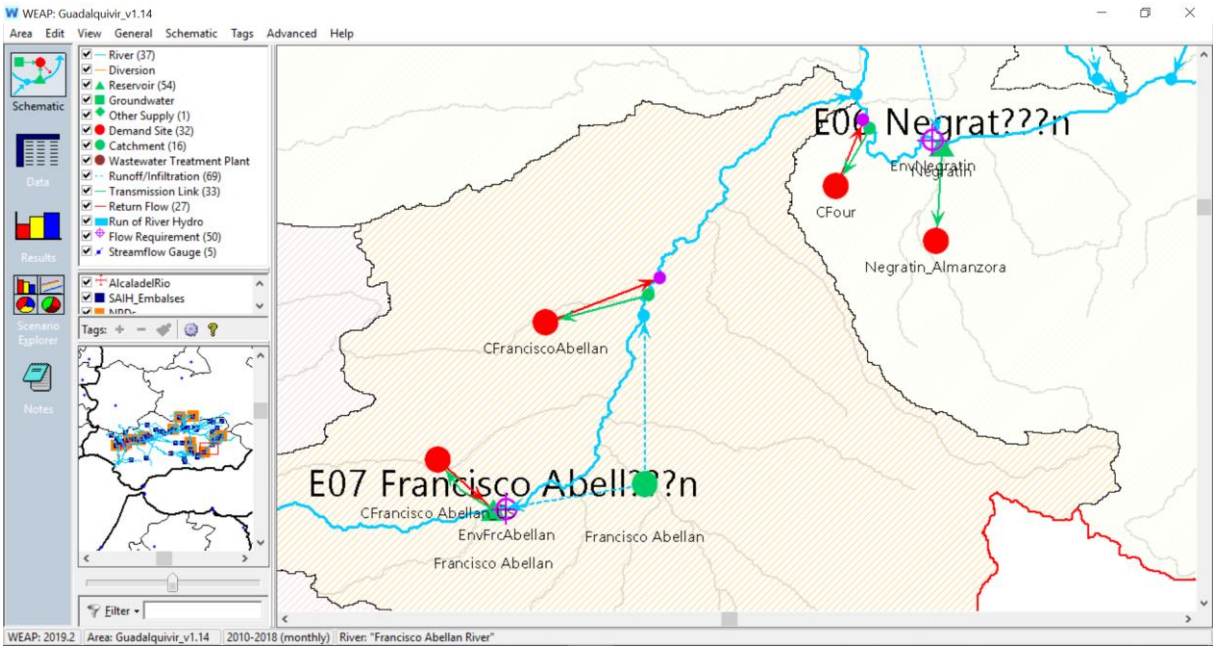

Figure 37: Example I on how the runoff is distributed within the catchments. The run/infiltration links from the catchments are given specified shares summing up to 100% and are connected to the areas upstream and downstream of the dam.

APPENDIX I: SCREEN DUMPS FROM THE WEAP MODEL

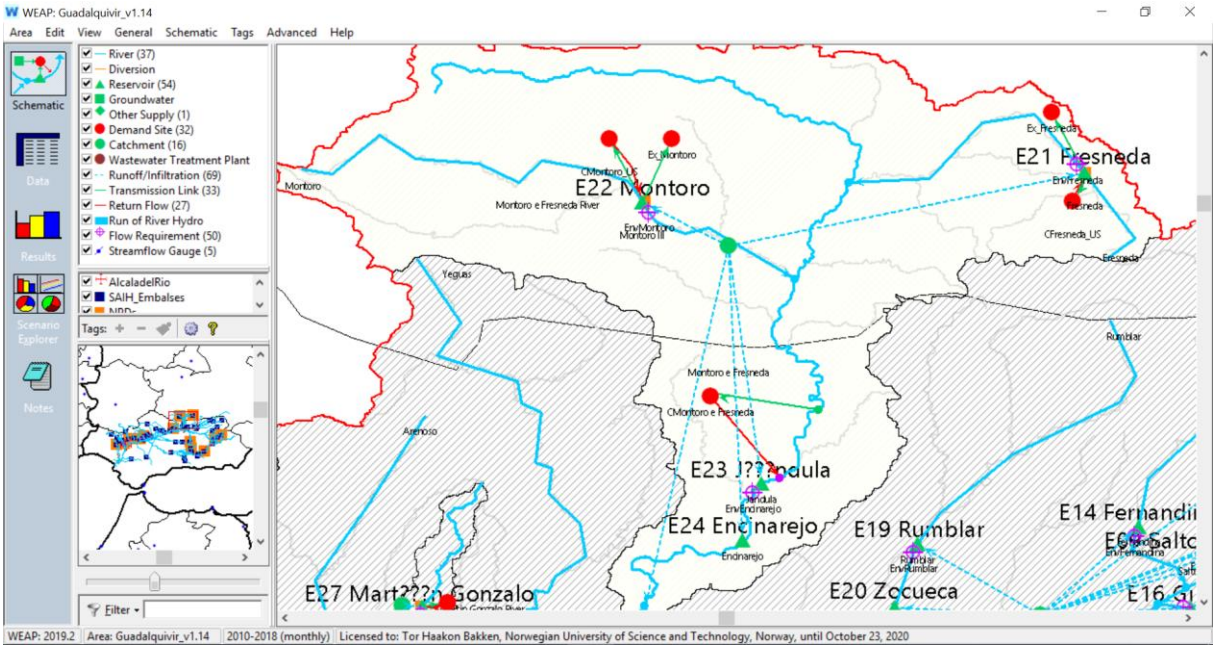

Figure 38: Example II on how the runoff is distributed within the catchments. The run/infiltration links from the catchments are given specified shares summing up to 100% and are connected to the areas upstream the individual dams and downstream the most downstream dam.

Key Assumptions

These are user-defined variables that can be referenced elsewhere in your analysis. For monthly variation, use Monthly Time-Series Wizard.

Key Assumption	2010	Scale	Unit
Humidity	MonthlyValues(Oct, 77.26, Nov, 73.19, Dec, 66.63, Jan, 64.79, Feb, 59.37, Mar, 54.48, Apr, 47.39, May, 49.26, Jun, 56.68, Jul, 67.21, Aug, 75.21, Sep, 77.97)		
Wind	MonthlyValues(Oct, 2.85, Nov, 3.13, Dec, 3.18, Jan, 3, Feb, 2.97, Mar, 2.89, Apr, 2.85, May, 2.77, Jun, 2.64, Jul, 2.73, Aug, 2.8, Sep, 2.97)		
Monthly variation	MonthlyValues(Oct, 9.524, Nov, 9.524, Dec, 5.079, Jan, 5.079, Feb, 5.079, Mar, 9.206, Apr, 9.27, May, 9.333, Jun, 9.397, Jul, 9.46, Aug, 9.524, Sep, 9.524)	Percent	share
FreezingPoint	-1		C
MeltingPoint	1		C
KC	MonthlyValues(Oct, 0.75, Nov, 0.75, Dec, 0.4, Jan, 0.4, Feb, 0.4, Mar, 0.725, Apr, 0.73, May, 0.735, Jun, 0.74, Jul, 0.745, Aug, 0.75, Sep, 0.75)		
ConsumptionRate	70	Percent	share
DeepConductivity	4		
DeepWaterCapacity	1850		
SoilWaterCapacity	1375		
RootZoneConductivity	4		
RunoffResistanceFactor	1.55		
InitUZ1	8	Percent	share
InitUZ2	8	Percent	share
PreferredFlowDirection	0.1		
Precip_corr	1.18		
ReducedWithdrawals	1		

Figure 39: Key assumptions applicable to all the catchments in the model.

APPENDIX I: SCREEN DUMPS FROM THE WEAP MODEL

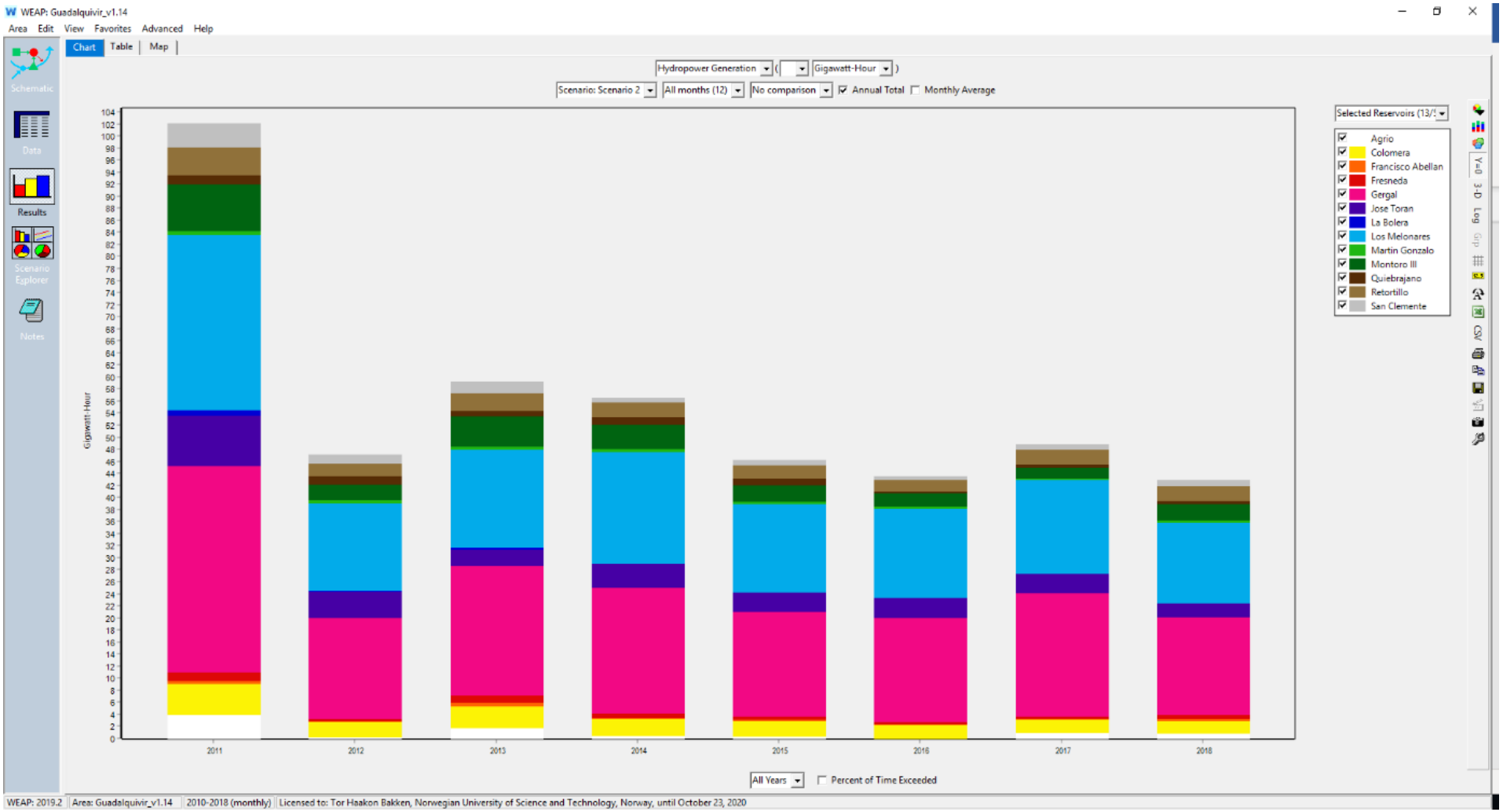

Figure 40: Example of the presentation of results in WEAP.

Nora Rydland Fjøsne

Demonstrating the retrofitting potential of non-powered dams for hydropower production

NTNU
Norwegian University of
Science and Technology